Alaska Range

Introduction

The heavily glacierized Alaska Range consists of a number of adjacent and discrete mountain ranges that extend in an arc more than 750 km long (figs. 1, 381). From east to west, named ranges include the Nutzotin, Mentasta, Amphitheater, Clearwater, Tokosha, Kichatna, Teocalli, Tordrillo, Terra Cotta, and Revelation Mountains. This arcuate mountain massif spans the area from the White River, just east of the Canadian Border, to Merrill Pass on the western side of Cook Inlet southwest of Anchorage. Many of the individual ranges support glaciers. The total glacier area of the Alaska Range is approximately 13,900 km^2 (Post and Meier, 1980, p. 45). Its several thousand glaciers range in size from tiny unnamed cirque glaciers with areas of less than 1 km^2 to very large valley glaciers with lengths up to 76 km (Denton

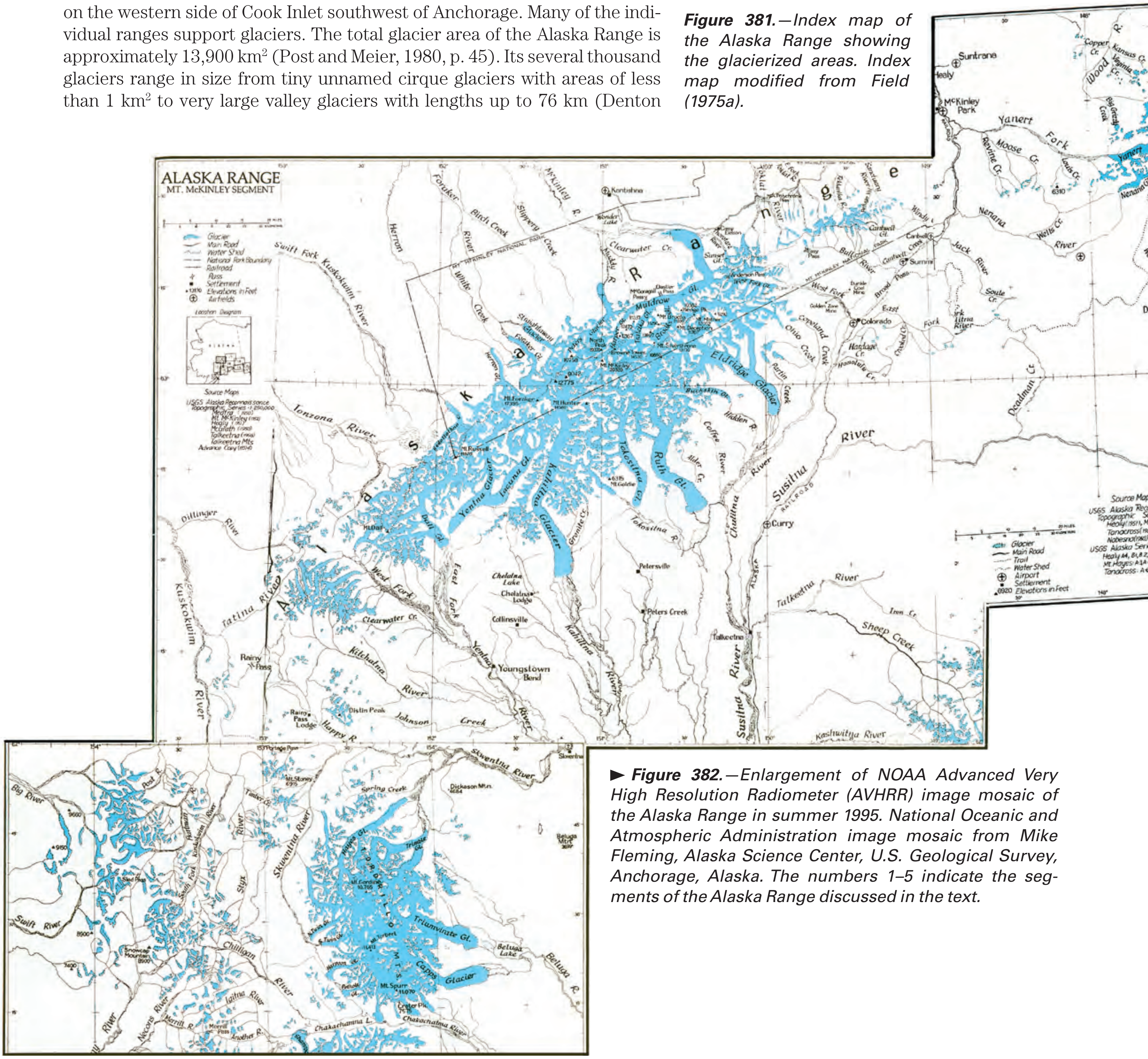

Figure 381.—Index map of the Alaska Range showing the glacierized areas. Index map modified from Field (1975a).

► *Figure 382.*—Enlargement of NOAA Advanced Very High Resolution Radiometer (AVHRR) image mosaic of the Alaska Range in summer 1995. National Oceanic and Atmospheric Administration image mosaic from Mike Fleming, Alaska Science Center, U.S. Geological Survey, Anchorage, Alaska. The numbers 1–5 indicate the segments of the Alaska Range discussed in the text.

and Field, 1975a, p. 575) and areas of greater than 500 km^2. Alaska Range glaciers extend in elevation from above 6,000 m, near the summit of Mount McKinley, to slightly more than 100 m above sea level at Capps and Triumvirate Glaciers in the southwestern part of the range.

From east to west, the Alaska Range can be divided into five principal segments (fig. 382): (1) the Mentasta and Nutzotin Mountains segment between the Canadian border and Mentasta Pass; (2) the Mount Kimball-Mount Gakona segment between Mentasta Pass and the Delta River; (3) the Mount Hayes-Mount Deborah segment between Delta River and Broad Pass; (4) the Mount McKinley-Mount Foraker segment between Broad Pass and Rainy Pass; and (5) the Mount Gerdine-Mount Spurr segment between Rainy Pass and Merrill Pass.

Landsat MSS images that cover the Alaska Range have the following Path/Row coordinates: 69/16, 70/16, 71/15, 71/16, 72/15, 72/16, 73/15, 73/16, 74/15, 75/15, 75/16, 76/15, 76/16, 76/17, 77/15, 77/16, 77/17, 78/15, and 78/16 (fig. 3, table 1). The glacierized areas of the Alaska Range are mapped on the USGS Nabesna, Alaska (1960), Tanacross, Alaska (1956), Mount Hayes, Alaska (1955), Healy, Alaska (1956), Talkeetna, Alaska (1958), Mount McKinley, Alaska (1958), McGrath, Alaska (1958), Lime Hills, Alaska (1958), and Lake Clark, Alaska (1958) 1:250,000-scale topographic maps (appendix A).

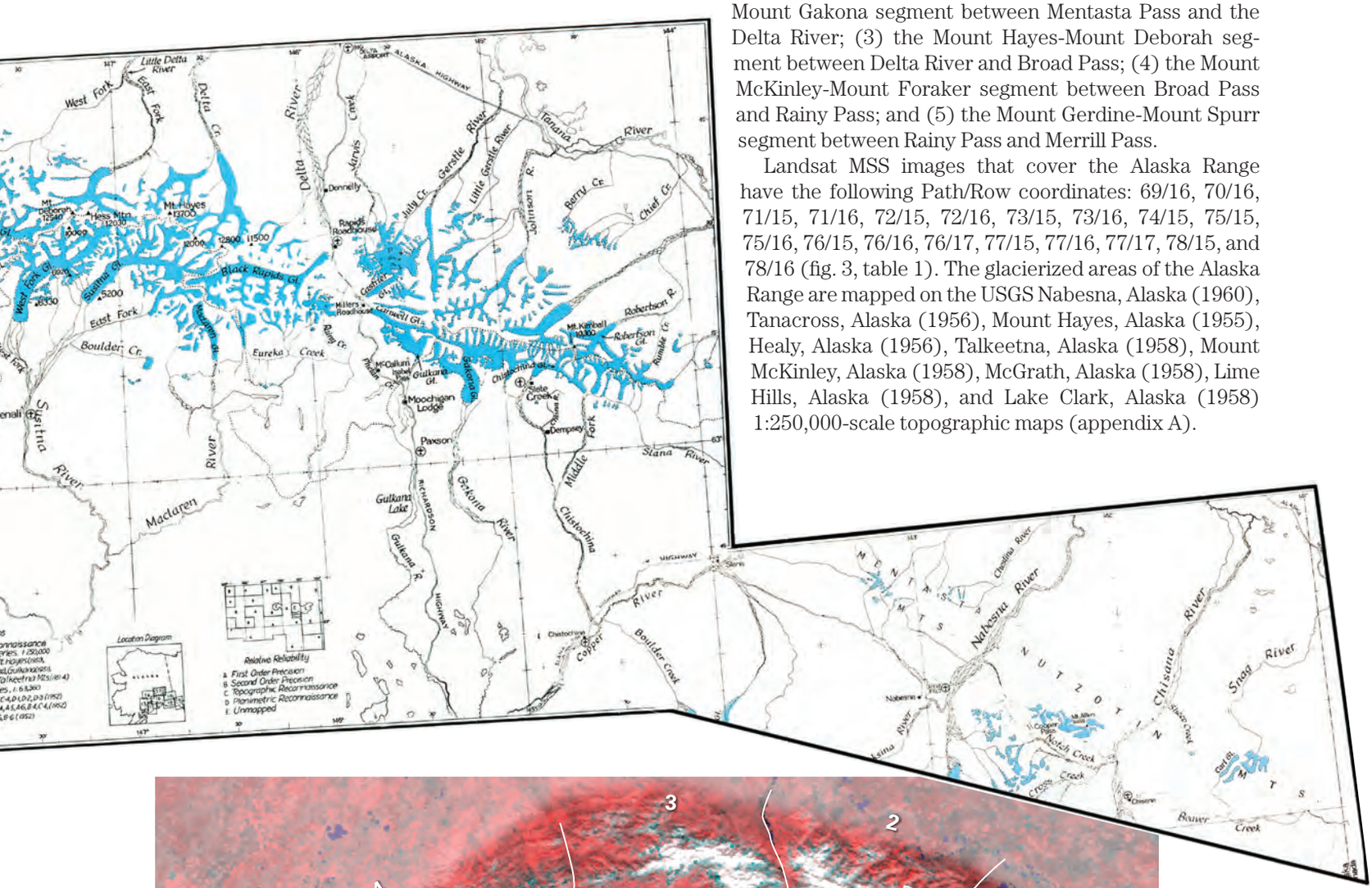

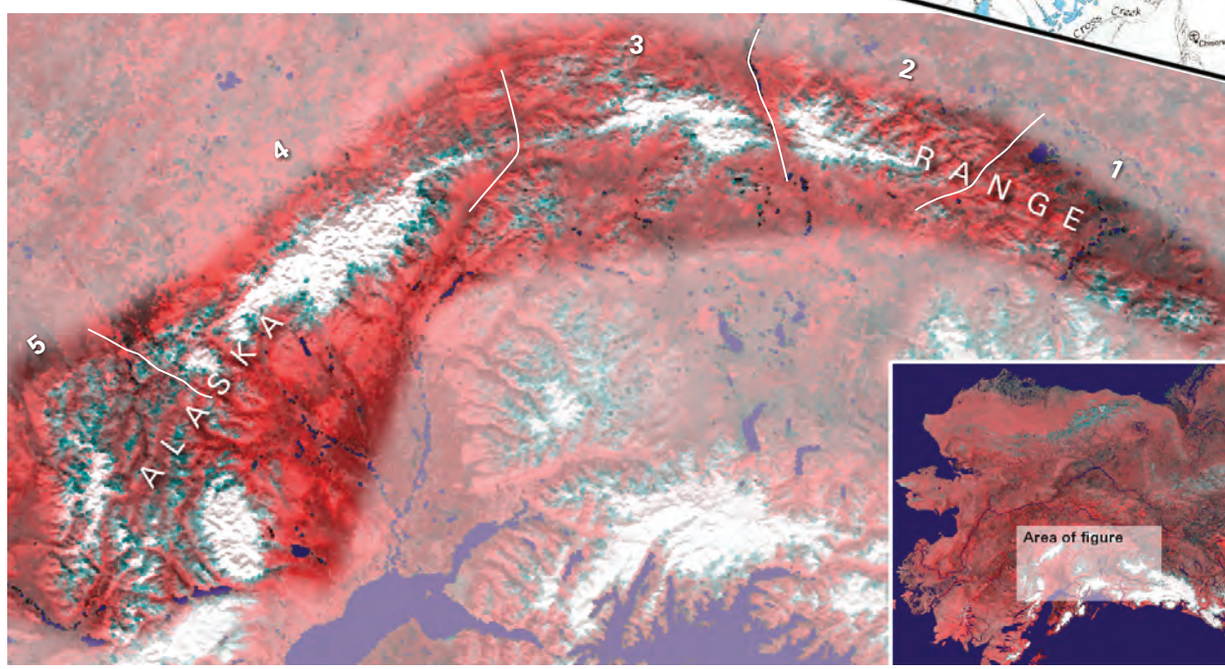

The Mentasta and Nutzotin Mountains Segment between the Canadian Border and Mentasta Pass

The Nutzotin Mountains extend for nearly 100 km from east of the Canadian border to the Nabesna River. Aside from several isolated glaciers, two areas support small concentrations of glaciers. Collectively, they contain as many as 100 small glaciers having a combined area of about 14.3 km^2 (Denton and Field, 1975a, p. 575). The first area, approximately 20 km west of the Canadian border, is located on the flanks of an unnamed ridge (fig. 383). Glaciers drain into Snag, Klein, Crescent, Baultoff, and Carl Creeks. Only one of the two largest glaciers is named (Carl Glacier, which is approximately 5 km long). When the area was photographed by the AHAP Program on 26 August 1981, all of its glacier termini, including the terminus of the large unnamed glacier that drains into Crescent Creek, showed multiple evidence of recent thinning and retreat.

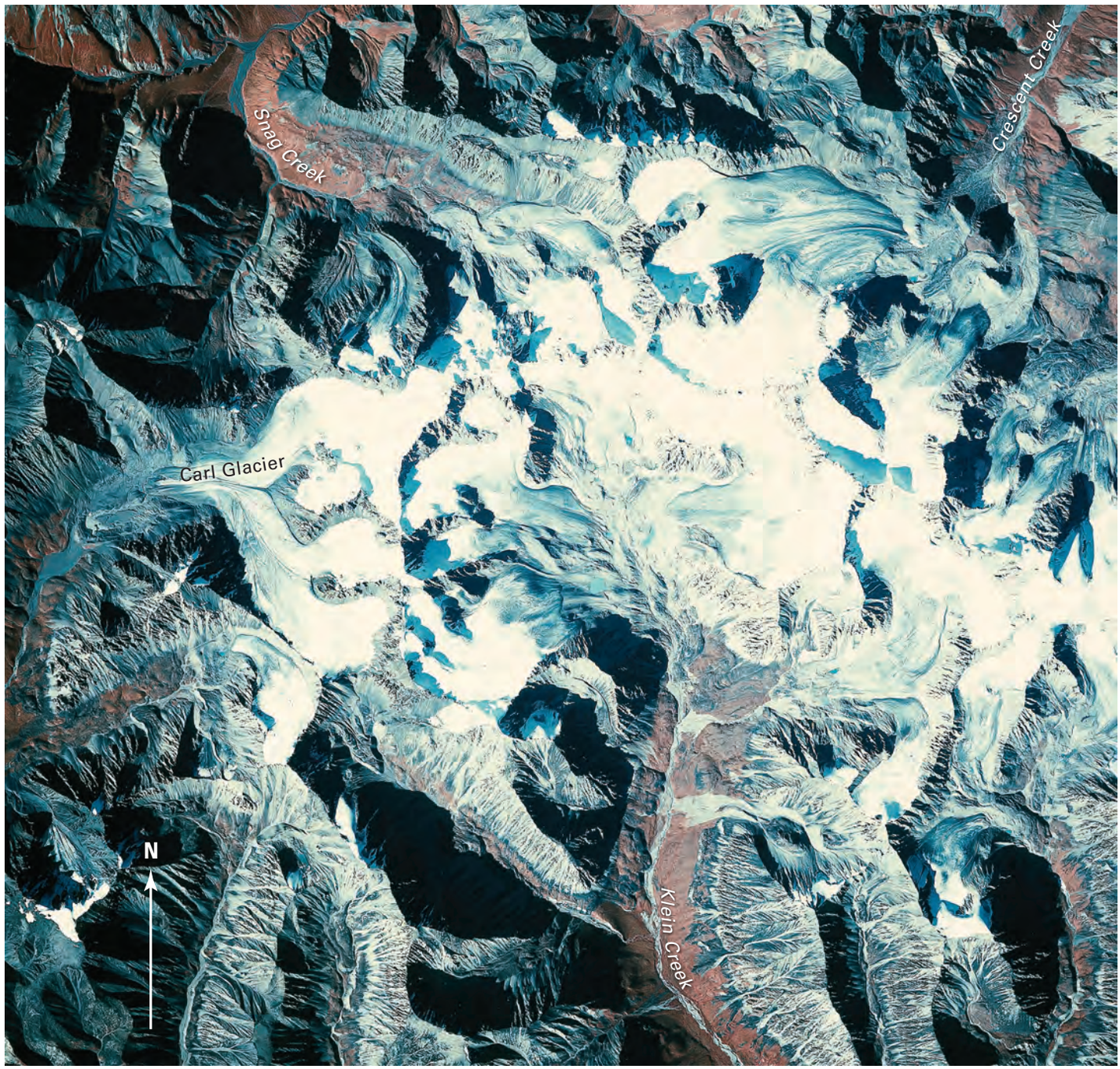

Figure 384.—*Two oblique aerial photographs of unnamed peaks in the Nutzotin Mountains and valleys showing the presence of small glaciers, rock glaciers, or both on 30 August 2000.* **A**, *The northern (left) of two cirques, located between the Nabesna River and Pickerel Lake, hosts a small glacier in a valley mantled by rock-glacier debris.* **B**, *Located southeast of Alder Creek, this unnamed tributary to Stuver Creek has several rock-glacier lobes in its valley and either a small glacier or rock glacier at its head. Photographs by Bruce F. Molnia, U.S. Geological Survey. Larger versions of these figures are available online.*

◄ ***Figure 383.***—*26 August 1981 AHAP false-color infrared vertical aerial photograph of the concentration of glaciers located southeast of Needle Peak in the eastern Nutzotin Mountains. All of the glacier termini, including the largest (Carl Glacier) and an unnamed glacier draining into Crescent Creek show multiple evidence of recent retreat and thinning, including elevated moraines, trimlines, abandoned moraines, and bare bedrock aprons. The unnamed glacier originates on the flank of an unnamed 2,606-m peak, the highest in the area. Four unnamed glaciers located in the upper reaches of Klein Creek appear to be the separated remnants of a single larger glacier that filled the head of Klein Creek within the last 100 years. Two other unnamed glaciers were also recently joined and probably were connected to the other Klein Creek glaciers during the "Little Ice Age." AHAP photograph no. L99F4712 from the GeoData Center, Geophysical Institute, University of Alaska, Fairbanks, Alaska.*

The second concentration of glaciers is located on the slopes of 2,591-m-high Mount Allen and on a west-trending ridge north of Cooper Pass and west of Chisana River. When the author observed the area from the air on 30 August 2000 (fig. 384), most cirques were ice free, whereas others supported small glaciers, rock glaciers, or both. Many of the glaciers of this area were observed at the beginning of the 20th century by Brooks (1900, 1906a, b, 1914), Moffit and Knopf (1909), and Capps (1910a, b) but have not received much attention since.

The Mentasta Mountains extend for more than 60 km from the Nabesna River to the Slana River. Because the elevations of the highest peaks are significantly lower than 3,000 m, the glaciers of this region all exist at relatively low elevations along a 30-km-long ridge. The largest concentration is located on the western flanks of a ridge between 2,511-m-high Noyes Mountain (see 24 August 1981 AHAP false-color infrared vertical aerial photograph no. L94F4128) and an unnamed 2,527 m-high-peak to its southeast. Approximately 5.5 km^2 of glacier ice exists in the western Mentasta Mountains (Denton and Field, 1975a, p. 575).

The Mount Kimball-Mount Gakona Segment between Mentasta Pass and the Delta River

The 100×60-km Mount Kimball-Mount Gakona segment supports a glacier-covered area of approximately 1,036 km^2 (Denton and Field, 1975a, p. 578–581). Most of the glaciers in this area descend from an 85-km-long southeast-to-northwest interconnected unnamed ice field. This unnamed ice field—topped in the east by Mount Kimball (3,140 m), in the center by Mount Gakona (2,875 m), and on the west by Mount Silvertip (~2,980 m)—is as much as 55 km wide from glacier terminus to glacier terminus. About 20 outlet valley glaciers that head in this ice field have lengths of 6 km or more, and most are named. The largest—the 33-km-long Johnson Glacier—has an area of 183 km^2 (Denton and Field, 1975a, p. 580) and forms the headwaters of the Johnson River. In 1902, a topographic map of part of this area made by Mendenhall and Gerdin (Mendenhall, 1905) showed the location and size of several of the area's larger south-flowing glaciers.

Outlet glaciers that drain the northern side of the unnamed ice field from east to west include (lengths and areas measured by Denton and Field, 1975a, p. 579–581, from USGS maps): (1) an unnamed glacier at the head of Rumble Creek (8 km, 18 km^2), the easternmost outlet of the ice field (see 24 August 1981 AHAP false-color infrared vertical aerial photograph no. L88F3863); (2) Robertson Glacier (22 km, 85 km^2), located at the head of Robertson

River; (3) Kimball Glacier, the western tributary of Robertson Glacier, which has a length of more than 10 km; (4) an unnamed glacier (24 km, 108 km^2) that forms the headwaters of the West Fork of Robertson River; (5) another unnamed glacier (10 km, 18 km^2) that forms the headwaters of an unnamed eastern tributary of the Johnson River; (6) Johnson Glacier; (7) Spur Glacier, so named because of the shape of its arcuate tributaries and straight terminus (12 km, 51 km^2); (8) Gerstle Glacier (fig. 385) (24 km, 80 km^2), which forms the headwaters of the Gerstle River; (9) an unnamed glacier at

Figure 385.—*South-looking oblique aerial photograph of the icefall of the Gerstle Glacier at an elevation of approximately 1,600 m on 22 August 1960. Both sides of the glacier show several trimlines, suggesting that the glacier has experienced significant thinning. University of Washington photograph no. 6-42 taken by Austin Post, U.S. Geological Survey.*

the head of July Creek (9 km, 25 km^2), which drains from the northern side of Mount Silvertip (~2,980 m); and (10) *Jarvis Glacier* (9 km, 19 km^2), the northwesternmost outlet glacier.

North of the unnamed ice field, a number of small unnamed glaciers drain in all directions from Mount Hajdukovich (2,698 m), located between Spur and Gerstle Glaciers, and from an unnamed isolated 2,383-m-high peak, located between the West Fork of the Robertson River and Johnson River. Riley Creek Glacier and several other small unnamed glaciers drain from an unnamed 2,520-m-high peak at the northwestern end of the ice field.

Outlet glaciers that drain the southern side of the unnamed ice field from east to west are (lengths and areas measured by Denton and Field, 1975a, p. 578–579, from USGS maps): (1) Tok Glacier, the easternmost outlet of the ice field, which forms the headwaters of the Tok River; (2) an unnamed glacier (9 km, 17 km^2), the largest of three glaciers that drain into the Slana River; (3) two unnamed glaciers (10 km, 15 km^2; 8 km, 9 km^2), both contributing their meltwater to the Middle Fork of the Chistochina River; (4) another unnamed glacier (6 km, 13 km^2), an eastern distributary of Chistochina Glacier; (5) Chistochina Glacier (13 km, 21 km^2) (see 24 August 1981 AHAP false-color infrared vertical aerial photograph no. L88F3868); (6) an unnamed glacier (17 km, 52 km^2) that forms the headwaters of the West Fork of the Chistochina River and was photographed by Moffit in 1910 (see USGS Photo Library photograph Moffit 418); (7) Gakona Glacier (32 km, 112 km^2), the largest south-flowing outlet glacier of the unnamed ice field; (8) Gulkana Glacier (10 km, 21 km^2), a glacier with a long history of 20th century scientific investigations (figs. 386, 387*A*); (9) West Gulkana Glacier, mapped during the IGY (AGS, 1960) and again in the late 1980s (figs. 386, 387*A*); (10) Canwell Glacier (24 km, 89 km^2); (11) Fels Glacier, mislabeled as Eel Glacier on the Mount Hayes, Alaska (1955), 1:250,000-scale (appendix A) and the

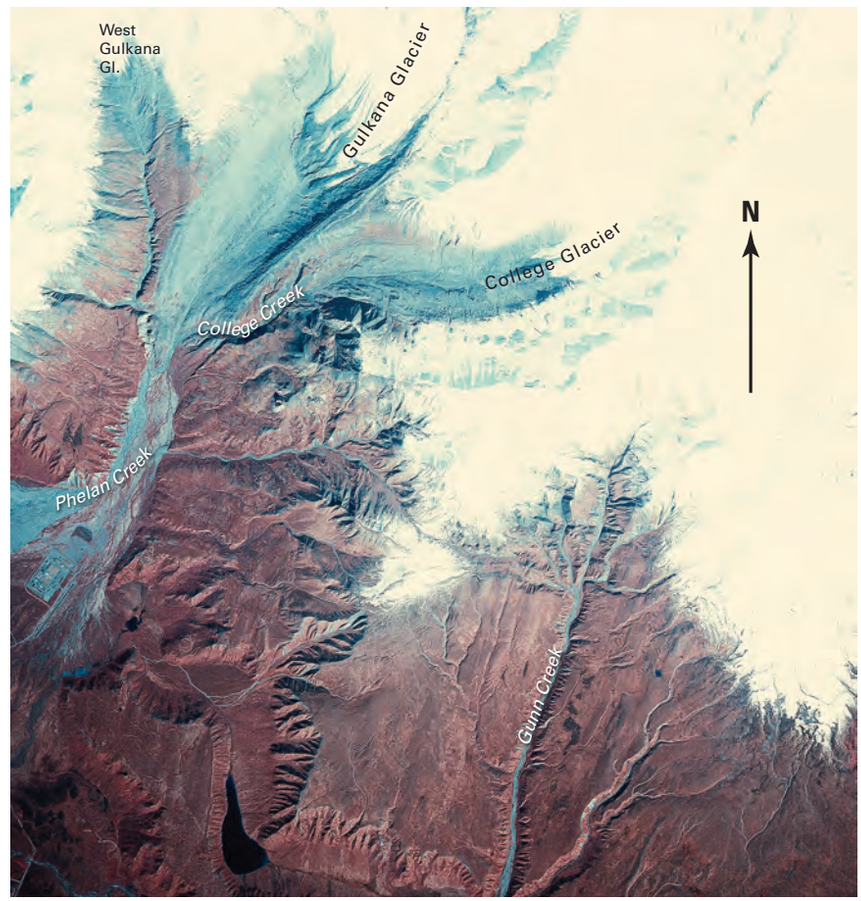

Figure 386.—*24 August 1981 AHAP false-color infrared vertical aerial photograph of the termini of Gulkana, West Gulkana, and College Glaciers. All three glaciers show evidence of ongoing recession and thinning. AHAP photograph no. L88F3873 from the GeoData Center, Geophysical Institute, University of Alaska, Fairbanks, Alaska.*

Mount Hayes B-4, Alaska (1955), 1:63,000-scale (appendix B) USGS topographic maps (15 km, 22 km^2); and (12) Castner Glacier (20 km, 79 km^2). The last three are west-flowing glaciers that drain into the Delta River.

Studies of Canwell and Castner Glaciers by Péwé (1957) found that both glaciers had advanced about 1.5 km during the early part of the "Little Ice Age" and that Canwell Glacier experienced a second smaller advance within the past 200 years. Canwell's advance was then followed by a retreat of nearly 2 km. During the first half of the 20th century, between 1902 and 1941, Canwell Glacier advanced again, a distance of approximately 1.5 km. Since then, its terminus has stagnated, thinned, and retreated.

Gulkana Glacier

The post-Pleistocene history of Gulkana Glacier has been described by a number of researchers. Calkin (1988) reported that the glacier occupied its Holocene maximum position about 5,700 yr B.P. at a location about 2.5 km forward of the 1962 ice margin. Péwé and Reger (1983) reported that cycles of retreat and advance followed; the glacier readvanced about 4,700 yr B.P., again at about 4,030 yr B.P., and again at about 800 yr B.P. Calkin (1988) used lichenometry to determine that Gulkana Glacier advanced about 560 yr B.P. and again at about 390 yr B.P. He stated that "historic evidence and lichen

***Figure 387.**—Four photographs showing changes in Gulkana Glacier during the 20th century.* **A**, *North-looking oblique aerial photograph of the terminus of Gulkana Glacier and parts of the termini of West Gulkana (west) and College (east) Glaciers on 31 August 1967. The trimlines along the Gulkana Glacier and in the former terminus region confirm that the glacier has experienced more than 4 km of retreat since photographed in July 1910 by F.H. Moffit (Photograph Moffit 427 from the USGS Photo Library, Denver, Colo.). Photograph 67-R4-87 by Austin Post, U.S. Geological Survey.* **B–D**, *see following pages.*

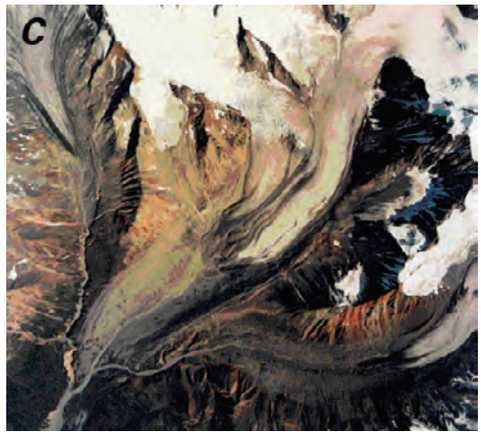

Figure 387.—**B**, *Oblique color aerial photograph of the terminus of Gulkana Glacier around 1975. The terminus has retreated about 30 m from its 1967 position. Undated photograph by Dennis C. Trabant, U.S. Geological Survey.* **C**, *Color vertical aerial photograph of the retreating termini of Gulkana and West Gulkana Glaciers on 11 July 1993. Since 1967, Gulkana Glacier has retreated more than 100 m. Photograph 1 No. 4 by AeroMap US, Inc.* **D**, *see following page. Larger versions of* B *and* C *are available online.*

data substantiate" an advance of the glacier after A.D. 1875. Mercer (1961a) determined that the rise in the firn limit of Gulkana Glacier may have been as much as 380 m since the "Little Ice Age" maxima.

Gulkana Glacier was photographed by Moffit on 15 July 1910 (see USGS Photographic Library photographs Moffit 423, 424, 427) and by Péwé on 12 July 1952. In the 42 years between photographs, the terminus of Gulkana Glacier retreated more than 4 km. Two oblique aerial photographs were acquired on 31 August 1967 (fig. 387*A*) and in 1975(?) (fig. 387*B*). General thinning occurred until 1976, but the glacier gained mass from 1976 to the early 1980s, and recession probably stopped (Mayo and Trabant, 1986). More recently, a comparison of a 1957 map of the glacier with data obtained during a geodetic airborne laser altimeter profiling survey carried out on 12 June 1993 allowed Echelmeyer and others (1996) to determine that Gulkana Glacier had retreated by about 1.75 km during the 36 years between data sets (an average annual retreat rate of 48.6 m a^{-1}) and that the glacier's area had decreased from 18.5 km^2 in 1957 to 17.0 km^2 in 1993 (a decrease of approximately 8 percent). The glacier also thinned an average of 10.9 m, and its volume decreased by 1.94×10^8 m^3. Between the 1950s and middle 1990s, on an annual basis, Gulkana Glacier thinned by 0.434 m a^{-1} and had a volume decrease of 0.00822 km^3 a^{-1}; between the middle 1990s and 1999, on an annual basis, Gulkana Glacier thinned by 0.748 m a^{-1} and had a volume decrease of 0.0136 km^3 a^{-1} (K.A. Echelmeyer, W.D. Harrison, V.B. Valentine, and S.I. Zirnheld, University of Alaska Fairbanks, written commun., March 2001). Figure 387*C* is a vertical aerial photograph acquired on 11 July 1993, one month after the geodetic airborne laser altimeter profiling survey. Figure 387*A–D* presents a photographic summary of changes in Gulkana Glacier during the 20th century.

Ostenso and others (1965) determined the configuration of the valley in which Gulkana Glacier flows by a gravimetric survey acquired by traverses across the glacier's surface. They determined that the subglacier valley of Gulkana Glacier consists of two parallel bedrock channels separated by a medial ridge. Ice in the eastern channel was about 225 m thick, whereas ice in the shallower western valley was only about 125 m thick. A recent study combining SAR and 50-MHz monostatic short-pulse radar data (Moran and others, 2000) determined that Gulkana Glacier's ice thickness in the upper 2 km of the eastern channel, above the juncture with the western tributary, was no thicker than 140 m and that the glacier's bed was steeply dipping, both parallel and transverse to the direction of ice flow. Because the locations of the gravity and radar surveys were not identical, no absolute change in thickness can be determined between the two. However, the maximum ice thickness measured by the radar survey is a third thinner than that measured by the earlier gravimetric survey.

In the early 1960s, the University of Alaska and the USGS began studies at Gulkana Glacier focused on characterizing its geophysical and glaciological parameters, including foliation patterns, structure, flow patterns, and ablation (Mayo and Péwé, 1963; Tangborn and others, 1977). Kennedy and others (1997) analyzed air temperature and precipitation data recorded at Gulkana Glacier basin between October 1967 and September 1996. The data set is important because it provides long-term climate information from the highest year-round climatological recording site in Alaska. Annual data summaries were calculated for each hydrologic year, from 1 October through 30 September, for years that have 12 months of data. Monthly precipitation-catch and average air temperature summaries were calculated for months with nine or fewer daily records missing. The average annual air temperature recorded at the site from hydrologic years 1968 through 1996 was -4.1°C. The coldest recorded year was 1972, which had an average annual temperature of -6.7°C. The warmest year was 1981, which had an average annual temperature of +2.6°C. The coldest month was January 1971, which had an

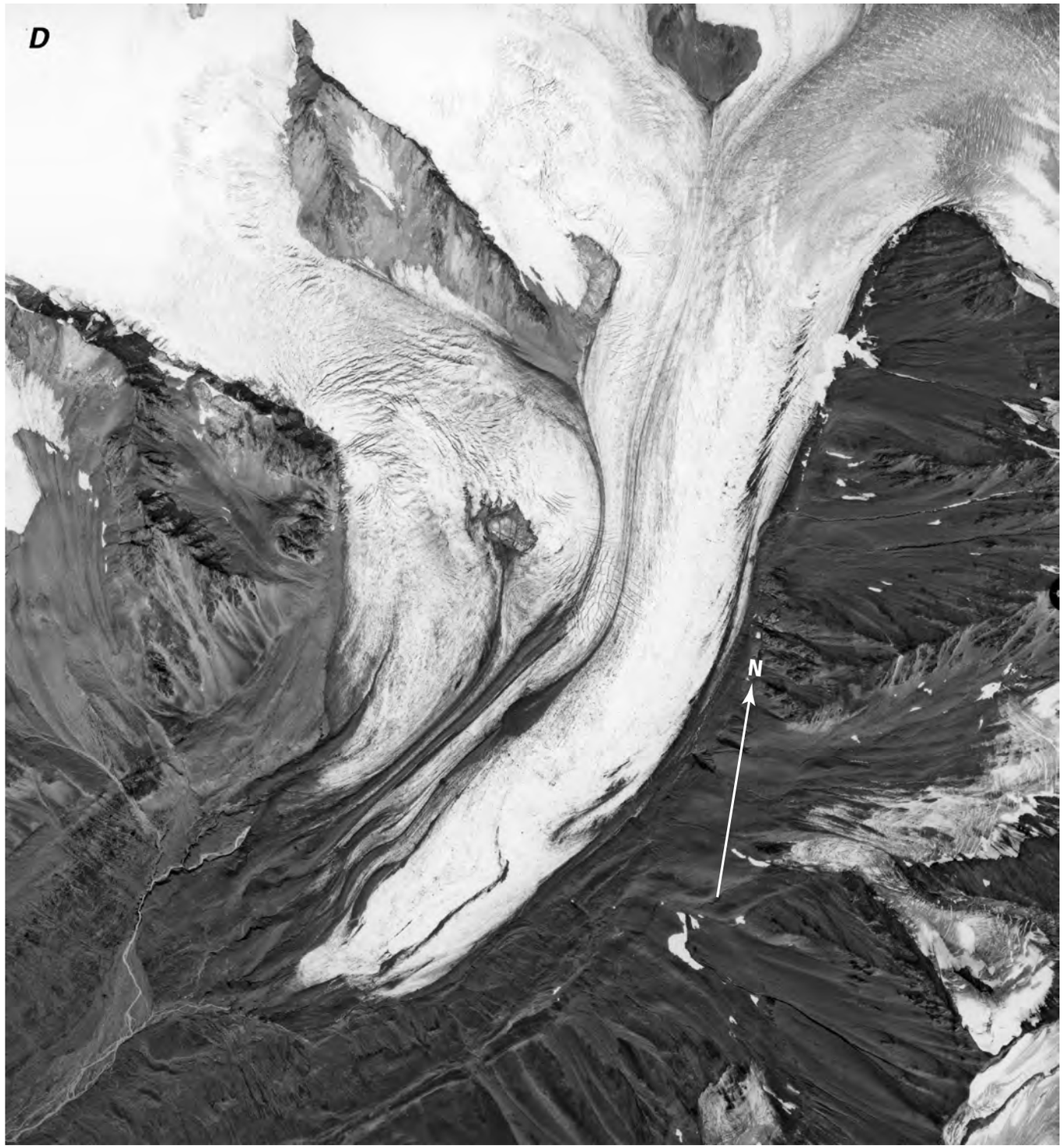

average temperature of -20.8°C. The warmest month was July 1989, which had an average temperature of +8.7°C. The coldest day was 17 January 1971, which had an average temperature of -35.0°C. The warmest day was 15 June 1969, which had an average temperature of +16.4°C.

The average annual precipitation gage catch recorded at the site from hydrologic years 1968 through 1992 was 1.02 m. The highest annual precipitation gage catch recorded was 1.572 m in 1981; the lowest was 0.555 m in 1969. The highest recorded monthly precipitation catch was 0.448 m in July 1981. In several different months, no precipitation was recorded. The highest daily precipitation gage catch was 9.9 cm on 12 September 1972. On

***Figure 387.*—D,** *Black-and-white 1:24,000-scale vertical aerial photograph of the retreating terminus of Gulkana Glacier on 18 August 1999. The response to changing climate has caused Gulkana Glacier to retreat more than 40 m and to thin by more than 5 m since the 1993 photograph. Photograph from U.S. Bureau of Land Management, roll 3, frame 333.*

many different dates, no precipitation was recorded. Because of low precipitation gage-catch efficiency, the reported annual precipitation gage-catch data are estimated to represent about 62 percent of the actual annual basin precipitation. Snowfall is the dominant form of precipitation on the glacier from September through mid-June. In 1976, glacier ice thickness from a single site near the highest measurement site was 180 m; two glacier cross profiles near midglacier indicated that the thickness was 270 m on the centerline; glacier ice was determined to be 150 m thick on the centerline at a downglacier measurement site.

The 1992 measured winter-snow, maximum winter-snow, net, and annual balances in the Gulkana Glacier basin were evaluated by March and Trabant (1996). Averaged over the glacier, the measured winter-snow balance was 0.97 m on 26 March 1992; the maximum winter-snow balance was 1.05 m on 19 May 1992; the net balance (from 8 September 1991 to 17 August 1992) was -0.29 m; and the annual balance (1 October 1991 to 30 September 1992) was -0.38 m. Annual stream runoff was 1.24 m averaged over the basin.

For 1993, March and Trabant (1997) found that the 1993 measured winter-snow balance was 0.81 m on 31 March 1993, 1.2 standard deviations below the long-term average; the maximum winter-snow balance, 0.84 m, was recorded on 10 May and 11 May 1993; the net balance (from 18 August 1992 to 8 September 1993) was -1.80 m, the most negative balance year on record at 2.8 standard deviations below the long-term average. The annual balance (1 October 1992 to 30 September 1993) was -1.64 m. Annual stream runoff was 1.996 m averaged over the basin, 0.2 standard deviations above the long-term average.

For 1994, March (1998) found that the measured winter-snow balance was 1.34 m on 29 April 1994, 0.9 standard deviation above the long-term average; the maximum winter-snow balance, 1.43 m, was recorded on 18 April 1994; the net balance (from 8 September 1993 to 17 September 1994) was -0.72 m, 0.7 standard deviation below the long-term average. The annual balance (1 October 1992, to 30 September 1993) was -0.88 m. Annual stream runoff was 1.93 m averaged over the basin.

For 1995, March (2000) found that the measured winter-snow balance was 0.94 m on 19 April 1995, 0.6 standard deviation below the long-term average; the maximum winter-snow balance, 0.94 m, was recorded on 25 April 1995; the net balance (from 18 September 1994 to 29 August 1995) was -0.70 m, 0.76 standard deviation below the long-term average. The annual balance (1 October 1994, to 30 September 1995) was -0.86 m. Annual stream runoff was 2.05 m averaged over the basin, approximately equal to the long-term average.

During the four-year period from 1992 through 1995, Gulkana Glacier's average measured winter-snow balance was +1.015 meters; its average maximum winter-snow balance was +1.0625 m; its average net balance was -0.88 m; and its average annual balance was -0.94 m. Average annual stream runoff was 1.804 m averaged over the basin. Retreat was continuing at the end of the 20th century, as shown on an 18 August 1999 vertical aerial photograph (fig. 387*D*).

West Gulkana Glacier

West Gulkana Glacier, a small valley glacier approximately 4 km long was mapped in 1957 (AGS, 1960) (figs. 386, 387*A*). Austin Post, who was a leader of the IGY team that mapped the glacier, reported it to be "virtually stagnant" and receding; almost no snow remained from the previous winter. The IGY map of West Gulkana Glacier shows a retreating glacier with a significant trimline on its eastern side (AGS, 1960). In 1987, a team from Arizona State University and the U. S. Military Academy at West Point, led by Melvin Marcus and L.S. Thompson remapped the glacier (Thompson and Smith, 1988).

A comparison of the two maps shows that the glacier retreated about 520 m and thinned and narrowed in the 30 years between maps.

West Gulkana Glacier was resurveyed in 1993 by a geodetic airborne laser altimeter profiler (Sapiano and others, 1998). Interpretation of a single profile acquired on 12 June 1993, field observations made in 1995, and a 1957 map showed that the terminus of West Gulkana Glacier had retreated by approximately 480 m during the 38 years between surveys, an average annual retreat rate of 12.6 m a^{-1}, and that the glacier's area had decreased from 4.2 km^2 in 1957 to 3.59 km^2 in 1993, a decrease of around 15 percent. During the 38 years of observation, the glacier thinned an average of 24 m, its volume decreased by 9.3×10^7 m^3, and its average annual mass balance was -0.61 m. Retreat was continuing at the end of the 20th century (fig. 387*C*) (see 18 August 1999 BLM vertical aerial photograph — Roll 3, Frame 323).

Jarvis Glacier

In 1955, Ostenso and Holmes (1962) used gravimetric techniques to study *Jarvis Glacier*. They found that it lies in a deep U-shaped valley with a cirque at its head. The cirque, which has a sill at its downglacier end, had ice thicknesses of as much as 321 m.

The Mount Hayes-Mount Deborah Segment between Delta River and Broad Pass

The 160-km-long Mount Hayes section, which includes Mount Hayes (4,216 m), Mount Moffit (3,957 m), and Mount Deborah (3,750 m), has a glacier-covered area of about 1,900 km^2 (Denton and Field, 1975a, p. 583–586). Most glaciers originate from an ice-covered interconnected upland accumulation area, an unnamed ice field that has a maximum width of more than 60 km. A number of isolated, generally small glaciers descend from individual peaks and ridges to the south, including several shown on the USGS Mount Hayes, Alaska (1955), 1:250,000-scale topographic map (appendix A) of the northern side of the Amphitheater Mountains named by Troy Péwé for the numerous cirques that are present (see 24 August 1981 AHAP false-color infrared vertical aerial photograph no. L88F3880). Most of the glaciers in this area are named and more than 15 glaciers have lengths of more than 7 km. According to Denton and Field (1975a, p. 583–586), who measured the following lengths and areas of glaciers, the longest are Black Rapids Glacier (fig. 388) (40 km, 341 km^2), West Fork Glacier (41 km, 311 km^2), and Susitna Glacier (36 km, 323 km^2). There are many surging glaciers in this section. The surge dynamics of glaciers in the Susitna River Basin were summarized by Clarke (1991).

Beginning on the northern side of the unnamed ice field (counter-clockwise, from east to west, starting west of Black Rapids Glacier) glaciers (lengths and areas measured by Denton and Field, 1975a, p. 583–586) include (1) two unnamed glaciers draining into the Delta River, the western one with a length of 10 km and an area of 13 km^2; (2) McGinnis Glacier (13 km, 33 km^2); (3) Trident Glacier (28 km, 222 km^2); (4) Hayes Glacier; (5) an unnamed glacier (7 km, 8 km^2), which descends from Mount Giddings and Mount Skarland; (6) Gillam Glacier (25 km, 144 km^2); (7) an unnamed glacier west of Gillam Glacier (8 km, 12 km^2); (8) an unnamed glacier draining into the Wood River; (9) Yanert Glacier (35 km, 183 km^2), which advanced about 5 km in a 1942 surge, stagnated for more than 57 years, and surged again in 2000 and 2001; (10) an unnamed glacier (8 km, 12 km^2), which descends from the western flank of Nenana Mountain; (11) Nenana Glacier, (16 km, 29 km^2); (12) West Fork Glacier (41 km, 311 km^2); (13) Susitna Glacier (fig. 389) (36 km, 323 km^2), which surged about 5 km in 1952 or 1953; (14) an unnamed glacier draining into the East Fork Susitna River (fig. 390) (17 km, 46 km^2), which has thinned more than 50 m and retreated several kilometers since being mapped in the 1950s; (15) Maclaren Glacier (17 km, 68 km^2); (16) Eureka Glacier, which is around 10 km long (estimated

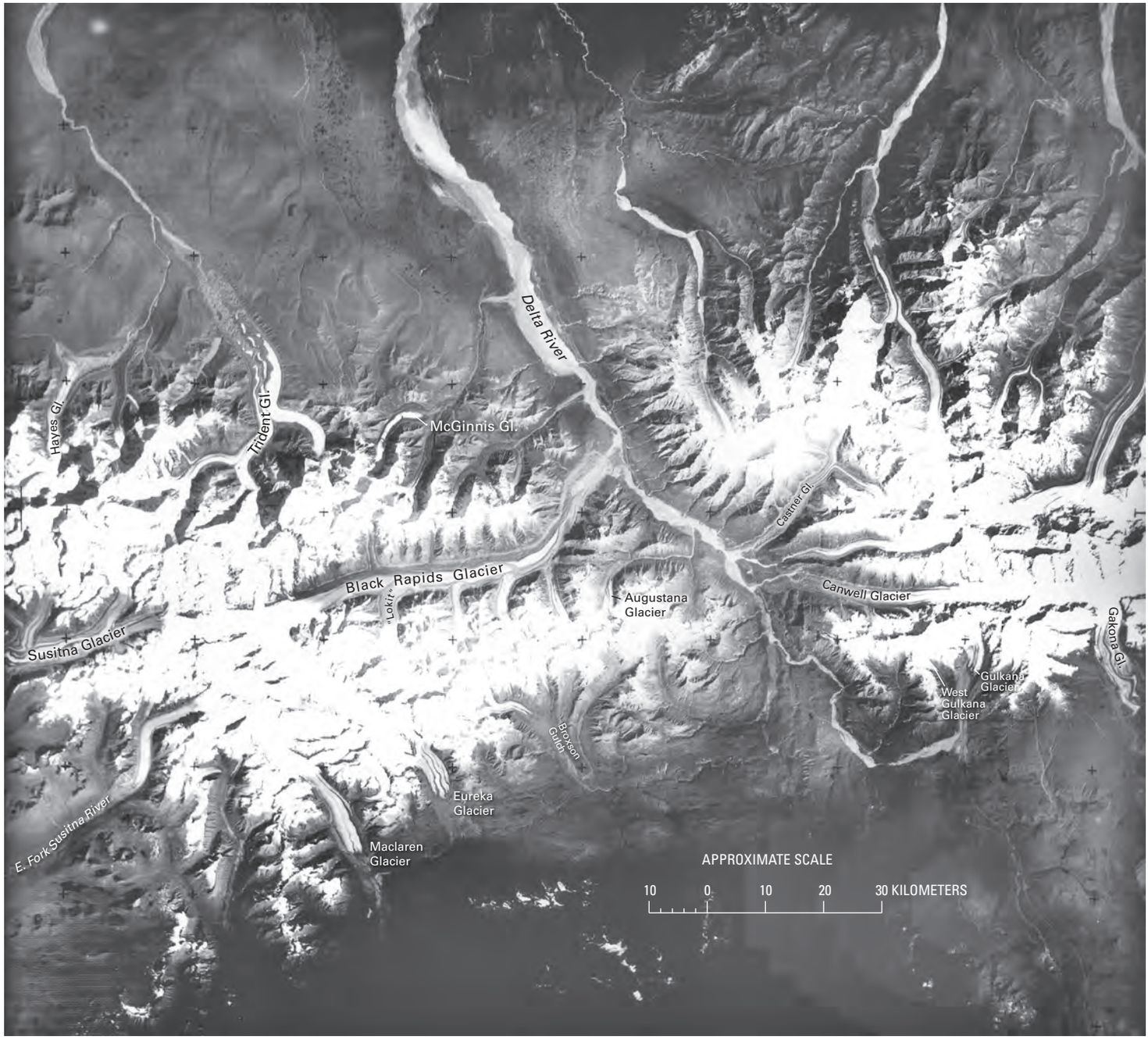

Figure 388.—*Annotated Landsat 3 return beam vidicon (RBV) image of Black Rapids Glacier, Susitna Glacier, Gulkana Glacier, West Gulkana Glacier, Canwell Glacier, Castner Glacier, and other glaciers in the Alaska Range. The Black Rapids Glacier has been long known to have unusual flow characteristics. During a surge in the winter of 1936–1937, the terminus advanced 4.8 km in about 3 months (Post, 1960). There are two indications of the cyclic nature of surges visible on this RBV image. The large tributary glacier, informally known as "Lokit," entering from the south near the mid-point of the Black Rapids is forcing a medial moraine across the main glacier; two other similar moraine loops from the same tributary are displaced about 8 and 16 km downglacier. These displacements occurred during 1936–1937 and an earlier surge. Also, the terminal moraine that formed in 1936–1937 is clearly visible about 2 km from the Delta River; a terminal moraine, an additional 2 km downvalley, was from a previous surge, which probably temporarily blocked the Delta River. The medial moraine patterns can also be used as an indicator of how the surge cycle is progressing; in 1981, the "Lokit" moraine loop was pushed nearly as far across the Black Rapids Glacier as the 1936–1937 "Lokit" loop had been at the time of that surge. This evidence suggests that the surge cycle was near completion; however, through 2004, no new major surge had begun. It is unlikely that a near-future surge of the Black Rapids Glacier would disrupt the Trans-Alaska Pipeline or Richardson Highway, both of which follow the Delta River. There are many other surging glaciers in this area (notably the Susitna and Gakona Glaciers). Mass balance has been measured at the Gulkana Glacier since 1965. There is evidence of more extensive past glaciation in the form of a moraine area covered with small lakes extending far to the north. It is not known if this larger glacier complex was affected by surges. Landsat 3 RBV image (31273–20304–D; 8 August 1981; Path 71, Row 15) from the USGS, EROS Data Center, Sioux Falls, S. Dak. Landsat image and caption courtesy of Robert M. Krimmel, U.S. Geological Survey.*

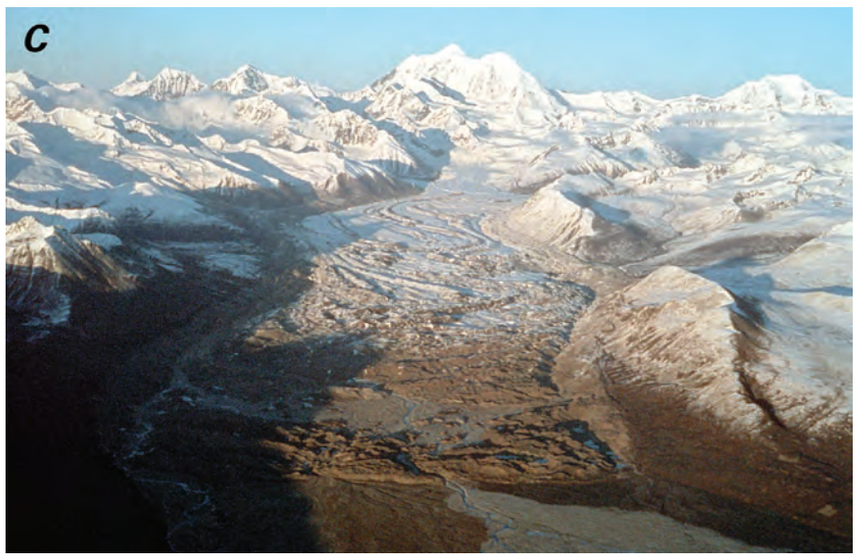

Figure 389.—*Three photographs of the debris-covered, stagnant terminus of Susitna Glacier (fig. 388).* **A**, *Pre-1915 northeast-looking photograph by F.H. Moffit of the hummocky, ablating terminus of Susitna Glacier. The presence of such a large number of thermokarst features suggests that its advanced state of stagnation began well before the start of the 20th century. Photograph Moffit 574 from the USGS Photo Library, Denver, Colo.* **B**, *August 1941 low-angle oblique aerial photograph of surge-contorted medial moraines on the surface of Susitna Glacier about 12 km above its stagnant terminus. Photograph (negative number 2804) by Bradford Washington, Museum of Science, Boston, Mass.* **C**, *Mid-1970s northeast-looking oblique aerial photograph of the debris-covered, stagnant terminus of Susitna Glacier. Folded loop moraines from a 1950s surge can be seen several kilometers above the terminus. The snow cover enhances the features. Mount Hayes is in the background. Photograph by Dennis C. Trabant, U.S. Geological Survey. A larger version of* A *is available online.*

Figure 390.—*14 September 1999 east-looking oblique aerial photograph of the terminus of an unnamed glacier that drains to the East Fork of the Susitna River. The western end of the lake corresponds to the 1955 position of the terminus. The large trimline suggests that the glacier has recently thinned significantly more than 50 m and retreated more than 2 km. Photograph by Bruce F. Molnia, U.S. Geological Survey.*

Figure 391.—*North-looking oblique aerial photograph of the terminus area of an unnamed rock glacier on the south side of Nenana Mountain on 14 September 1999. The rock glacier, which is more than 4 km long, heads in a cirque. Photograph by Bruce F. Molnia, U.S. Geological Survey. A larger version of this figure is available online.*

by the author); (17) an unnamed glacier approximately 8 km long (estimated by the author) draining into Broxson Gulch; (18) Augustana Glacier, which is about 6 km long (estimated by the author); and (19) Black Rapids Glacier (fig. 388) (40 km, 341 km^2).

Rock glaciers exist on many mountains, including Nenana Mountain (fig. 391). Some occur at the mouths of valleys that were glacier filled during the "Little Ice Age," whereas others are isolated bodies on the flanks of mountains and ridges.

As are the majority of glaciers in the Alaska Range, the glaciers in this area are stagnant, thinning, and (or) retreating. Aside from an occasional surge-produced thickening or advance, no glaciers below 2,000 m were observed to be either thickening or advancing. No late 20th or early 21st century surge events have resulted in terminus displacements.

Black Rapids Glacier

Between 1912 and 1936, Black Rapids Glacier retreated about 5 km. In 1936, the stagnation and retreat of Black Rapids Glacier were interrupted by a catastrophic surge that began in September or October (Moffit, 1942) and was the first to receive attention from the popular media. The 1 March 1937 issue of Time Magazine described the surge: "The Black Rapids Glacier, long dying in its valley 125 miles south of Fairbanks, has come to life. Its mile-and-a-quarter face was shoving toward the Delta River and the Richardson Highway (sole motor road from Fairbanks to the coast), rearing ice crests to 500 ft., breaking off great land icebergs which tumbled thunderously ahead onto the mossy valley floor" (Time Magazine, 1937). O.W. Geist, a geologist at the then Alaska Territorial School of Mines (now the University of Alaska Fairbanks), observed the surge and reported that "The glacier is bifurcated. One fork is moving into the other, grinding and crunching at a point five miles back. The intersection is the scene of a giant upheaval.... Three days ago we could walk to the face of the glacier. Now so much water is flowing that we could not walk to the front" (Time Magazine, 1937).

During a three-month period during the winter of 1936–37, Black Rapids Glacier advanced 4.8 km (Post, 1960). By February 1937, the glacier had reached a position that threatened the Richardson Highway adjacent to the Delta River. This location, fortunately, was close to the point of maximum advance. Retreat and downwasting began in the summer of 1937 and continues to the present. During the period of maximum surge, Black Rapids Glacier advanced as much as 30 to 65 m d^{-1}. Since then, the glacier has been stagnant, has become thinner, and has had several of its tributaries undergo

significant retreat, as an 18 August 1999 vertical aerial photograph shows (fig. 392). As a result of the surge, the media nicknamed Black Rapids Glacier "Galloping Glacier" and "Runaway Glacier."

Since 1971, the USGS and the University of Alaska Fairbanks (Heinrichs and others, 1995, 1996) have measured systematic mass balances,

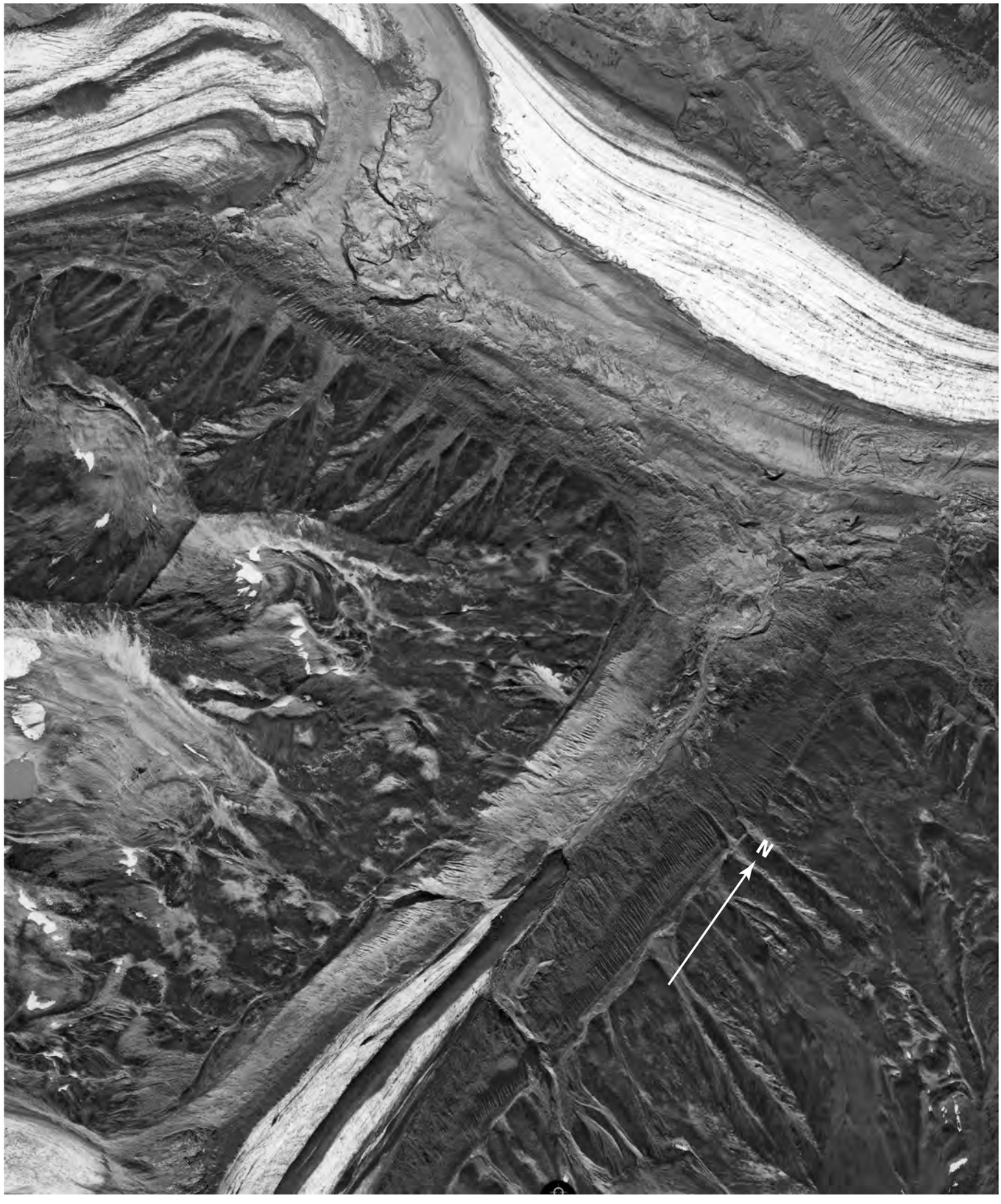

equilibrium line elevations (ELA), surface elevations, ice thicknesses, near-surface temperatures, and ice velocities. Heinrichs and others (1995) summarized the behavior of Black Rapids Glacier during a quiescent period from 1970 to 1992. Typically, they made semi-annual measurements of surface velocity, surface elevation, and mass balance at 10 sites along the centerline of the glacier. Their measurements show "synchronous interannual fluctuations" with a variability of about 20 percent and a period of 4 to 9 years. A winter-summer oscillation of about the same magnitude also exists. They also found large seasonal changes in surface speed of as much as 400 percent, caused primarily by changes in basal motion. During May through July 1993, the velocity of several surface markers along the glacier was measured twice daily; seismic-reflection measurements of the bed and ice-radar measurements were made daily. A subglacier stream originating at the terminus was monitored continually throughout the summer to investigate the glacier's basal hydrology. Measurements included stage, dye tracing, electrical conductivity, and turbidity. Acquiring the data simultaneously permitted direct measurement of changes at the bed that were correlated with changes in the velocity on the glacier's surface. Subglacier draining of several ice marginal lakes produced large increases in surface speed.

Raybus and Fatland (2000) compared SAR-interferometric techniques with conventional surface-velocity measurements to test whether the interferometric data are "quantitatively consistent with terrestrial velocity measurements." (p. 119). They compared velocities derived from two ERS–1 SAR images collected on 22 and 25 January 1992 with surface measurements made in 1987, 1990, and 1996 and concluded that the "interferometric and terrestrial datasets are mutually consistent." (Raybus and Fatland, 2000, p. 127).

Between the 1950s and the middle 1990s, on an annual basis, Black Rapids Glacier thickened by 0.343 m a^{-1}, and its volume increased by 0.099 km^3 a^{-1}. Much of this increase was in the form of replenishment in the accumulation area of the ice mass displaced during the 1936–37 surge. Between the middle 1990s and 1999, on an annual basis, Black Rapids Glacier thinned by 0.655 m a^{-1}, and its volume decreased by 0.189 km^3 a^{-1} (K.A. Echelmeyer, W.D. Harrison, V.B. Valentine, and S.I. Zirnheld, University of Alaska Fairbanks, written commun., March 2001).

Rock Avalanches onto Glaciers Resulting from the 3 November 2002 Earthquake (*M* 7.9) on the Denali Fault

A large-magnitude (*M* 7.9) earthquake on 3 November 2002 generated three large surface ruptures, which had a cumulative length of approximately 320 km. The largest was a 225-km-long rupture of the Denali Fault (fig. 393), which had a maximum right-lateral slip displacement of almost 9 m (Harp and others, 2003). The earthquake epicenter was located near an icefall in a tributary of West Fork Glacier. The westernmost surface rupture (first subevent of *M* 7.2) was a thrust fault that offset the surface of Susitna Glacier (fig. 389). Truffer and others (2002) presented a summary of the impact of the earthquake on glaciers within the Alaska Range. They reported that glaciers are located in many valleys aligned with the Denali Fault; consequently, more than 40 percent of the surface rupture resulting from the event can be seen on glaciers. Surface rupture was observed not only on Susitna Glacier but also on Black Rapids, Canwell, Gakona, and Chistochina Glaciers (fig. 388). In addition, offset glacier ice was observed near the terminus of West Fork Glacier where Susitna Glacier fault intersects it. Truffer and others (2002) reported that offsets in glacier ice have variable morphologies. Almost all seracs in the icefall toppled during the quake. The Denali Fault laterally offset preexisting crevasses on the northern side of Canwell Glacier, and vertical offset was observed at many localities. At some locations, one or more long linear cracks appeared along the glacier surface, often following medial moraines. Truffer and others (2002) suggested that

◀ ***Figure 392.*** *— 18 August 1999 black-and-white 1:24,000-scale vertical aerial photograph of the part of Black Rapids Glacier west of its terminus. The tributary entering from the south has retreated more than 2 km in the 44 years since it was mapped. The small unnamed glaciers have either completely disappeared or have retreated and lost contact with their main trunks. Photograph from U.S. Bureau of Land Management, roll 3, frame 322.*

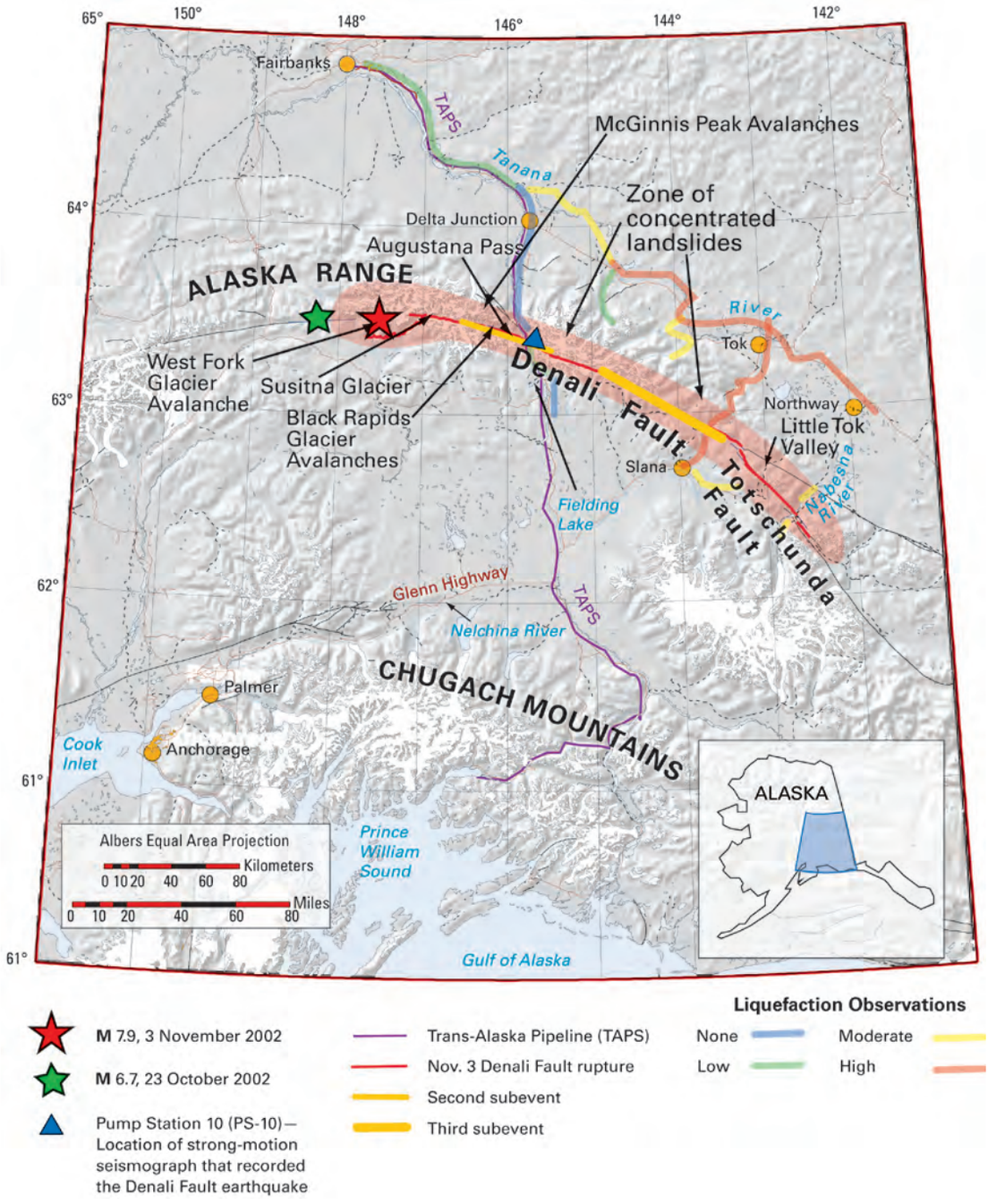

moraines represent areas of weakness. The Susitna Glacier fault appears to make a sharp turn to the west where it follows a looped moraine across the glacier. At some locations along the Denali Fault, cracks in the ice are oriented perpendicular to the fault trace. Their observations suggest that careful examination of glacier morphology must be considered when delineating the trace of a fault across a glacier.

The earthquake also produced thousands of rock avalanches, many of which covered parts of glaciers in the Alaska Range. Most of the rock avalanches were located in a zone approximately 30 km wide that straddled fault-rupture zones along the Totschunda and Denali Faults. McGinnis, Black Rapids, and West Fork Glaciers were affected by large rock avalanches, many of which consisted of a mixture of rock, snow, and glacier ice.

According to Harp and others (2003) the largest rock avalanche on McGinnis Glacier (fig. 394*A*) had a volume of greater than 30×10^6 m^3. They reported that two large rock avalanches originated at two different sites on the flanks of McGinnis Peak, the largest part resulting from the collapse of

Figure 393.—*Map showing mainshock, foreshock, zone of fault rupture, concentrated landslides, individual landslides on glaciers in the Alaska Range, and observations of liquefaction effects triggered by the Denali Fault earthquake of 3 November 2002. Modified from Harp and others (2003, fig. 1, p. 5).*

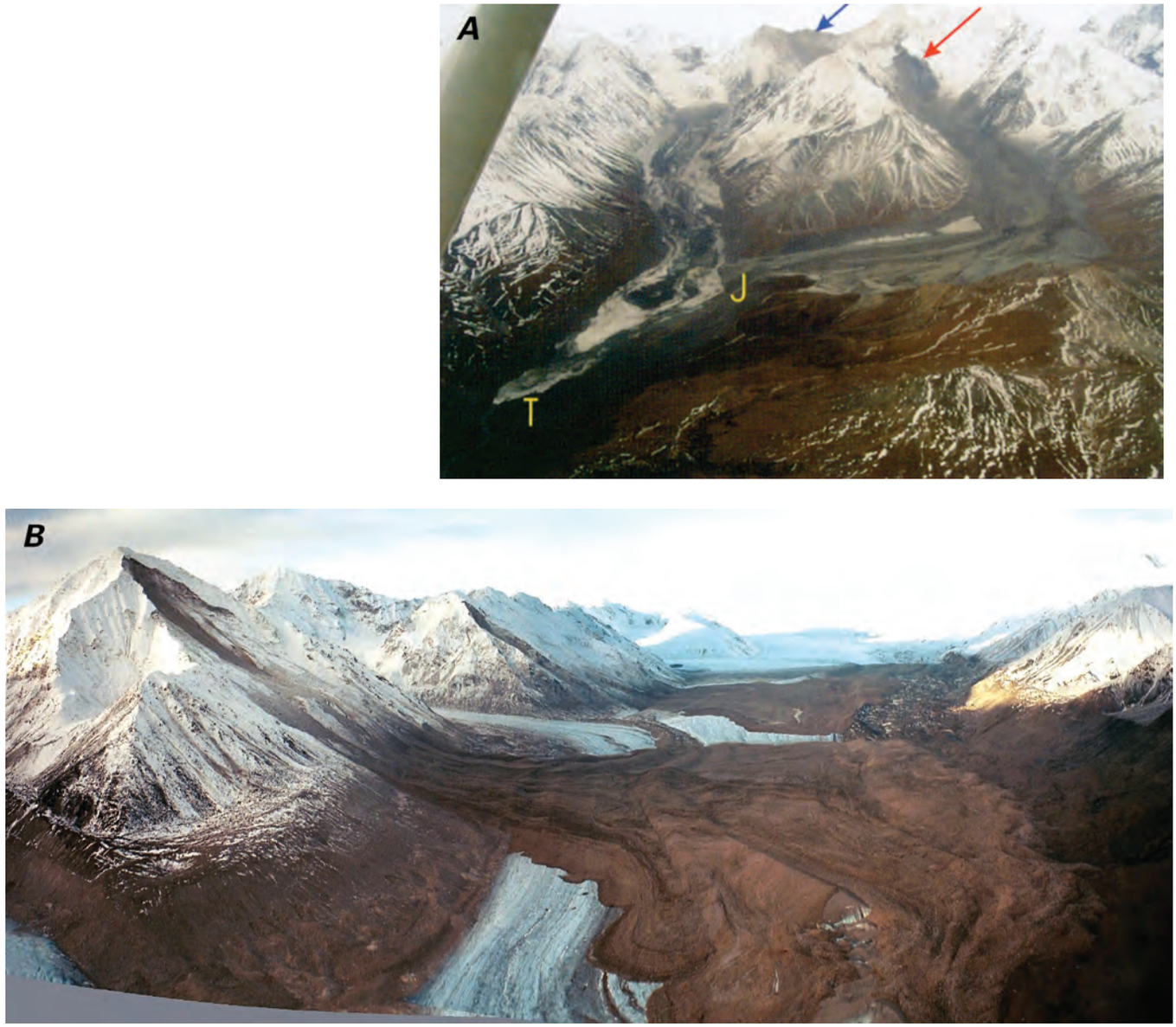

Figure 394.—**A**, *Oblique aerial photograph of landslides from McGinnis Peak onto McGinnis Glacier modified from Harp and others (2003, fig. 2, p. 6). Two huge rock avalanches originated from different flanks of McGinnis Peak. The rock avalanche to the right (red arrow denoting head scarp) is composed mainly of rock and is approximately 30 x 10^6 m^3 in volume. The runout path of the rock avalanche is approximately 10 km. The avalanche to the left (blue arrow denoting head scarp) has more ice and snow included within the avalanche debris. The landslides converged in the center part of the photo (J), and the avalanche on the left continued down to the toe of McGinnis Glacier (T).* **B**, *Oblique aerial photographic mosaic, taken on 7 November 2002, of multiple rock avalanches on Black Rapids Glacier. On 3 November 2002, a moment magnitude (M)7.9 earthquake occurred along the Denali Fault in central Alaska (fig. 393). It was the largest earthquake in the United States since 1987 and ties for the 9th largest earthquake in the United States in the last 100 years (comes from USGS list of top 10 largest earthquakes in the United States). The earthquake ruptured 225 km of the Denali Fault with measured offsets as much as 8 m. The fault is of interest to glaciologists because 130 km, or about half, of the rupture lies under glaciers. The fault rupture crosses the West Fork, Susitna, Black Rapids, Canwell, Gakona, and Chistochina Glaciers, and numerous smaller glaciers. In this oblique aerial photographic mosaic, the composite of three rockfall avalanches from the south wall of the Black Rapids Glacier can be seen blanketing about 13 km^2 of the ablation area or about 5 percent of the total glacier area. The blanketing effect of these rockfalls is expected to increase the glacier's mass balance by about +0.2 m a^{-1} by reducing the melting of glacier ice during subsequent summer melt periods. The Denali Fault underlies this reach of Black Rapids Glacier. The 3 November 2002 earthquake fractured the glacier surface from its confluence with the Susitna Glacier (upper center of the photo) to just below the bottom of the photo, along a 30-km-long path near the northern margin (right margin in this photo) of Black Rapids Glacier. Caption and photograph courtesy of Dennis C. Trabant and Rod S. March, U.S. Geological Survey.*

a 750-m-high rock wall. Debris flowed down each of the glacier's two major tributaries on relatively low-angle slopes before converging and flowing to the toe of the 10-km-long glacier.

Harp and others (2003) also reported that large rock avalanches occurred at Black Rapids Glacier (fig. 394*B*) when granite slopes on the southern side of the glacier failed. The three largest rock avalanches each had volumes of several million cubic meters of debris that together covered about 13 km^2 of the ablation area or about 5 percent of the total glacier area. Truffer and others (2002) suggested that the blanketing effect of the rock avalanches will increase the glacier's mass balance by about 0.2 m a^{-1} by insulating the ice from warm summer temperatures. The rock avalanches, which descended from elevations of several thousand meters, completely crossed the glaciers and flowed up the opposite valley walls, similar to the Shattered Peak rock avalanche, which flowed onto the Sherman Glacier during the March 1964 Great Alaskan earthquake (fig. 229). The rock-avalanche deposits were generally 2 to 3-m thick and relatively uniform in their distribution. Lateral margins of the flows were quite sharp. Harp and others (2003) described the rock-avalanche debris flowing up and over a 5 to 6-m-high medial moraine and blanketing it and the surrounding glacier with a uniform thickness.

Harp and others (2003) also described large rock avalanches that were triggered onto the surface of West Fork Glacier above a thrust fault that ruptured during the 2002 earthquake.

Metamorphic rock debris that fell from the valley walls encountered the adjacent medial moraine and became airborne before it landed on the surface of the glacier and fanned out. The largest rock block that they observed was more than 20 m on its largest side. The thickness of the deposit ranged from 3 to 15 m.

A large rock and ice fall also occurred on upper Gakona Glacier. Truffer and others (2002) postulated that this rock and ice fall will not affect the glacier's mass balance immediately because it was deposited onto its accumulation area. They concluded that these rock falls will be a readily visible surface feature for the next 200 to 400 years or more. Before the 3 November 2002 earthquake, large rock and ice-fall debris cover was not evident on the glaciers of the region, suggesting that an earthquake event of similar magnitude has not occurred in at least 200 years and perhaps longer.

Geospatial Inventory and Analysis of Glaciers: A Case Study for the Eastern Alaska Range

By William F. Manley[1]

Abstract

Recent advances in Geographic Information Systems (GIS) make it possible to assemble large empirical multiparameter datasets that provide important information on environmental variation, process, and change. Such a GIS-based application is presented here for glaciers in the eastern Alaska Range. Data sources include USGS Digital Line Graphic (DLG), Digital Raster Graphic (DRG), and Digital Elevation Model (DEM) files, which were derived from USGS topographic quadrangle maps representing glacier and landscape conditions from 1948 to 1954. Information from 10 USGS 1:63,360-scale topographic quadrangle maps was combined and processed in the GIS to summarize parameters and to analyze spatial relationships. The 279 glaciers shown on the 10 maps occupy a total area of 1,229 km^2. Data trends are dominated by a disproportionate decrease in the frequency distribution of glaciers by area.

[1] Institute of Arctic and Alpine Research (INSTAAR), University of Colorado Boulder, CO 80309-0450; william.manley@colorado.edu; 303-735-1300

A "typical" glacier in the region measures only 0.6 km^2 in area, is as wide as it is long, and occupies a basin only slightly larger than the glacier itself (for example, a cirque glacier). In contrast, the relatively few named or previously measured glaciers yield median values of 19.5 km^2 for area, 4.0 for the ratio of length to width, and 1.7 for the ratio of basin area to glacier area (large valley glaciers). Other parameters are not found to be strongly related to glacier area, including median elevation and the shape of hypsometric curves. The GIS layers of glacier extent form a comprehensive digital inventory revealing a range of morphologic relationships that quantitatively define feedbacks between glacier dynamics and mountainous terrain. The geospatial data are also useful for mapping and visualization, selection or analysis of "representative" glaciers, deriving or applying scaling relationships, modeling of ice dynamics and retreat, and as a decades-old baseline for comparison with recent airborne and satellite remote-sensing measurements. As a complement to field measurements, maps, geodetic airborne laser-altimetry, aerial photographs, and satellite imagery, the GIS approach takes advantage of spatial variation to better understand environmental controls on glacier distribution and geometry.

Introduction

Inventories of glaciers and glacier systems in Alaska and elsewhere are important in the assessment of water resources, glacier hazards, the response of glaciers to climate change, and, under negative mass-balance conditions, their excess meltwater contribution to sea-level rise (for example, Fountain and others, 1997; Kääb and others, 2002; Paul, 2003; Meier and Wahr, 2002; Meier and others, 2003). Recent studies have shown that Alaska's glaciers are undergoing pronounced thinning and retreat and that mass balances are consistently negative (Echelmeyer and others, 1996; Hodge and others, 1998; Arendt and others, 2002) as a result of historically unprecedented Arctic warming (cf. Serreze and others, 2000). However, less than 1 percent of Alaska's glaciers by area has been included in a global inventory (for example, the World Glacier Monitoring Service's World Glacier Inventory) (National Snow and Ice Data Center, 1999, 2003), and existing tabular databases are limited in their capability to spatially represent the three-dimensional context of glaciers within mountain environments.

This section provides a new approach to documenting and investigating glaciers by means of GIS. The study takes advantage of detailed and extensive aerial photographic interpretation and glacier mapping done by the USGS in the early 1950s. Goals of the study are to (1) develop, test, and apply a series of procedures to create a glacier atlas in the form of a geospatial database; (2) in addition to mapping and visualization, use spatial analysis to investigate geomorphic relationships resulting from the interplay of climate, topography, and ice dynamics; and (3) make a glacier inventory – and the specific GIS algorithms used to create it – available for further research. This study is part of a broader project using GIS to document and analyze glaciers, environments, and climate across the State of Alaska.

The study area, in the eastern Alaska Range, lies in the east-central interior of Alaska (fig. 395) and spans approximately 100 km from the Delta River valley on the west to Mentasta Pass on the east. The mountainous terrain and its glaciers are further described and illustrated in the section on the Mount Kimball-Mount Gakona Segment between Mentasa Pass and the Delta River. The region includes the relatively well studied Gulkana Glacier (cf. Mayo and Trabant, 1986; March and Trabant, 1996; Hodge and others, 1998). This "benchmark" glacier and the adjacent West Gulkana Glacier were included in recent studies of volumetric change determined from laser altimetry (Echelmeyer and others, 1996; Sapiano and others, 1998; Arendt and others, 2002). Glaciers in the area are not yet a part of the World Glacier Inventory (National Snow and Ice Data Center, 1999, 2003), but 19 of them were cataloged in a preliminary inventory by Denton and Field (1975a; see also

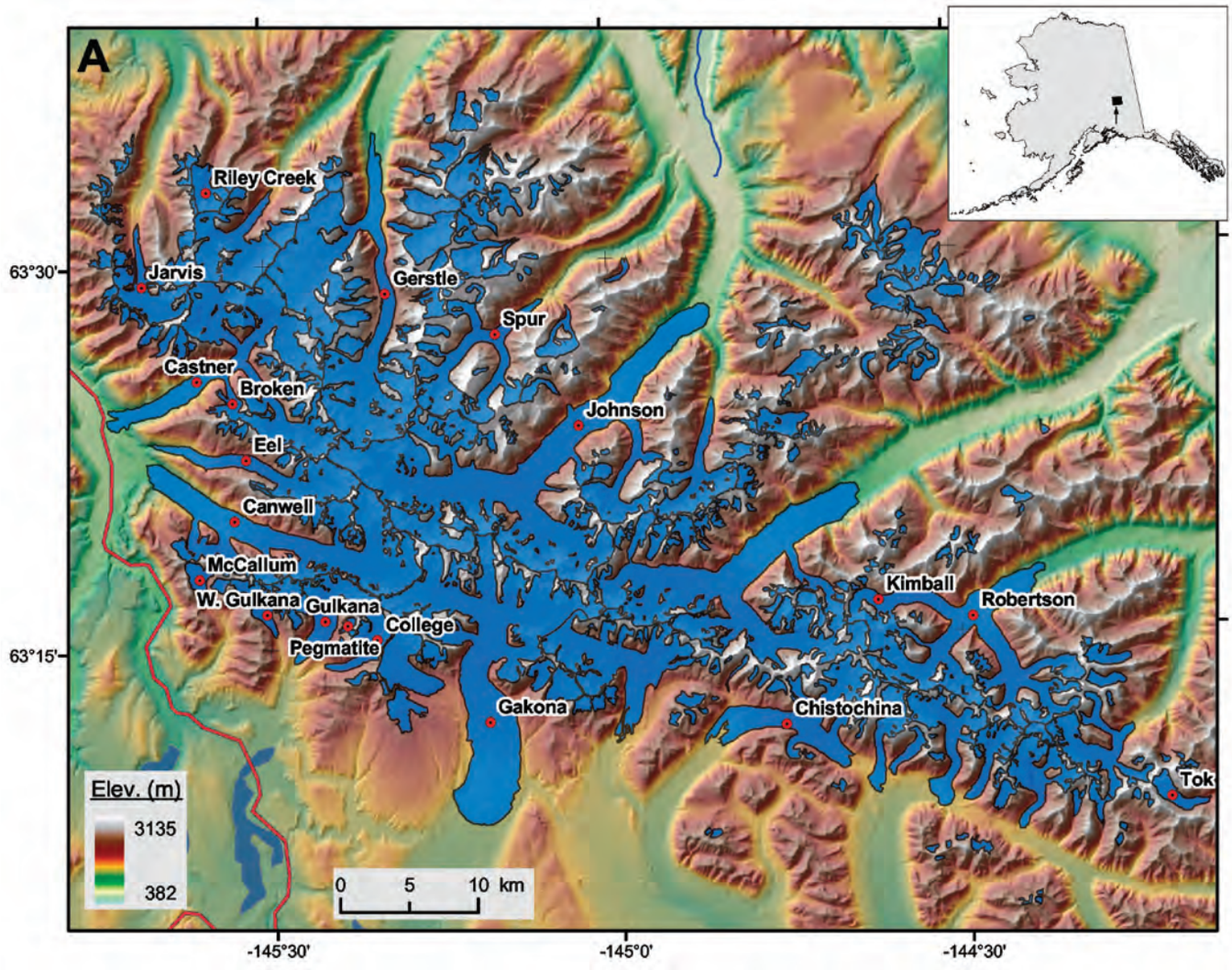

Field, 1958). The region has a continental climate, partially shielded from transport of moisture from the Gulf of Alaska by the Wrangell, Talkeetna, and Chugach Mountains, and the St. Elias Mountains to the south.

***Figure 395.**—Maps of glaciers and terrain in the eastern Alaska Range.* **A**, *Glacier polygons in the digital inventory are overlain on color-coded topography and shaded relief. Three small glaciers in the database, northeast of Tok Glacier, are not shown. Tick marks display the boundaries of 1:63,360-scale, 15-minute topographic maps for the area.* **B**, *The glacier polygons, representing the areal extent of glacier ice during 1948–1954, are shown as black lines over a GeoCover Landsat mosaic. This orthorectified false-color composite displays TM bands 7, 4, and 3 from imagery acquired in approximately 1990. Although glacier termini are obscured by debris-covered ice, the mosaic reveals in detail some evidence for thinning and ice-marginal retreat.*

Methods

Three types of data from the USGS were used as the foundation of this study (fig. 396). Hydrographic DLG files are vector representations of water features as digitized from the USGS 1:63,360-scale 15-minute topographic quadrangle maps that include polygons having "Minor1" values of 103 or 411 encode features, originally mapped as a "Glacier or permanent snowfield" (USGS, 1998a, b). DRG files are images scanned from the topographic quadrangle maps. The DEM used in this study was derived from the USGS National Elevation Dataset (NED) files, which were compiled from the 15-minute DEMs for Alaska, which, in turn, are based on contours, spot heights, and other terrain features on the topographic quadrangle maps. Thus, all three datasets used here were derived from the same source: 10 15-minute topographic quadrangle maps for the eastern Alaska Range (Mount Hayes A1-A3, B1-B4, and C2-C4). The maps were originally compiled by using stereophotogrammetric mapping technology and 1948–54 vertical aerial photographs acquired by the USAF for the AMS. Because the datasets share a common origin, they have the advantage of sharing the same spatial registration and temporal basis (for example, a maximum of 6 years from oldest to youngest aerial photographic coverage).

To process and analyze the GIS data, more than 90 individual "scripts" were written, tested, and applied, where each "script" is a stepwise semiautomated

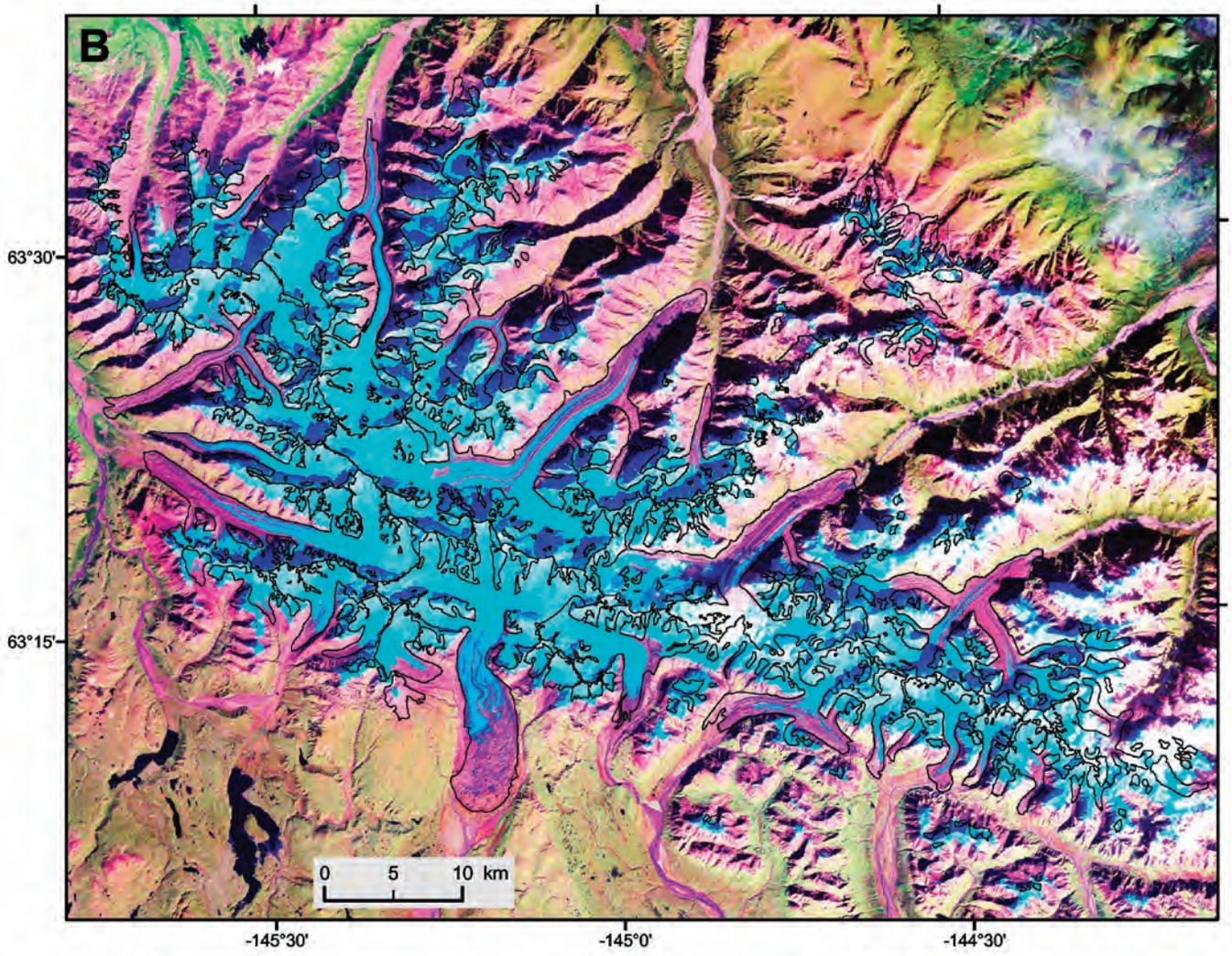

procedure that may include macros (prerecorded series of actions executed with a single command) or programming code for direct GIS processing. For example, five scripts were used to import the NED DEM, project it from an original map projection, datum, and resolution (Geographic NAD 27 with 2-arc-second spacing) to UTM zone 6 with 60-m spacing, and clip it (trim to eliminate data outside the study area). GIS processing was handled by ArcGIS Desktop (ArcInfo), as well as MFWorks, a simple raster program used for some of the final geometric calculations. Error assessment is presented in the next section.

Major processing steps (fig. 396) began with database preparation and quality editing. An extensive review of metadata was undertaken to assure that the three types of data sources were temporally compatible, all derived from the original 1950s topographic quadrangle maps, which are compiled from 1948–54 vertical aerial photographs. Ten DLG files were imported and projected to Universal Transverse Mercator (UTM). Glacier polygons were extracted and mosaicked to yield "unedited ice polygons." These features were compared directly with the DRG files (fig. 397*A*). In most cases, the unedited ice polygons very closely matched the glacier outlines as shown on the topographic quandrangle maps (within a 60-m grid-cell tolerance commensurate with the DEM). However, some of the ice polygons displayed digitization and other unexplainable errors that required intensive manual editing. Thus, "edited ice polygons" were created that more closely depict the complex glaciers and contiguous ice masses in the study area, as the topographic quadrangle maps show.

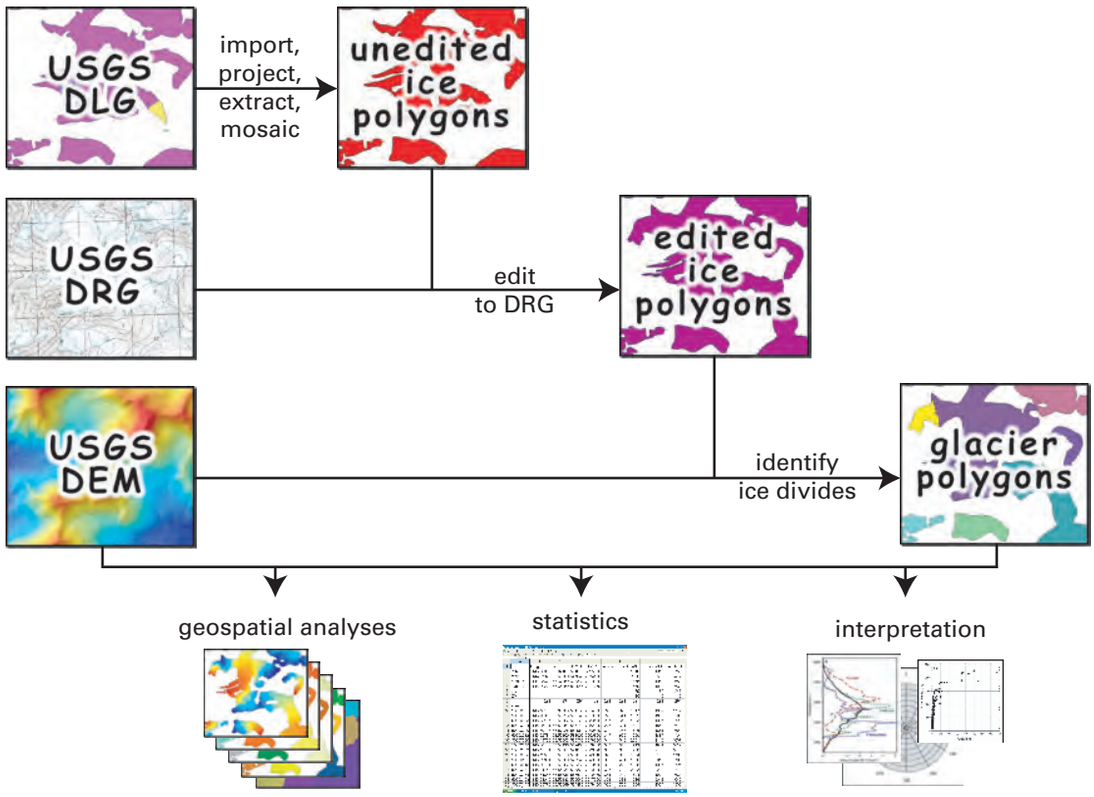

Figure 396.—*Flow diagram for processing of the original cartographic source material to create and analyze the glacier spatial database. DLG, Digital Line Graph; DRG, Digital Raster Graphic; DEM, Digital Elevation Model. See text for additional details.*

The next major step addresses the fundamental "geospatial definition" of a glacier. The ice masses shown on topographic maps are rarely simple, isolated cirque or separate valley glaciers. They commonly are complex features joined at drainage divides from which separate glacier ice bodies flow downslope. To "cut" the "ice polygons" into "glacier polygons" along ice divides, an algorithm was developed that takes advantage of watershed functions in ArcInfo. This script identifies glacier "toes" as parts of each ice polygon that lie below the median elevation of the polygon and uses the toes as "pour points" for the watershed function. The resulting, often contiguous glacier polygons (fig. 397) then can be analyzed separately. Automated processing avoids subjective and time-intensive manual editing. A byproduct is a GIS layer of separate glacier basins, each enclosing a glacier and the upslope area that sheds snow or meltwater onto its surface.

Finally, a variety of raster commands were used to measure a variety of parameters for each glacier on the basis of the glacier outlines and the coregistered DEM (table 7). This approach builds upon that of Allen (1998) (see also Paul and others, 2002; Paul, 2003) and relies on zonal functions acting on each glacier's 60×60-m grid cells. The DEM has sufficient resolution for this task: 26 grid cells for the smallest glacier, a median glacier area of 160 grid cells, and more than 42,000 grid cells for the largest glacier.

Parameters were measured for the purposes of compiling a digital inventory as well as for geospatial and glaciologic analysis. Location is described by the **latitude** and **longitude** of the centroid grid cell. The GIS readily calculates **minimum**, **maximum**, **median**, and **average elevation** as well as the **range in elevation** for each glacier. Basic geometric parameters for each glacier include **area**, **perimeter**, average **slope angle**, and average **aspect** (following directional statistics presented by Davis, 1986). **Compactness**, a nondimensional measure of shape, was calculated as 4π multiplied by area, divided by perimeter squared (cf. Davis, 1986; Allen, 1998). This parameter varies from 0.0 for infinitely narrow or convoluted shapes to 1.0 for a circle. Glacier **length** is difficult to quantify objectively with an automated script owing to the constraints imposed by raster processing but was estimated

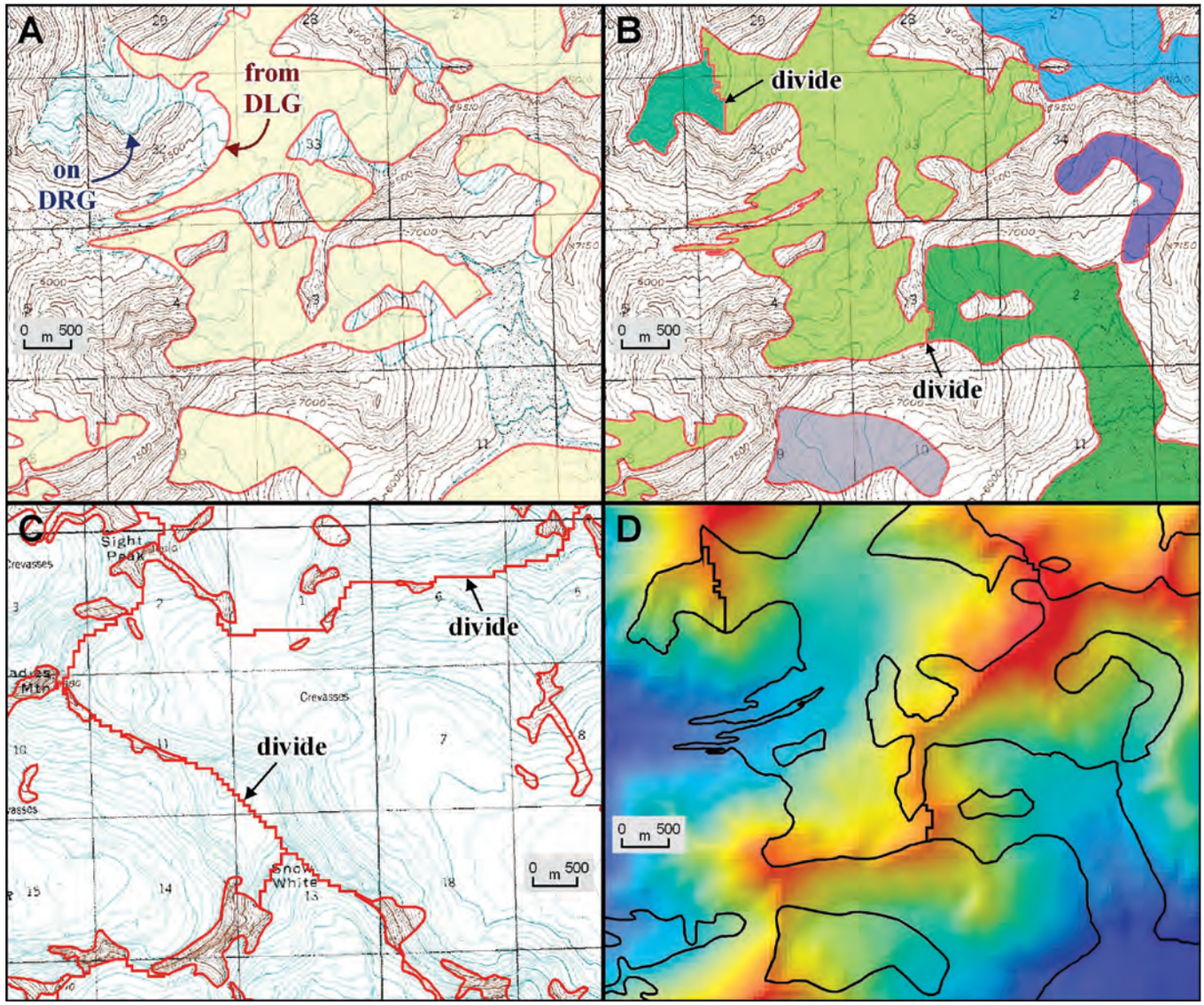

Figure 397.—*Close-ups of selected GIS processing steps and results.* **A**, *Close-up of DLG polygons shown over the DRG for a small area northeast of Gerstle Glacier. Glacier extents in the DLG files did not everywhere match those depicted on the DRGs owing to digitization and other errors.* **B**, *The glacier features were edited to agree with the DRGs, and the "ice polygons" were cut along automatically identified drainage divides to form separate "glacier polygons."* **C**, *Example of ice divides at the upper limits of the Johnson, Canwell, Fels, and Gerstle Glaciers. The jagged nature of ice divides is inherited from the processing of 60-m DEM grid cells.* **D**, *Glacier polygons as black outlines over the DEM for the area shown in* A *and* B.

as the longest flowline using a downhill FLOWLENGTH command. Glacier **width** is similarly difficult to process consistently as a human would measure and is simply calculated here as area divided by length, yielding also the **length/width ratio** as a second metric for shape. The **basin coefficient** is defined as **basin area** divided by glacier area, a relative measure of the upslope area available for avalanching and snowdrift onto the glacier surface. A few other parameters, including backwall height, were estimated as part of a broader study related to estimated ELAs but are not presented here.

The spatial variables extracted from the GIS for each glacier are based on all 60×60-m cells that make up the glacier. Thus, mean elevation is the true mean, not simply the average of minimum and maximum elevations. Similarly, slope angle is averaged across the entire glacier, not simply derived from elevation range and length. As an aside, calculation of average aspect for each glacier involves circular statistics to avoid the problems resulting from geometric means of azimuthal data.

Also, with each glacier's surface geometry represented in the GIS, it is possible to quantify **area-altitude distribution**. A script was developed that determines the cumulative area for each glacier grid cell as the percent of that glacier's area lying above the elevation of that grid cell. The area-altitude grid can then be used to plot hypsometric curves related to mass balance for individual glaciers or entire ranges.

TABLE 7. *Results of the spatial analysis of 279 glaciers in the eastern Alaska Range.*[1]

	Longitude DD	Latitude DD	Minimum Elevation (m)	Maximum Elevation (m)	Median Elevation (m)	Average Elevation (m)	Elevation Range (m)	Area (km^2)	Perimeter (km)	Compact-ness	Aspect (degrees)	Slope (degrees)	Length (km)	Width (km)	Length/ width ratio	Basin area (km^2)	Basin coefficient
All glaciers																	
Minimum			756	1424	1237	1216	90	0.09	1.6	0.01	0	8	0.1	0.2	0.1	0.13	1.0
Maximum			2472	3135	2599	2590	2276	154.52	360.5	0.65	359	37	34.4	6.1	11.1	277.92	8.2
Median							459	0.57	5.4	0.26			0.7	0.8	1.0	1.12	1.8
Average			1638	2241	1910	1913					6	18					
Sum								1229									
Selected glaciers																	
Minimum			756	1826	1518	1630	411	0.89	7	0.01	5	8	1.0	0.9	1.2	1.62	1.1
Maximum			1549	3135	2091	2040	2276	154.52	360	0.35	325	20	34.4	6.1	11.1	277.92	2.4
Median							1606	19.45	64	0.06			9.9	2.3	4.0	38.83	1.7
Average			1117	2681	1790	1785						13					
Sum								950									
Canwell	-145.45884	63.32222	808	2721	1639	1630	1913	70.76	176.9	0.03	307	10	24.4	2.9	8.4	117.03	1.7
Castner / Broken	-145.52845	63.43713	766	2935	1818	1758	2169	70.58	208.2	0.02	260	13	20.8	3.4	6.1	114.57	1.6
Chistochina	-144.72919	63.20041	1139	2974	1518	1666	1835	35.09	108.1	0.04	214	9	11.0	3.2	3.5	72.46	2.1
College	-145.35955	63.25648	1257	2420	1754	1729	1163	8.54	31.6	0.11	214	11	6.8	1.3	5.4	15.67	1.8
Eel / Fels	-145.47815	63.36497	863	2718	1865	1803	1855	21.52	65.9	0.06	278	12	15.4	1.4	11.1	43.76	2.0
Gakona	-145.18597	63.24145	1059	2944	1644	1642	1885	108.72	203.4	0.03	184	8	17.9	6.1	2.9	155.16	1.4
Gerstle	-145.32490	63.46235	821	2993	2091	2040	2172	86.84	204.2	0.03	41	12	23.4	3.7	6.3	136.33	1.6
Gulkana	-145.42431	63.27445	1141	2431	1834	1786	1290	19.45	60.7	0.07	182	10	8.5	2.3	3.7	27.38	1.4
Jarvis	-145.66714	63.48103	1283	2794	1763	1792	1511	14.76	64.1	0.05	325	13	9.3	1.6	5.9	23.85	1.6
Johnson	-145.13283	63.36141	756	2963	1758	1766	2207	154.52	360.5	0.01	36	11	34.4	4.5	7.7	277.92	1.8
McCallum	-145.60371	63.29947	1415	1826	1670	1649	411	3.14	10.7	0.35	146	10	2.3	1.4	1.7	5.05	1.6
Pegmatite	-145.38774	63.26542	1549	2008	1783	1777	459	0.89	7.3	0.21	265	17	1.0	0.9	1.2	1.62	1.8
Riley Creek	-145.58049	63.55183	1540	2483	2023	2013	943	6.01	17.8	0.24	35	20	2.7	2.3	1.2	6.46	1.1
Robertson / Kimball	-144.51903	63.24377	912	3135	1664	1731	2223	72.41	219.1	0.02	28	12	17.0	4.3	4.0	158.60	2.2
Spur	-145.22050	63.43740	1105	2928	1958	1999	1823	29.12	110.5	0.03	42	15	13.0	2.2	5.8	70.86	2.4
Tok	-144.20409	63.13876	1401	2206	1788	1800	805	4.27	15.1	0.23	105	10	4.7	0.9	5.1	9.10	2.1
W. Gulkana	-145.51717	63.28298	1296	2435	1723	1734	1139	6.34	25.4	0.12	178	15	3.7	1.7	2.2	9.33	1.5
AL-6308/14424	-144.39882	63.15864	1161	2767	1857	1845	1606	15.36	57.7	0.06	197	14	4.4	3.5	1.3	25.86	1.7
AL-6310.5/14417	-144.31543	63.17109	1135	2768	1750	1764	1633	18.35	73.7	0.04	70	14	6.8	2.7	2.5	33.16	1.8
AL-6310/14431	-144.53144	63.18256	1117	2603	1755	1722	1486	16.27	55.7	0.07	193	13	9.9	1.6	6.1	39.39	2.4
AL-6310/14437.5	-144.61454	63.18722	1111	2648	2031	1861	1537	9.13	31.1	0.12	200	12	5.8	1.6	3.7	13.87	1.5
AL-6313-14459	-145.00096	63.23897	1161	2612	1685	1698	1451	38.83	118.9	0.03	157	9	12.2	3.2	3.8	52.95	1.4
AL-6317/14450	-144.81841	63.28315	850	3126	1586	1630	2276	100.14	262.6	0.02	31	11	24.7	4.0	6.1	185.73	1.9
AL-6322/14453	-144.87769	63.35569	1073	2867	1850	1846	1794	16.37	56.9	0.06	5	17	10.4	1.6	6.6	38.83	2.4
AL-6331.5/14532	-145.54385	63.51268	1215	2720	1950	1939	1505	23.07	60.6	0.08	27	16	8.8	2.6	3.3	32.53	1.4

[1] Median values shown in summary sections at top for parameters that are not normally distributed. Named glaciers (below) include those identified by Denton and Field (1975) with alphanumeric codes.

Error Analysis

A thorough analysis of error is difficult to accomplish because of the lack of independent, detailed measurements related to these glaciers for the time period of acquisition of the aerial photographs (1948–54) used for map compilation. Some of the potential sources of error are not significant. Changes in glacier area over the 6-year span of aerial photography are probably negligible, and photographs for 8 of the 10 quadrangle maps were taken during the same year (1954). Co-registration errors among the DEM, DLGs, and DRGs are also negligible. Most of the GIS processing to estimate glacier parameters (such as **area**, **elevation**, and **aspect**) adds negligent numerical error due to GIS processing alone. More important are errors associated with the source data.

The primary elevation datasets (the 15-minute DEMs) are probably a source of error. USGS national map-accuracy standards (USGS, 1998b) state that root mean square errors (RMSEs) for Level 2 DEMs are less than one half of the contour interval [15 m (50 ft) or 30 m (100 ft) for these quadrangles; for example, RMSE < 15 m]. The average vertical RMSE for the 10 topographic quadrangle maps used in this analysis, as reported in DEM metadata and based on 300 geodetic control points, is 3.6 m. However, other glacier studies utilizing 15-minute DEMs (Aðalgeirsdóttir and others, 1998; Arendt and others, 2002) have documented vertical errors of about 45 m (standard deviation of random error with negligible systematic offset) for upper accumulation areas on glaciers. The lack of contrast on vertical aerial photographs of snow-covered glaciers precludes the use of stereophotogrammetric plotters to determine accurate surface-elevation data (for example, a "floating" white dot in the plotters cannot be accurately positioned on a "white" surface by the photogrammetrist). All elevations of the snow-covered areas of glaciers (accumulation area) depicted on topographic maps are unreliable. This error affects calculation of average elevation and — to a lesser extent — of median elevation. It probably also adds error to the identification of ice divides.

For the glacier polygons, this study relies on the original USGS mapping by cartographers during the late 1940s and early 1950s, among which were included (as best as can be determined) glaciologists specifically tasked with glacier delineation. The original USAF vertical aerial photographs acquired for the AMS are generally of high quality. By definition, the polygons include "permanent snowfields," although polygons less than 0.1 km^2 (a commonly accepted lower limit for glaciers) were excluded from analysis. A related conceptual "error" reflects how to quantitatively and objectively define a glacier (see "Methods" and "Discussion"). But the greatest source of uncertainty for this study is probably associated with the subjective nature of glacier mapping by cartographers from stereoscopic pairs of vertical aerial photographs — a process that is not exactly reproducible because of variation in the skills of the cartographers.

In general, the possible errors are random rather than systematic in nature. On the basis of the discussion above, the glacier-elevation measurements (**min**., **max**., **median**, and **average elevations** and **elevation range**) are probably accurate within approximately 50 m. The error for glacier area is roughly 5 percent for small glaciers and approaches about 1 percent for large glaciers. Derived parameters such as average slope angle and aspect probably carry a very small uncertainty, with the exception of length and width, which are difficult to objectively measure in automated fashion, and may vary about 15 percent from how a glaciologist would manually measure such values on a map. Errors for any single glacier or grid cell may be significant but are minimized with mean or median calculations for individual glaciers and for relationships among glaciers with a large sample size (n=279).

It is instructive to compare this GIS analysis with previously published information for Gulkana Glacier. The GIS analyses are based on the USGS-

mapped extent as interpreted from aerial photographs taken in 1954 (most of the glacier) and 1949 (the lower kilometer). The geospatial results include an area of 19.45 km^2, a length of 8.5 km, a minimum elevation of 1,141 m, and an average slope angle of 10°. These values compare with (1) an estimate of area (18.5 km^2) using the same maps (Echelmeyer and others, 1996); (2) estimates of length (8 km), terminus elevation (1,180 m), and slope angle (7°) based on a 1993 geodetic airborne laser altimeter profiling survey (Echelmeyer and others, 1996); (3) a description of area (19.3 km^2) and length (8.5 km) by Hodge and others (1998); and (4) a listing of area (20 km^2) that apparently used the same maps (Arendt and others, 2002). The GIS results appear comparable, and other methodologies may carry uncertainties in detail.

Another "test" is a comparison with previously published data for 19 glaciers (fig. 398). Denton and Field (1975a) presented a summary of glaciers in the area, based on the USGS 1955 1:250,000-scale topographic quadrangle map for Mount Hayes. The Mount Hayes map was compiled by the AMS from USAF aerial photographs acquired between 1948 and 1955, using the same source materials that were used for the 10 15-minute topographic quadrangle maps used in the GIS analyses of glaciers. Their estimates of area and length are thus associated with a smaller scale Level 1 (equivalent in DEM terms to a 90-m grid cell) data source and manual map measurements. Discrepancies for area are minor, probably related to the smaller scale mapping. Discrepancies for length are more significant and probably reflect differences between manual and GIS-based approaches (see "Methods" section). In general, the regressions – only for the largest glaciers in this region – affirm the reliability of the geospatial approach.

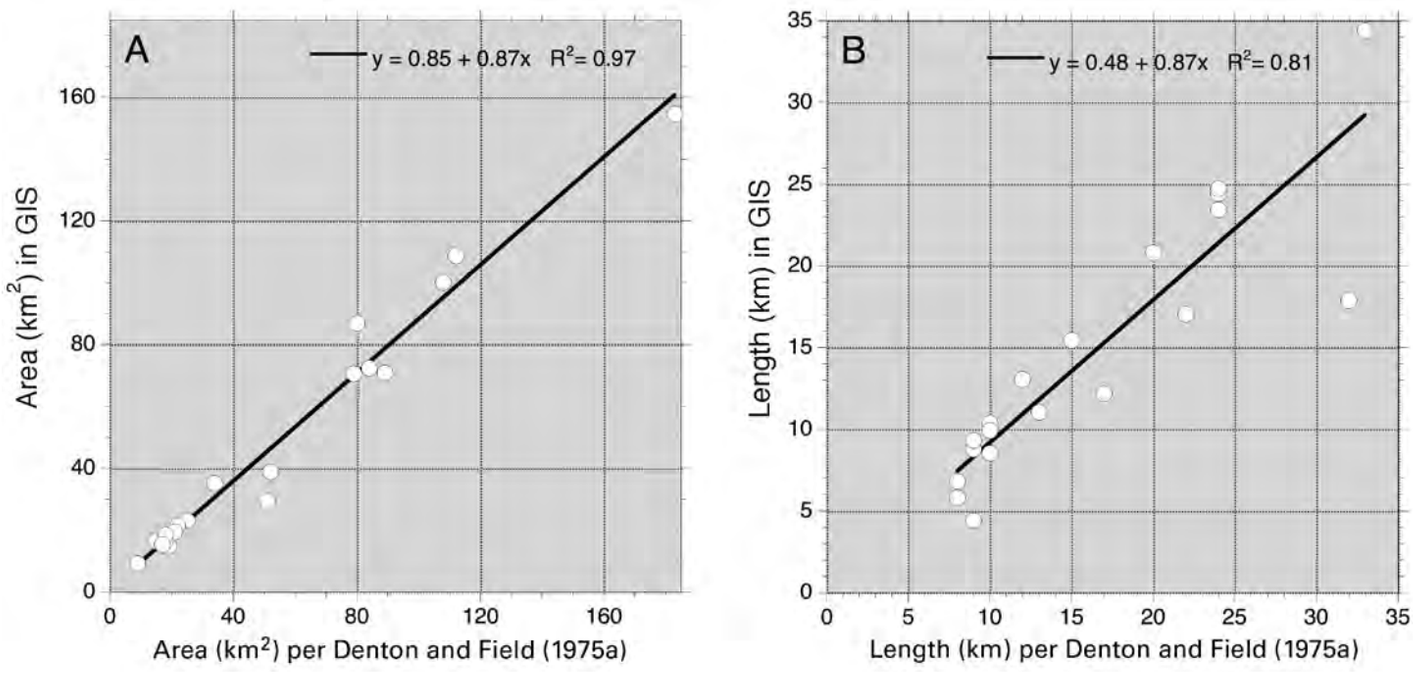

***Figure 398.**—Comparison of GIS results for* **A** *(area) and* **B** *(length) with the 19-glacier inventory of Denton and Field (1975a).*

Results

The geospatial analysis yields details for 279 glaciers thus identified for the eastern Alaska Range. Summary statistics are given in table 1 for all glacier polygons, along with summary results and individual measurements for the 19 previously measured or named glaciers. Selected parameters are shown in map form in figure 399. Relationships among glacier parameters were also explored through correlation analysis. Log-normal transformations were applied to elevation range, area, perimeter, length, width, length/width ratio, basin area, and basin coefficient.

The cirque, valley, and complex mountain glaciers range in size from 0.1 km^2 (the minimum threshold for inclusion in the GIS processing) to 154.5 km^2 (Johnson Glacier); the average area is 4.4 km^2, and the median area is 0.6 km^2. Total glacier area is 1,229 km^2. The total comprises about 8 percent of the glacierized area of the entire Alaska Range and less than 2 percent of the glacier area for the entire State (Post and Meier, 1980) but more than twice the area of glaciers in the lower 48 States (about 513 km^2, cf. Meier, 1961; about 580 km^2, Krimmel, 2002). The largest glaciers flow from the central divide of the range; smaller glaciers are clustered around nunataks, on ridges standing above valley glaciers and their tributary glaciers, and on isolated massifs mainly north of the range divide (fig. 399*A*). Taken as a whole, the glacierized area extends from a minimum elevation of 756 m at the toe of Johnson Glacier to a maximum of 3,135 m at the upper limit of Robertson Glacier.

The results for the calculation of glacier area, illustrated in figures 399*A* and 400, highlight a dominant trend: small glaciers are much more common than large ones. The frequency distribution by area is similar in form to the combined exponential and power relationships noted for other detailed regional inventories (including the Brooks Range) and as applied through geometrical scaling to a global scale (Meier and Bahr, 1996; Bahr, 1997; Bahr and Meier, 2000). It is not surprising, therefore, that the number of small glaciers is disproportionately higher than the number of large ones. The results here document a systematic area-scaling relationship empirically for a relatively small region. The results also exemplify the ability of semiautomated GIS analysis to comprehensively examine relationships among all glaciers in a region, including small glaciers that are not commonly inventoried or studied.

Some of the fundamental parameters of glacier geometry are not strongly related to glacier area. For example, glacier aspect varies throughout the cardinal directions of the compass. North-facing glaciers are concentrated on the northern side of the range (fig. 399*B*), and there is a weak but marginally preferred aspect of 6° ($p = 0.10$, with a mean resultant vector length of 0.09) (Davis, 1986). However, aspect is not significantly related to glacier area (fig. 401) *(*$r = 0.06$; $p = 0.29$). [Editors' note: r is a correlation coefficient where 1 indicates perfect correlation between variables and 0 indicates no correlation; p is a probability ranking where higher values show higher relation between variables.] Median glacier elevation ranges from 1,237 m (a north-facing cirque glacier 11 km north-northeast of Robertson Glacier) to 2,599 m (for a small southwest-facing glacier 9 km east of Johnson Glacier); the average for the region is 1,910 m. Higher values exist for the northern and western glacierized areas of the region (fig. 399*C*), with a trend surface dipping 10.9 m km^{-1} at an azimuth of 186°; RMSE = 134 m; $r^2 = 0.46$; $p < 0.0001$. The median elevation of glaciers may be closely related to the regional long-term ELA (cf. Braithwaite and Müller, 1980). However, for this region, median elevation is not convincingly related to glacier area ($r = -0.12$; $p = 0.05$). A closely related parameter, average glacier elevation, exhibits similar spatial and statistical relationships.

A few geometric parameters are significantly but weakly related to glacier area. Slope angles range from 8° (for Gulkana Glacier) to 37° (for a small

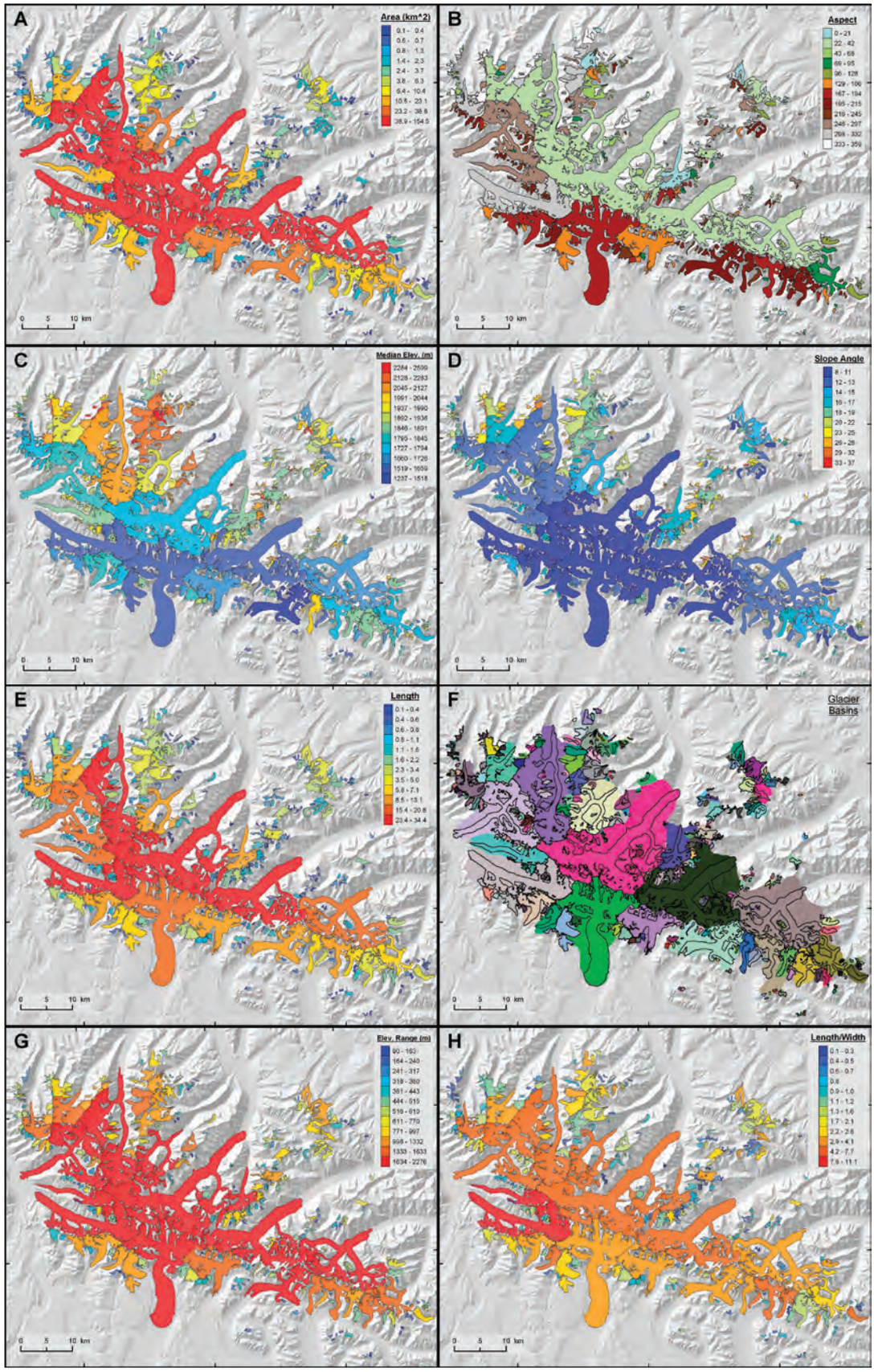

Figure 399.—*Shaded-relief maps of the glaciers color-coded for selected GIS results:* **A**, *area;* **B**, *aspect;* **C**, *median elevation;* **D**, *slope angle;* **E**, *length;* **F**, *glacier basins randomly colored;* **G**, *elevation range; and* **H**, *length-to-width ratio.*

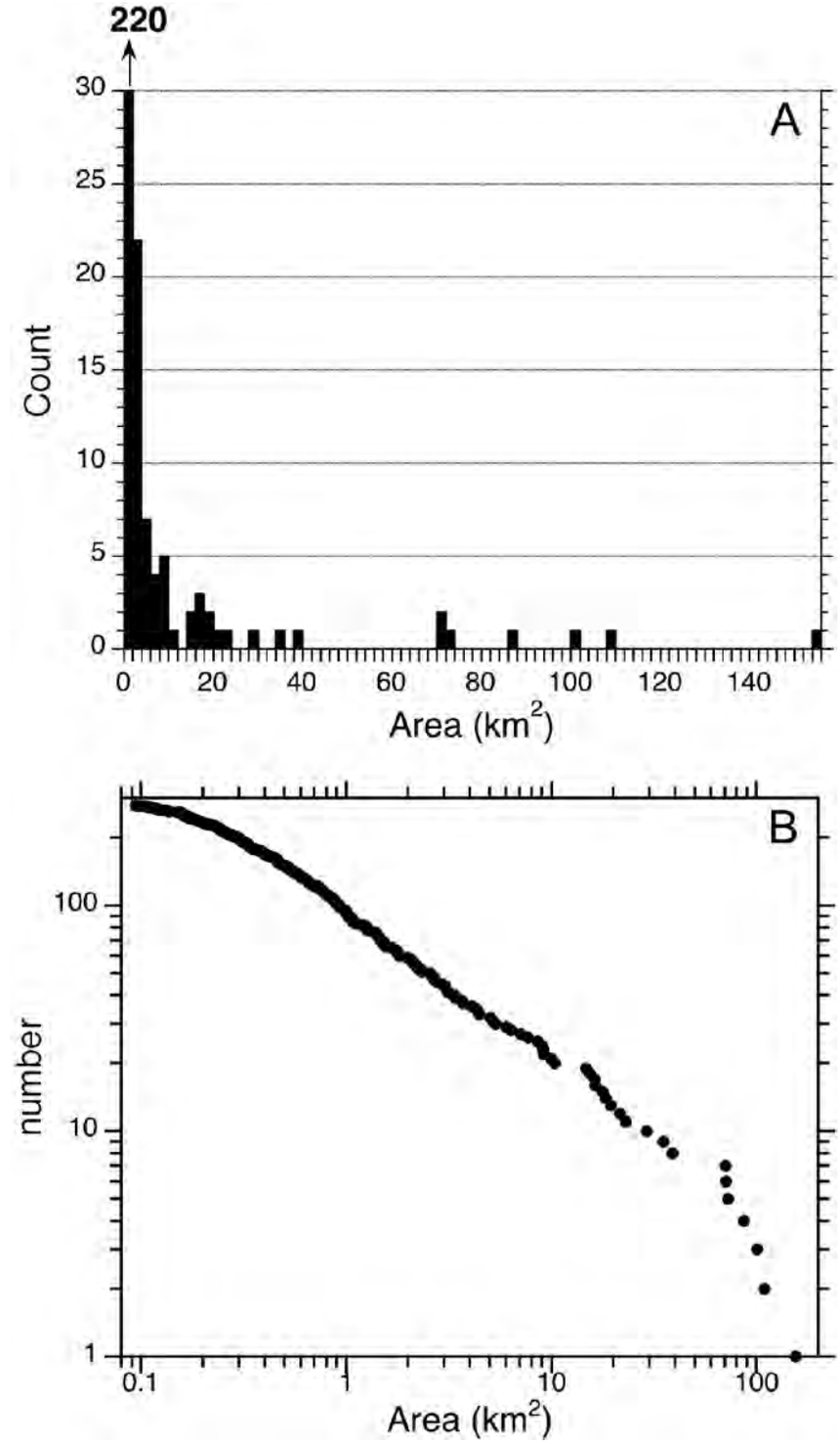

Figure 400.—*Frequency distribution of glaciers by area.* **A**, *Shown as a histogram. The leftmost column extends beyond the Y-axis limit of the graph.* **B**, *Log-log plot of cumulative number of glaciers greater than a given area. Compare with Meier and Bahr (1996) and Bahr (1997).*

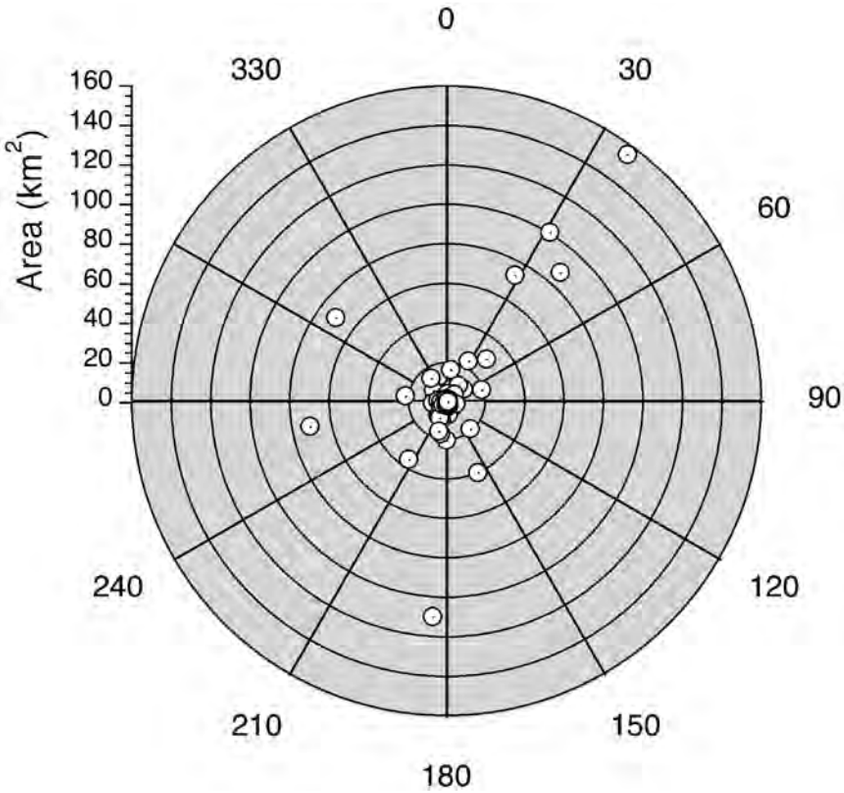

Figure 401.—*Polar diagram of glacier area versus aspect. Most glaciers fall close to the central origin, with the largest glaciers facing northeast, south, and west.*

glacier 8 km west of Kimball Glacier); the regional average is 18° (fig. 399*D*). Not surprisingly, the smallest glaciers tend to have steep surfaces (fig. 402*A*). However, correlation with area is weak ($r = -0.40$; $p < 0.0001$). Similarly, the basin coefficient varies from 1.0 (for example, the glacier completely occupies its basin) to 8.2 (for example, the basin is eight times larger than the glacier area); the median value is 1.8. This proportional metric is highest for small glaciers (fig. 402*B*), but correlation with area is weak ($r = -0.26$; $p < 0.0001$). To summarize, many of the glaciers are typical cirque glaciers that have steep surfaces and are bounded by ice-free headwall areas, whereas large valley glaciers typically have low slopes and relatively small ice-free catchments. However, not all of the glaciers analyzed fall within this spectrum.

Other morphologic parameters are strongly related to glacier area. Not surprisingly, strong relationships exist between area and length (figs. 399*E*, 402*C*) ($r = 0.96$), width ($r = 0.85$), perimeter ($r = 0.98$), and basin area (cf. fig. 399*F*) ($r = 0.96$). Larger glaciers tend to have a greater range in elevation from head to toe (figs. 399*G*, 402*D*) ($r = 0.85$). They also tend to be more elongate, having high length-to-width ratios (fig. 399*H*) ($r = 0.66$), whereas smaller glaciers are more circular in shape (for example, compactness) ($r = 0.66$). These parameters strongly express, in a quantitative sense, a range in morphology normally described qualitatively – from niche and cirque glaciers to simple valley glaciers or those with numerous tributaries and compound accumulation basins. They similarly characterize morphologic changes for alpine glaciers as they advance and retreat in mountainous terrain.

Another parameter relates strongly to area. Only the largest glaciers in the region have been studied previously. Glaciers given names on the USGS topographic quadrangle maps and included in the inventory by Denton and Field (1975a) comprise only 7 percent of the glaciers in the eastern Alaska Range. Not surprisingly, these 19 glaciers have morphologies that differ greatly from the "typical" values for the range (table 7). For example, they are much larger (19.5 km^2 versus 0.6 km^2), longer (9.9 km versus 0.7 km), and elongate (length-width ratio of 4.0 versus 1.0) and have a greater range in elevation (1,606 m as opposed to 459 m), than could be considered "representative"

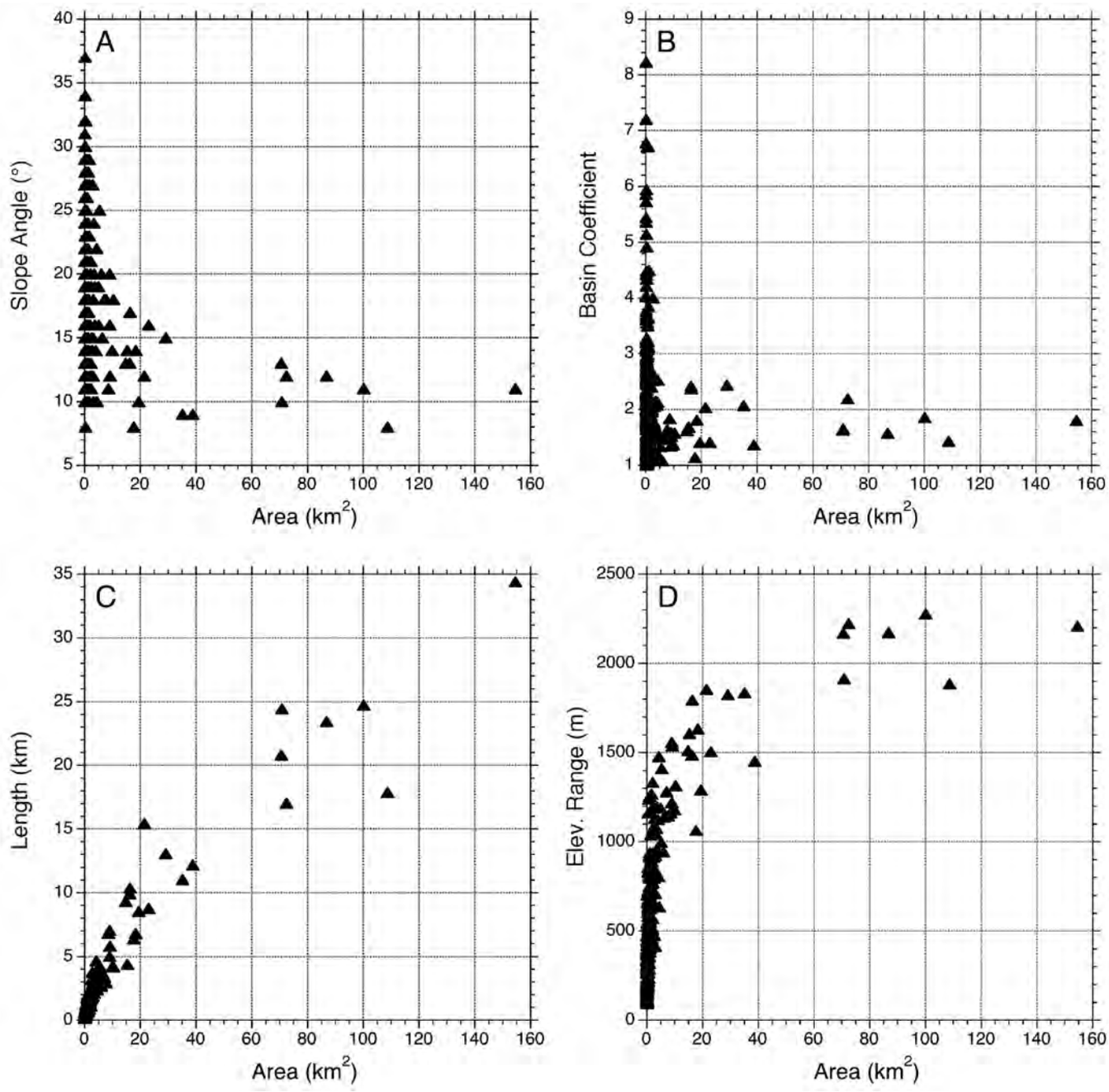

***Figure 402.**—Plots of four geospatial measurements versus glacier area.* **A**, *Slope angle;* **B**, *basin coefficient;* **C**, *length; and* **D**, *elevation range.*

(see "Discussion"). Conversely, the 19 glaciers together cover 950 km² or 77 percent of the total glacierized area in the region.

Finally, the area-altitude distribution, or hypsometry, can be plotted and evaluated for selected glaciers and for the region as a whole (fig. 403). Glacier ice integrated across the range displays a normal distribution with elevation and yields a characteristic sigmoidal curve when plotted as cumulative area versus elevation (cf. Arendt and others, 2002). Some glaciers show skewed concentrations of surface area in their higher (for example, Gerstle Glacier) or lower (for example, Chistochina and Gakona Glaciers) reaches. Others such as Gulkana Glacier, do not fully encompass the vertical range of ice in the region but display bell-shaped distributions that mirror the distribution for the range as a whole. Still others yield normal distributions that are shifted above (for example, Riley Creek Glacier) or below the regional curve. Together with climate and flow dynamics, glacier hypsometry is closely linked to mass balance.

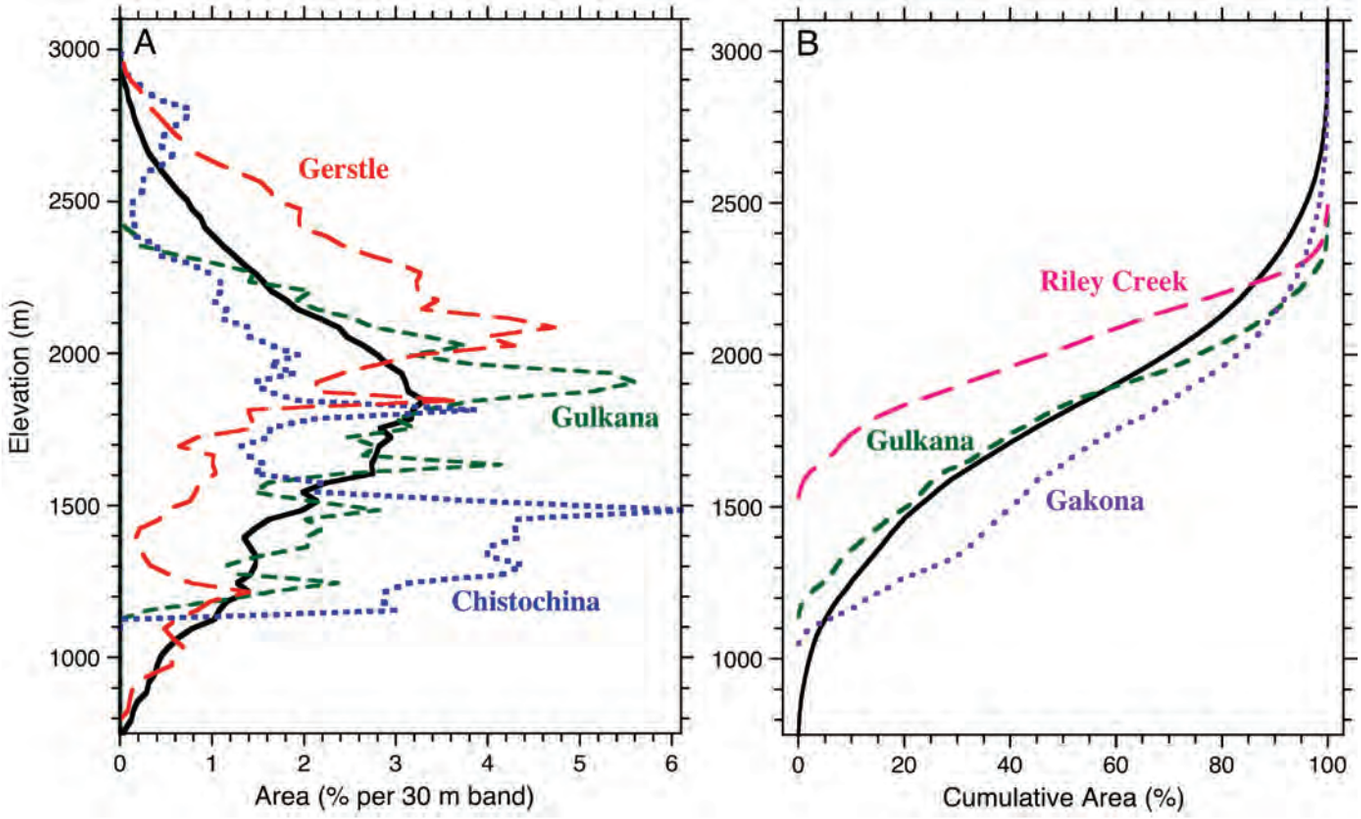

Figure 403.—*Area-altitude distribution integrated for all glacier ice in the region (black lines) compared with curves for selected glaciers.* **A**, *Plotted as percent area per 30-m elevation band.* **B**, *Cumulative area, in percent, versus elevation.*

Discussion

Presented here is a new digital inventory of glaciers in the eastern Alaska Range as they existed during the 1948–54 period. Nineteen glaciers were previously detailed by area, length, width, and other parameters (Denton and Field, 1975a). None of the glaciers are currently in the World Glacier Inventory (National Snow and Ice Data Center, 1999, 2003). The region includes Gulkana Glacier, a well-studied "benchmark" glacier (cf. Echelmeyer and others, 1996; Hodge and others, 1998; Molnia, this volume). The geospatial database of glacier extent builds upon extensive mapping and GIS layers produced by the USGS. A total of 279 glaciers (only 19 have formal names) cover an area of 1,229 km^2. Beyond mapping and visualization, the advantages of using GIS to study these glaciers include the capability of investigating all of the glaciers in the region, statistically analyzing glaciological properties, and sharing the digital inventory for other uses.

Quantitative geospatial analysis is a relatively new approach to studying glacier systems. Studies to date include objective glacier classification, digital inventory, and analysis of change (for example, Allen, 1998; Paul and others, 2002; Kääb and others, 2002; Ommanney, 2002b; Paul, 2003). The technique used here relies on spatial rather than temporal variability. As such, it is complementary to time-series studies of glacier change based on field measurements and (or) remote sensing (cf. Arendt and others, 2002; Paul, 2002, 2003), which are commonly limited to only a limited number of "selected" glaciers in any given glacierized region.

This study takes advantage of a large, comprehensive, empirical dataset. Created from glacier extents shown on 1:63,360-scale USGS topographic quadrangle maps, the spatial dataset includes all glaciers in the eastern Alaska Range at moderately high resolution, including very small ones. The glacier polygons include debris-covered areas, which are problematic for automated processing of satellite imagery. Measurement error for individual glaciers may be higher than that which exists with intensive manual editing. However, semiautomated GIS processing yields a large sample size that reveals coherent patterns among morphologic parameters.

Most of the 15 parameters of glacier morphology are strongly linked to a prominent trend: large glaciers are much less common than small ones. The area of the largest glacier measures 154 km^2, whereas the median glacier area is only 0.6 km^2. Glaciers ranging from 0.1 to 1.0 km^2 in size account for 6 percent of the glaciers by area and 67 percent by number. Properties that are correlated with glacier area yield average or median values that are characteristic of small cirque or niche glaciers: the "typical" glacier is almost as long (0.7 km) as it is wide (0.8 km), occupies a small basin (1.1 km^2), slopes 18° on average, and spans 460 m in elevation. Glaciers in the region have only a weak statistical preference to form north-facing surfaces. The glaciers commonly have "normal" bell-shaped distributions of area versus elevation.

Geospatial data help to address the question "Is Gulkana Glacier generally 'representative' of all the glaciers in the region?" In other words, are studies to date on this "benchmark" glacier regionally significant (cf. Echelmeyer and others, 1996; Hodge and others, 1998)? On the one hand, Gulkana Glacier is much larger, longer, wider, elongate, and more gently sloped than the typical glacier and has a greater elevation range and basin size. However, other metrics imply that Gulkana Glacier is indeed "representative" in terms of mass balance. Its median and mean elevations are close to "typical"; more importantly, its elevational distribution (hypsometric curve) is closely similar to that for glacier ice integrated across the region as a whole. At any rate, the issue depends largely on the specific question at hand, and the digital inventory can help to identify additional glaciers for study that are — in various ways — "representative."

As geospatial analysis of glaciers becomes more common, it will be important to reduce redundant effort and to assure comparability among datasets. In this regard, the digital inventory is available as an attributed vector GIS layer from the Quaternary GIS Laboratory at the Institute of Arctic and Alpine Research (INSTARR), University of Colorado [http://instaar.colorado.edu/QGISL/]. The stepwise algorithms are also available and can be applied to other glacierized regions. Among other methodologic issues, the "scripts" help address a fundamental concern: an objective, quantitative, geospatial definition of a "glacier." The definition is inherently linked to how drainage areas and ice divides are identified. Similarly, parameters such as length and width are dependent in detail on the chosen analytical approach. Hopefully a community consensus or protocol for standardized geospatial processing will emerge, perhaps as part of the Global Land Ice Measurements from Space (GLIMS) Program (Keiffer and others, 2000; Bishop and others, 2004) or as presented in the important Ph.D. dissertation by Paul (2003). The digital inventory is valuable for other studies. Though limited in extent, the database would assist in the regional analysis of the following glacier parameters: (1) derivation of, or application of, scaling relationships to estimate such quantities as thickness, volume, activity index, response times, and so on; (2) analysis and modeling of mass balance, ELAs, and local to regional controls on glacier-climate relationships; (3) analysis and modeling of glacier hazards, meltwater runoff, and contribution to sea-level rise; and (4) studies of glacier change as a decades-old baseline for comparison with recent satellite imagery and other remotely sensed measurements of glacier response to climate change.

Acknowledgments

Extensive GIS editing and processing were done by Denise Dundon and Evan Burgess (University of Colorado). Thanks also go to Mark F. Meier and Mark B. Dyurgerov (University of Colorado) for guidance and discussions. Most important, this study would not have been possible without the considerable efforts and skills of USGS cartographers and earth scientists involved in the compilation and publication of the topographic quadrangle maps and derived GIS layers.

The Mount McKinley-Mount Foraker Segment between Broad Pass and Rainy Pass

The Mount McKinley-Mount Foraker segment, which is about 275 km long and almost 80 km wide, contains the highest mountain in North America, Mount McKinley (6,195 m) (Brooks, 1911). Two views of this segment and its glaciers are presented (figs. 404, 405). Although it is officially named Mount McKinley (fig. 406), this mountain is popularly called *Denali*, meaning the *Great* or *High One* in the Athapaskan language. Other high peaks in this region include Mount Foraker (5,303 m), the third highest summit in Alaska; Mount Hunter (4,443 m); Mount Brooks (3,640 m); and Mount Russell (3,558 m). This segment also includes the Kichatna Mountains.

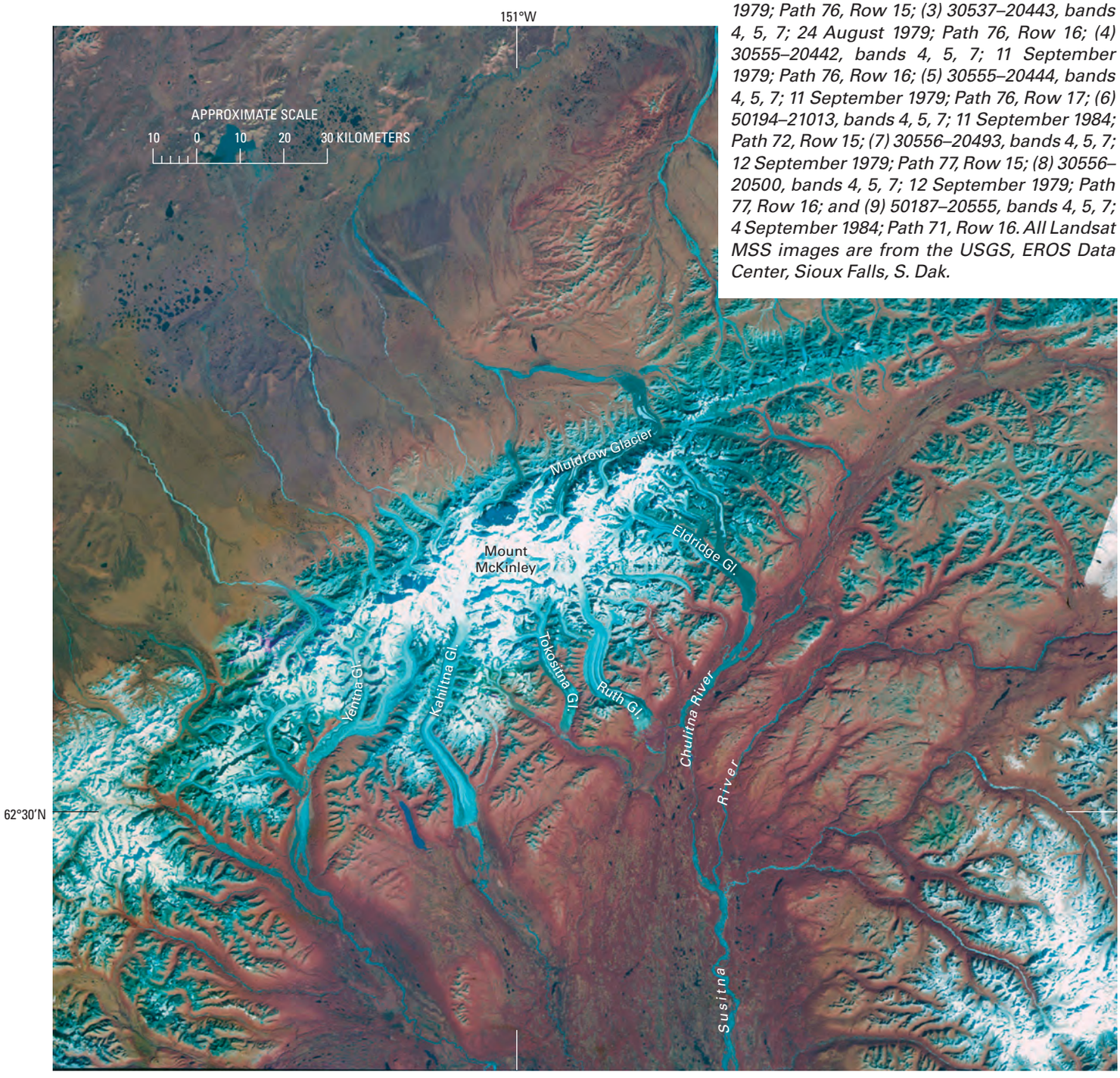

Figure 404.—*Landsat 3 and 5 MSS false-color infrared composite image mosaic of Mount McKinley area and environs, Alaska Range, Alaska, used for the 1:250,000-scale, experimental satellite image map of Denali National Park and Preserve, Alaska, published by the USGS in 1984. Numerous glaciers are visible on the flanks of the massif. Yentna Glacier (center) shows contorted medial moraines characteristic of a surging glacier. Reddish hues represent various types of vegetation. The following 9 Landsat 3 and 5 MSS images were used to compile the mosaic: (1) 30914–20281, bands 4, 5, 7; 4 September 1980; Path 75, Row 16; (2) 30537–20441, bands 4, 5, 7; 24 August 1979; Path 76, Row 15; (3) 30537–20443, bands 4, 5, 7; 24 August 1979; Path 76, Row 16; (4) 30555–20442, bands 4, 5, 7; 11 September 1979; Path 76, Row 16; (5) 30555–20444, bands 4, 5, 7; 11 September 1979; Path 76, Row 17; (6) 50194–21013, bands 4, 5, 7; 11 September 1984; Path 72, Row 15; (7) 30556–20493, bands 4, 5, 7; 12 September 1979; Path 77, Row 15; (8) 30556–20500, bands 4, 5, 7; 12 September 1979; Path 77, Row 16; and (9) 50187–20555, bands 4, 5, 7; 4 September 1984; Path 71, Row 16. All Landsat MSS images are from the USGS, EROS Data Center, Sioux Falls, S. Dak.*

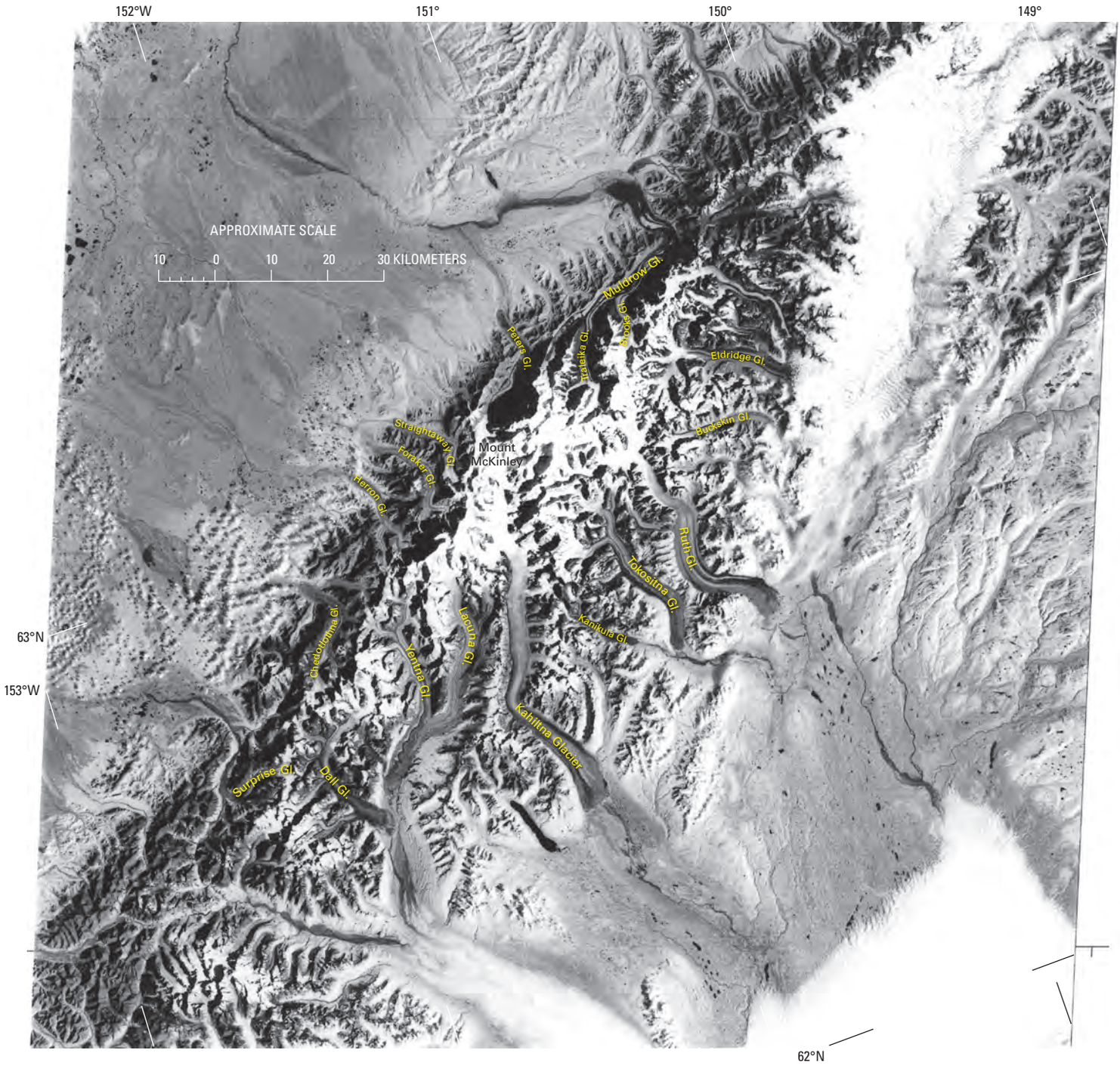

Figure 405.—*Annotated Landsat 1 MSS image of Mount McKinley and Denali National Park and Preserve. Mount McKinley (6,195 m) supports numerous large glaciers. Many of the glaciers on the northwest side of the McKinley massif surge, including the Straightaway, Peters, and Muldrow Glaciers. Muldrow Glacier had a strong surge that began in the winter of 1956–1957. During the course of the surge, which lasted less than 1 year, the terminus advanced 6.6 km, and surface levels dropped up to 100 m in the upper glacier area and increased 200 m in the lower glacier (Post, 1960). The contorted medial moraines of the Muldrow Glacier can be clearly seen on this image. Peters Glacier had a strong surge in 1986. The large glaciers on the south side of the massif — the Kahiltna, Ruth, and Eldridge Glaciers — do not show evidence of surging. The Tokositna Glacier surged in 1971–72 and in 2002–02. Landsat 1 MSS image (5865–19312, band 7; 31 August 1977; Path 77, Row 16) from the USGS, EROS Data Center, Sioux Falls, S. Dak. Landsat image and caption courtesy of Robert M. Krimmel, U.S. Geological Survey.*


A

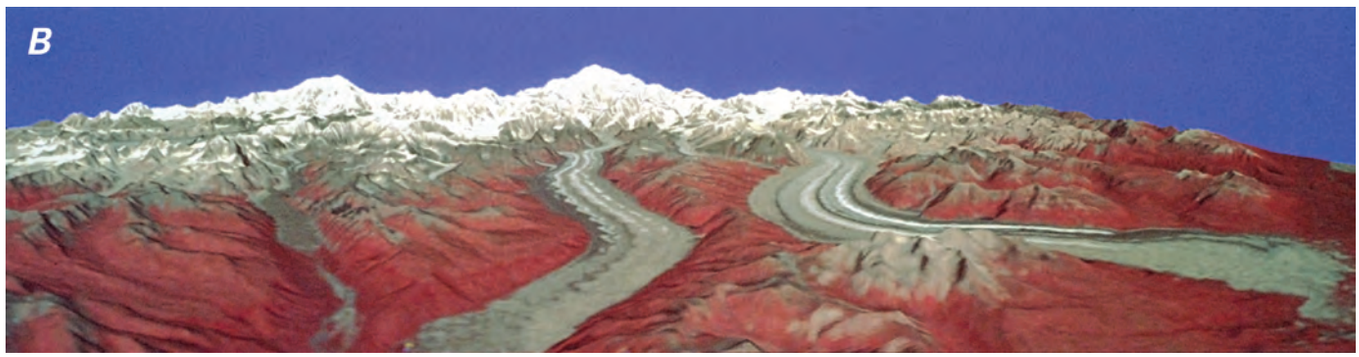
B


C

Figure 406.—*Three views of Mount McKinley.* **A**, *1923 photograph by Blanchard of Mount McKinley from the north side of the hummocky stagnant ice terminus of Muldrow Glacier. Photograph Alaska 100 from the USGS Photo Library, Denver, Colo.* **B**, *A computer-generated north-looking view of the central Alaska Range including Mount McKinley and Mount Foraker produced by combining part of the Landsat image mosaic used in figure 404 with corresponding digital elevation data. The point of view is located about 4,500 m above the Tokositna River. From east to west, key foreground features are: Ruth Glacier, the Tokosha Mountains, Tokositna Glacier, and Kanikula Glacier. Produced by the USGS, EROS Data Center, Sioux Falls, S. Dak., courtesy of the author.* **C**, *Oblique aerial photograph taken in October 1965 looking towards the summit of Mount McKinley across the snow-covered upper part of the Traleika Glacier (including its West Fork) a major tributary of the Muldrow Glacier. U.S. Air Force Cambridge Research Laboratories photograph taken by T/Sgt. Roland E. Hudson, courtesy of Richard S. Williams, Jr., U.S. Geological Survey.*

More than 20 glaciers with lengths of greater than 8 km descend from many isolated peaks to the east and a broad interconnected accumulation area to the west. The unnamed ice field is more than 115 km in length. Six glaciers have lengths of greater than 40 km. From east to west, in a counter-clockwise direction, these are (according to lengths and areas measured by Denton and Field, 1975a, p. 588–590 and p. 593 from USGS maps): Muldrow Glacier (fig. 407) (61 km, 516 $km^{2)}$; Yentna Glacier (51 km, 487 km^2); Kahiltna Glacier (76 km, 580 km^2); Tokositna Glacier (fig. 408) (44 km, 240 km^2); Ruth Glacier (63 km, 449 km^2); and Eldridge Glacier (48 km, 485 km^2). Many of the glaciers in this segment surge, including Tokositna, Lacuna, Yentna, Straightaway, Peters, and Muldrow Glaciers. These glaciers and many others show multiple evidence of surging. Tokositna, Lacuna, and Yentna Glaciers have large looped and folded moraines (Meier, 1976) that result from long periods of near stagnation alternating with brief periods of extremely high surge flow.

Beginning on the northern side of the unnamed ice field, moving counter-clockwise from east to west, the major glaciers are listed with approximate lengths and approximate areas measured by Denton and Field (1975a, p. 588–593) from USGS maps: (1) an unnamed glacier draining to the East Fork Toklat River; (2) Polychrome Glacier; (3) an unnamed glacier draining to the Toklat River (8 km, 15 km^2), which, on an annual basis between the middle 1950s and the middle 1990s, thinned by 1.82 m a^{-1} and decreased in volume by 0.016 km^3 a^{-1} (K.A. Echelmeyer, W.D. Harrison, V.B. Valentine, and S.I. Zirnheld, University of Alaska Fairbanks, written commun. March 2001); (4) Sunset Glacier (9 km, 9 km^2); (5) Muldrow Glacier (61 km, 516 km^2); (6) Peters Glacier (27 km, 123 km^2), which surged in 1986; (7) an unnamed glacier draining into Slippery Creek (8 km, 11 km^2); (8) Straightaway Glacier (fig. 409) (22 km, 71 km^2); (9) Foraker Glacier (fig. 410) (25 km, 74 km^2); (10) Herron Glacier (25 km, 79 km^2); (11) an unnamed glacier draining into Swift Fork (8 km, 27 km^2); (12) Chedotlothna Glacier (see 1925 Capps photograph, USGS Photo Library photograph Capps 1103) (27 km, 97 km^2); (13) an unnamed glacier draining into Ripsnorter Creek (7 km, 8 km^2); (14) Surprise Glacier (15 km, 47 km^2), which has retreated more than 2 km since 1958, opening an ice-marginal lake adjacent to

Figure 407.—*13 September 1986 oblique aerial photograph of Muldrow Glacier, the largest glacier on the north side of Mount McKinley; it had a major surge from 1956 to 1957. The aerial photograph shows only the middle part of the glacier; the lower glacier extends another 15 to 20 km beyond the photograph to the right. The large, arcuate moraine loop in the foreground was displaced to its present position from in front of the major left tributary in the middle of the photograph by the 1957 surge (Post, 1960). Presumably, the foreground loop will be displaced downglacier and replaced by the loop now forming in front of the major left tributary during the next surge. Photograph no. 86–R3–182 and caption courtesy of Robert M. Krimmel, U.S. Geological Survey.*

Figure 408.—*Oblique aerial photograph of Tokositna Glacier on 30 August 1984; the glacier is located on the south side of Mount McKinley and has frequent minor surges. This view, looking down the glacier, shows well the characteristic contorted medial moraines of surging glaciers. These features on the Tokositna Glacier are barely large enough to be seen on the Landsat MSS image mosaic (fig. 404) and image (fig. 405). Photograph no. 84–R2–248, 30 August 1984, by Robert M. Krimmel, U.S. Geological Survey.*

▲ ***Figure 409.***—*14 September 1999 north-looking oblique aerial photograph of the terminus area of Straightaway Glacier showing its hummocky, debris-covered surface and the development of thermokarst features. A vegetation-covered lateral moraine has developed on the east side of the glacier. Photograph by Bruce F. Molnia, U.S. Geological Survey. A larger version of this figure is available online.*

◄ ***Figure 410.***—*14 September 1999 northwest-looking oblique aerial photograph of the terminus area of Foraker Glacier showing its hummocky, debris-covered surface and the development of thermokarst features. Of all the large glaciers observed in 1999 flowing out of the Alaska Range, Foraker Glacier appeared to have experienced the greatest amount of recent thinning and retreat, thinning by as much as 75 m. Photograph by Bruce F. Molnia, U.S. Geological Survey.*

its terminus; (15) an unnamed glacier draining from Mount Dall (16 km, 55 km^2); (16) Dall Glacier (36 km, 243 km^2); (17) Yentna Glacier (fig. 411) (51 km, 487 km^2), which surged in 1972 and again in 2000, while its major tributary, Lacuna Glacier (fig. 412), which had been stagnant for about 60 years, surged in 2001; (18) an unnamed glacier (10 km, 25 km^2); (19) an unnamed glacier (10 km, 14 km^2); (20) the stagnant Kahiltna Glacier (76 km, 580 km^2) (see 1910 Capps photograph, USGS Photographic Library photograph Capps 312), some of whose unnamed tributaries were studied and photographed by Capps in 1910 (fig. 413); (21) Kanikula Glacier (18 km, 48 km^2); (22) Tokositna Glacier (44 km, 240 km^2), which surges about every 25 to 30 years; (23) Ruth Glacier (fig. 414) (63 km, 449 km^2); (24) an unnamed glacier at the head of the Coffee River (11 km, 11 km^2); (25) Buckskin Glacier (23 km,

47 km^2), which retreated more than 2 km between 1958 and 1999; (26) Eldridge Glacier (48 km, 485 km^2); and (27) two unnamed glaciers draining into Ohio Creek, one having a length of 8 km and an area of 12 km^2 and the other having a length of 14 km and an area of 17 km^2. Other glaciers, the lengths and (or) areas of which have been estimated by the author, are the 6-km-long West Fork Glacier (one of three glaciers with that name in Alaska) and an unnamed glacier that drains into Boulder Creek that has a length of about 8 km and an area of about 10 km^2 and originates from an isolated unnamed peak west of Chedotlothna Glacier.

Figure 411.—*31 August 1967 north-looking oblique aerial photograph of the upper part of Yentna Glacier at an elevation of approximately 1,600 m. Although trimlines are close to the ice surface, elevated lateral and medial moraines and a thick marginal sediment zone on many tributaries suggest that the Yentna Glacier has undergone some recent thinning. Because the date of this aerial photograph is 5 years prior to the 1972 surge, it is doubtful that any of the thinning seen here is related to surge drawdown. Photograph no. 67–R3–67 by Austin Post, U.S. Geological Survey.*

Figure 412.—*31 August 1967 north-looking oblique aerial photograph of the upper part of Lacuna Glacier at an elevation of approximately 1,500 m. Folded loop moraines provide evidence of a past surge. Trimlines and elevated lateral and medial moraines suggest that the glacier has experienced recent thinning. Few glaciers have the number of potholes that are seen on the surface of this glacier. Photograph 67–R3–60 by Austin Post, U.S. Geological Survey.*

Figure 413.—*Two 1910 photographs by S.R. Capps mosaicked to show two unnamed retreating glaciers located at the head of Hidden Creek, a 9-km-long eastern tributary to the valley of the Kahiltna Glacier. Both glaciers have elevated lateral moraines and are fronted by large debris aprons. Photographs Capps 306 and 307 from the USGS Photo Library, Denver, Colo.*

Figure 414.—**A**, *4 September 1966 north-looking oblique aerial photograph of The Great Gorge of Ruth Glacier, with Mount McKinley in the background. Elevated lateral moraines located on both sides of the valley suggest that here, more than 30 km above the terminus, at an elevation of approximately 1,000 m, recent thinning has occurred. Photograph no. 665–82 by Austin Post, U.S. Geological Survey.* **B**, *14 September 1999 south-looking oblique aerial photograph of a large thermokarst lake in the central terminus area of Ruth Glacier. This lake is the result of the coalescence of many individual thermokarst pits. Photograph by Bruce F. Molnia, U.S. Geological Survey.*

Tokositna Glacier

Tokositna Glacier surged in 1970 and in 1972. Neither surge resulted in the displacement of the terminus. Essentially stagnant since the end of the surge in 1972, Tolisitna suddenly began surging in late February 2001, moving forward at a rate of approximately 2 m d^{-1}. The 1971–72 surge resulted in about 2 km of displacement. The 2001 surge produced significantly less displacement and did not impact the terminus. Before the early 1970s surge, Post (1969) had identified Tokositna Glacier as a surge-type glacier on the basis of contorted moraines that resulted from a pre-1957 surge.

Polychrome Glacier

Polychrome Glacier, a north-flowing 4-km-long valley glacier at the eastern end of this group of glaciers, discharges into an unnamed eastern fork of the Toklat River; it was mapped by the AGS during the IGY (AGS, 1960). In the notes accompanying the map, Post (AGS, 1960, p. 21) described an ablation moraine covering the lower 1.5 km of the glacier that effectively protected the covered ice so that "little or no retreat was evident." Post (AGS, 1960, p. 21) also noted that almost no snow remained from the previous winter and that he doubted if "the glacier had experienced a positive snow budget for many years at any point in the basin." In 1995, Polychrome Glacier was resurveyed by a geodetic airborne laser altimeter profiler (Sapiano and others, 1998). A comparison of two profiles collected on 28 June 1995 with profiles constructed from a 1957 map showed that the 1995 terminus of Polychrome Glacier was very close to its 1957 position, a change of 10±5 m during the 38 years between surveys. The glacier's area, however, had decreased from 1.84 km^2 in 1957 to 1.7 km^2 in 1995, a decrease of about 9 percent. The glacier had thinned an average of 8.5 m, its volume had decreased by 1.5×10^7 m^3, and its average annual mass balance was -0.2 m.

Muldrow Glacier

Muldrow Glacier (figs. 405, 406, 407) flows to the northeast from high on the slopes of Mount McKinley, ending at a moraine-covered terminus near the Eielson Visitors Center in Denali National Park. Two named tributary glaciers, Brooks and Traleika Glaciers (fig. 406*C*), are the primary sources of ice for Muldrow Glacier. From May of 1956 through the summer of 1957, Muldrow Glacier surged a distance of about 6.6 km (Post, 1960). The maximum observed velocity during the peak of movement was about 350 m d^{-1} or about 24 cm min^{-1}. The glacier surface elevation decreased up to 100 m in the upper glacier area and increased 200 m in the lower glacier. For almost a decade before the surge, a wave of thickening ice moved down the upper part of the glacier at a rate of approximately 0.75 m d^{-1}. Post (1960), who described the 1956–57 surge, reported that an analysis of moraine patterns on the surface of Muldrow Glacier suggests that at least four prior surges have occurred within the past several hundred years, the most recent pre-1956 surge occurring between 1906 and 1912. A large moraine visible from the Eielson Visitors Center was formed by a late 16th or early 17th century advance that represents the "Little Ice Age" maximum position of Muldrow Glacier. Ice stagnation and retreat followed, but, about 150 years ago, the recession was interrupted by a new surge that deposited a second set of moraines approximately 1.5 to 4.5 km behind the 16th or 17th century moraines. The 1957 surge overrode much of the second set of moraines and reached to within 5 km of the park road. In 1976 and 1977, Bradford Washburn, acting on the recommendation of the Swiss glaciologist Fritz Müller and working jointly with the Museum of Science (Boston, Massachusetts) and the Swiss Foundation for Alpine Research, mapped the lower 37 km of the Muldrow Glacier from vertical aerial photographs acquired on 21 August 1976 by Air Photo Tech of Anchorage, Alaska (Field, 1990). The orthophoto contour map, which has a 10-m contour interval on the glacier (20-m contours on steep off-glacier topography), was published as five 1:10,000-scale sheets, each covering about 8×10 km (Washburn, 1983).

When the author observed it from the air in 1978, in September 1999, and on 3 September 2002, vegetation covered the ablating, stagnant, ice-cored moraine for a distance of 2 km or more from the glacier's terminus. For the next 15 km further upglacier, this continuous morainic cover graded into areas of debris-covered stagnant ice and bare ice. More than 25 km further upglacier, the glacier's surface was a mixture of bare ice and contorted moraines.

Kichatna Mountains

The Kichatna Mountains (fig. 415*A*, *B*) support several dozen glaciers, seven of which are more than 8 km long. Many of the smaller glaciers, which sit in cirques or small valleys, were retreating when they were first observed at the start of the 20th century (fig. 415*A*). The largest radiate like claws from the northern flanks of Augustin Peak, Gurney Peak, Cathedral Spires, and Lewis Peak. The glaciers, whose lengths and areas have been measured by Denton and Field (1975a, p. 590–591), include four unnamed glaciers (8 km, 9 km^2; 10 km, 21 km^2; 15 km, 26 km^2; about 6 km, about 5 km^2, estimated by the author); Shadows Glacier (14 km, 24 km^2); Cul-de-sac Glacier (12 km, 14 km^2); and Tatina Glacier (10 km , 11 km^2).

Glaciers of this area were used to compare the capabilities of two of the first satellite remote sensing systems and their ability to resolve glaciological

Figure 415.—*Two views of cirque and small valley glaciers in the Kichatna Mountains.* **A**, *1902 panoramic photographs by A.H. Brooks of several glaciers in the south-central Kichatna Mountains, probably east of Caldwell Glacier. The unnamed glaciers show multiple evidence of retreat and thinning. Photographs Capps 878 and 879 from the USGS Photo Library, Denver, Colo.* **B**, *24 August 1979 east-looking oblique aerial photograph of the summits of several unnamed, approximately 2,000-m-high Kichatna Mountains peaks adjacent to Augustin Peak. Because only the snow-covered heads of these glaciers can be seen, the status of their terminus regions cannot be determined. Photograph no.79–R2–233 by Austin Post, U.S. Geological Survey.*

features from space. Hall and Ormsby (1983) compared a Landsat image (30177–20455, 29 August 1978) of the Alaska Range and a SEASAT SAR image (03800083, 23 July 1978) that was also analyzed by Ford and others (1980). Both images show glaciers in the area. They concluded that Landsat and SEASAT SAR images were equally useful in determining the position of glacier termini, delineating medial moraines, and depicting terminal moraine areas. Landsat images can be used to determine the snowline; SEASAT SAR images cannot. Ford (1984) was also able to delineate glacial lakes, fluted ridges, and drumlinized topography along the valleys of the Chulitna and Tokositna Rivers.

The Mount Gerdine-Mount Spurr Segment between Rainy Pass and Merrill Pass

This segment, which has a maximum length of approximately 140 km, includes the Tordrillo Mountains, which hosts both the largest concentrations of glacier ice and the largest glaciers; the Terra Cotta Mountains; the Revelation Mountains; and some isolated accumulation areas from which a number of small glaciers descend.

Peaks of the Tordrillo Mountains that support large glaciers include Mount Torbert (3,480 m), Mount Gerdine (3,432 m) and Mount Spurr (3,374 m) (fig. 416), the only active volcano in the Alaska Range. More than 15 glaciers longer than 8 km descend from a broad interconnected accumulation area more than 45 km long and located between Hayes River and Chakachamna Lake. The three longest — Hayes, Triumvirate, and Capps Glaciers — all drain eastward and are longer than 40 km (Denton and Field, 1975a, p. 595–596).

The named glaciers of the Tordrillo Mountains, whose lengths and areas have been measured by Denton and Field, 1975a, p. 595–597, are (from the north in a clockwise direction): Hayes Glacier (48 km, 207 km^2), which is known to surge (fig. 417*A*) and originates on the western side of Mount Gerdine; Trimble Glacier (33 km, 286 km^2) (fig. 417*B*), which originates on the eastern side of Mount Gerdine, Triumvirate Glacier (45 km, 402 km^2)

Figure 416.—*Annotated Landsat 2 image of the Tordrillo Mountains, southwestern Alaska Range. There are numerous ice-dammed lakes, surge-type glaciers, and glaciers on volcanoes in this area. Chakachamna Lake has not been ice-dammed in recent years; however, an advance of the Barrier Glacier or a debris flow from Mount Spurr, which had major eruptive activity in 1953 and was becoming active again in 2004, could easily dam the lake again. Strandline Lake has a history of repeated jökulhlaups (Juhle and Coulter, 1955; Post and Mayo, 1971; Sturm and Benson, 1985). The Hayes Glacier is known to surge (Post, 1969), as does the Harpoon Glacier, which was actively surging in 1984. This Landsat image barely shows the characteristic contorted medial moraines of surge-type glaciers on the Hayes, Harpoon, and Capps Glaciers. Landsat 2 MSS image (21288–20253, band 7; 2 August 1978; Path 76, Row 17) from the USGS, EROS Data Center, Sioux Falls, S. Dak. Landsat image and caption courtesy of Robert M. Krimmel, U.S. Geological Survey.*

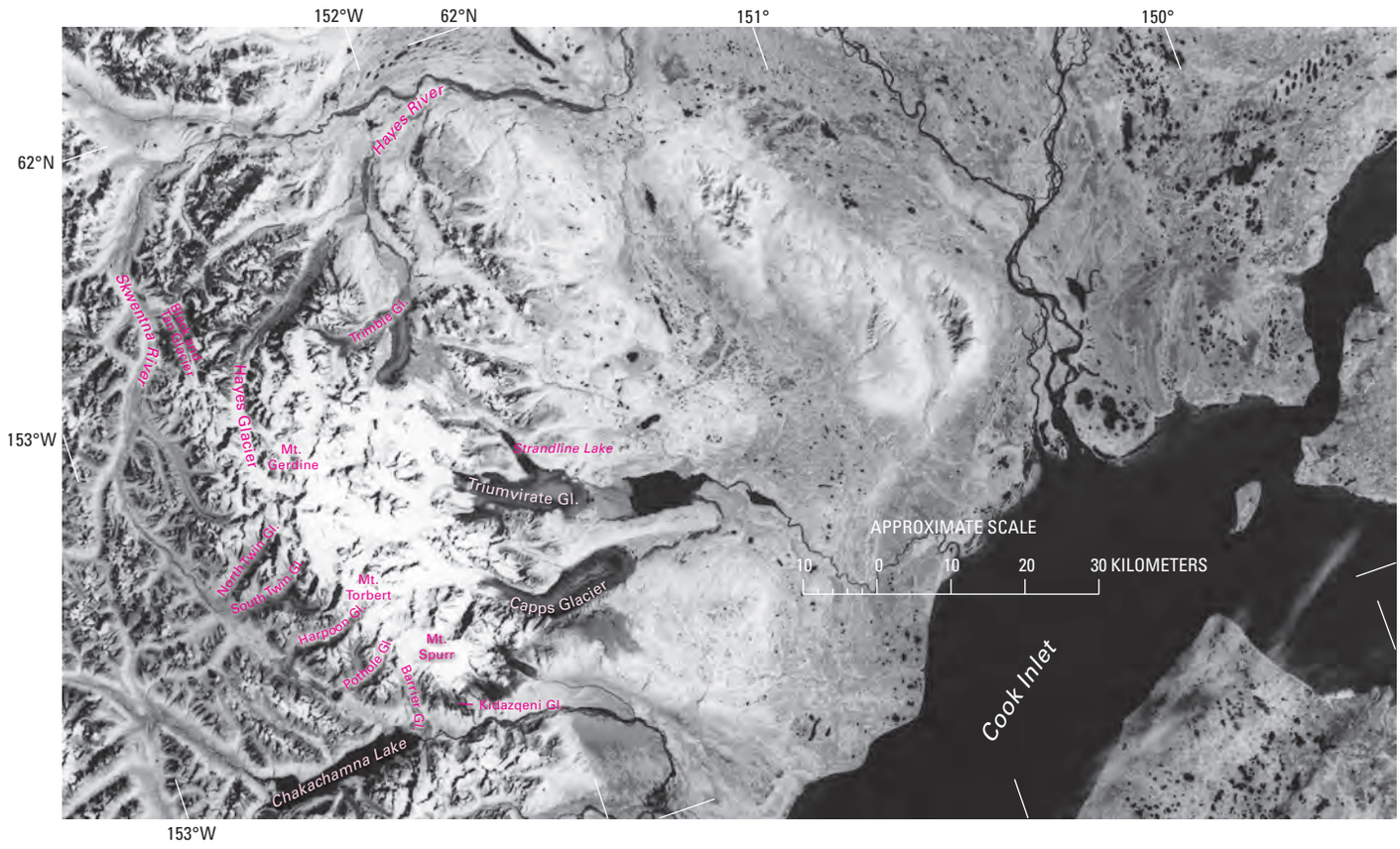

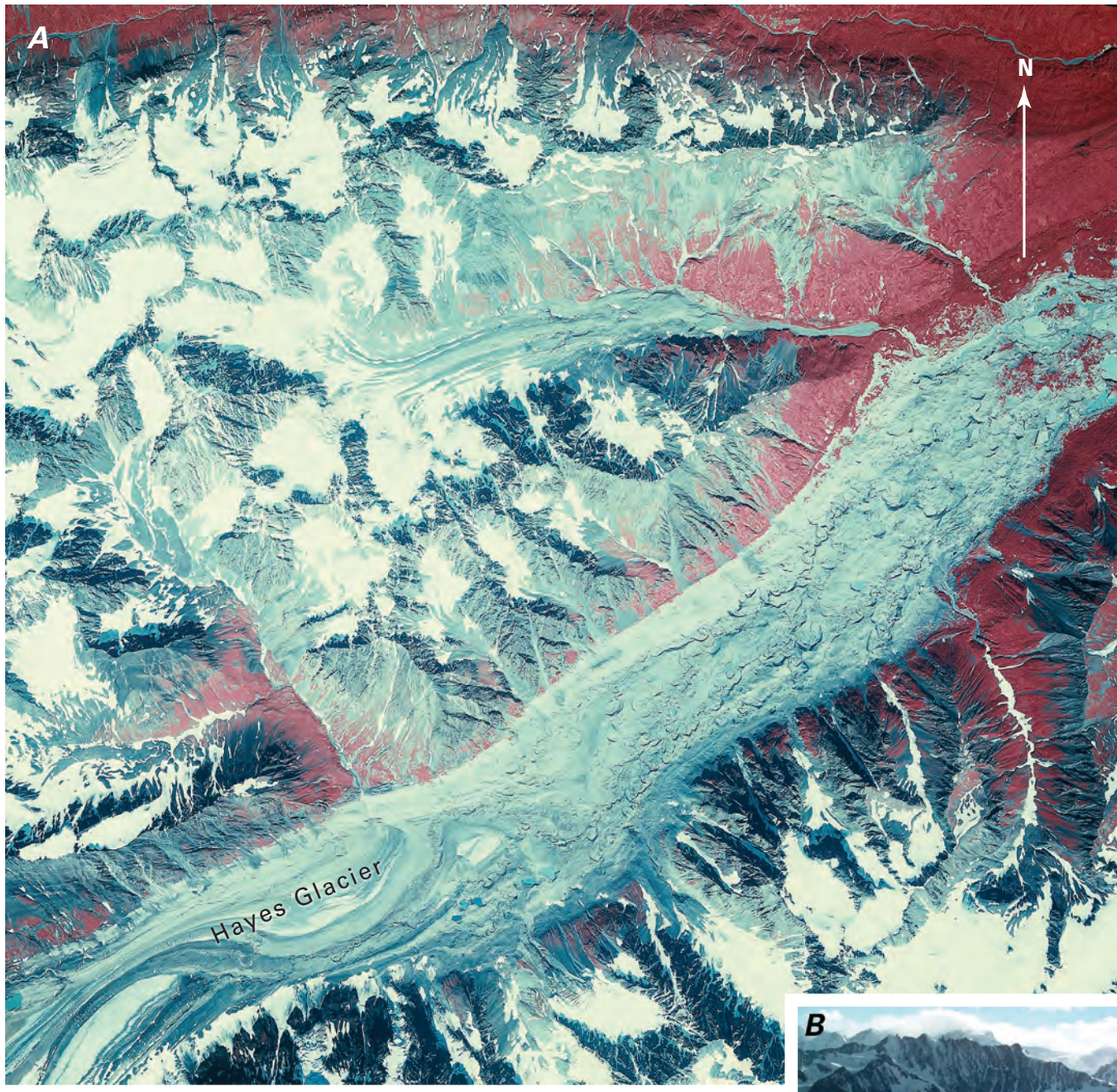

Figure 417.—**A**, *20 July 1982 annotated AHAP false-color infrared vertical aerial photograph of the lower part and terminus of the Hayes Glacier, an unnamed glacier to the north, and a number of cirques containing small glaciers. Hayes Glacier shows multiple evidence of stagnant ice, retreat, and thinning, including the growth of vegetation on its terminus. The surface of its lower 15 km is mantled by ablation debris and is covered by hundreds of thermokarst pits and lakes. Trimlines rim the two glaciers. The cirques are either deglacierized or the glaciers have retreated so much that they no longer make contact with Hayes Glacier or the unnamed glacier. AHAP photograph no. L102F9235 from the GeoData Center, Geophysical Institute, University of Alaska, Fairbanks, Alaska.* **B**, *8 September 2000 west-looking oblique aerial photograph of the upper part (North Branch) of the Trimble Glacier showing a distinct trimline and sediment accumulation on the southern margin of the glacier. Photograph by William R. Reckert, Volunteer for Science, U.S. Geological Survey. A larger version of* B *is available online.*

(fig. 418), which originates on the southern side of Mount Gerdine and from the flanks of a number of unnamed peaks. It has a small northern distributary that dams Strandline Lake, which has a history of repeated glacier outburst floods (jökulhlaups) (Juhle and Coulter, 1955; Post and Mayo, 1971; Sturm and Benson, 1985). Continuing clockwise is (1) Capps Glacier (fig. 419) (42 km, 293 km^2), originating on the eastern side of Mount Torbert and the northern side of Mount Spurr [Capps Glacier was reported to be surging during September 2000 by Austin Post (oral commun., 8 September 2000), but the surge was not affecting the terminus region]; (2) an unnamed glacier

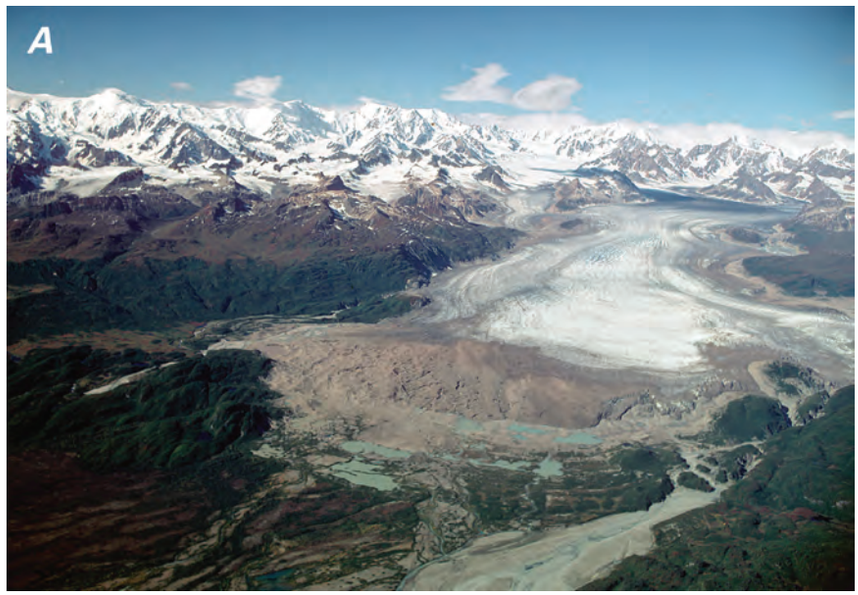

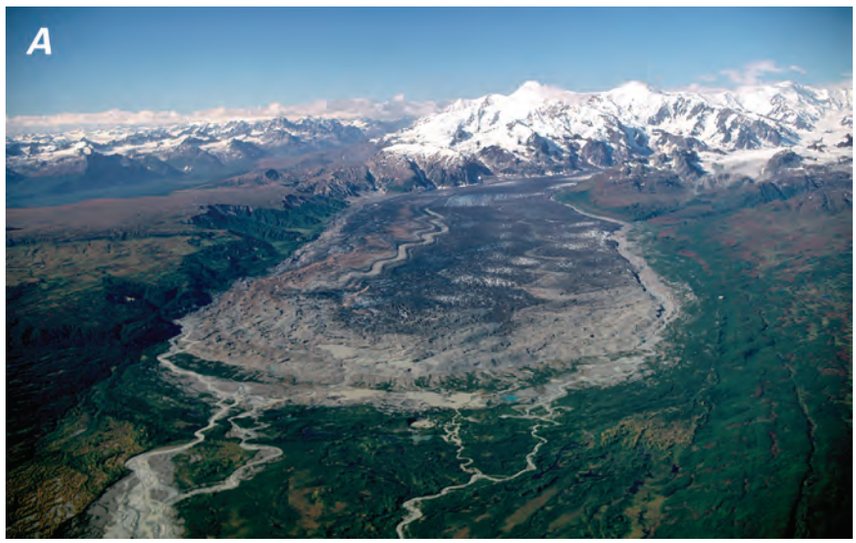

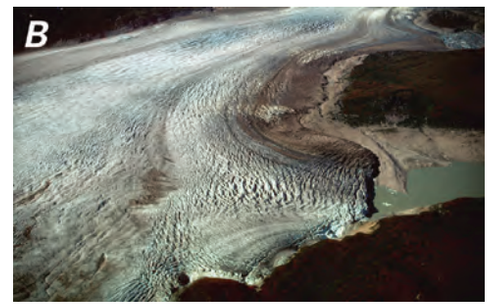

Figure 418.—*Two 8 September 2000 oblique aerial photographs of the terminus of Triumvirate Glacier showing multiple evidence of stagnant ice, retreat, and thinning.* **A**, *West view upglacier from above the outwash plain that fronts the glacier and its sequence of multiple, recessional moraines, many with interlobe lakes. Other features include the development of a hummocky pitted surface, large trimlines, a large ice-marginal lake, Strandline Lake, and significant accumulations of glaciofluvial sediments along the margins of the glacier.* **B**, *View of the retreating ice margin adjacent to Strandline Lake and to a second lake to the west. Continued thinning of Triumvirate Glacier results in a lowering of the surface level of both lakes. The water level in both lakes is low enough that water is no longer flowing along the northern margin of the glacier. In the past, a thicker glacier would block the outflow from both lakes resulting in a period of glacier outburst floods (jökulhlaups). Photographs by William R. Reckert, Volunteer for Science, U.S. Geological Survey. A larger version of* B *is available online.*

Figure 419.—*Two 8 September 2000 oblique aerial photographs of Capps Glacier.* **A**, *View looking west across the terminus of Capps Glacier showing evidence of stagnant ice, retreat, and thinning, including the development of a hummocky pitted surface with thermokarst lakes, trimlines, an ice-marginal lake, and large volumes of sediment accumulating along the margins of the glacier. The folded medial moraines are indicative of past surge behavior. Photograph by William R. Reckert, Volunteer for Science, U.S. Geological Survey.* **B**, *Oblique aerial photograph looking southwest across the central part of the glacier showing the fractured vertical margin and shattered surface indicative of a surge in the middle part of the glacier. Photograph no. C–26 by Austin Post, U.S. Geological Survey. A larger version of* B *is available online.*

Figure 420.—*Three photographs of Kidazqeni Glacier.* **A**, *September 1966 northwest-looking oblique aerial photograph of the summits of Mount Spurr and Crater Peak showing two glaciers on the south side of Mount Spurr. The eastern one, incorrectly mapped as Kidazgeni (with a g) Glacier in 1958 is actually unnamed. The western glacier is Kidazqeni Glacier (with a q). The unnamed glacier has a heavily tephra-covered piedmont lobe. Aside from exposed bedrock in its bed, an elevated lateral moraine on its west side, a small barren halo around the terminus of Kidazqeni Glacier, and an elevated lateral moraine on the east side of the unnamed glacier, neither glacier shows significant evidence of thinning or retreat. In the 8 years between the 1958 map and the photograph, no change could be detected in either glacier. Photograph no. 666–6 by Austin Post, U.S. Geological Survey.* **B**, *2 September 1970 north-looking oblique aerial photograph of the summit of Crater Peak and Kidazqeni Glacier. Steam is rising from Crater Peak. In the 4 years between photographs, no significant change could be detected in Kidazqeni Glacier. Photograph no. 7OR2–252 by Austin Post, U.S. Geological Survey.* **C**, *22 September 1992 oblique aerial photograph of the summit of Mount Spurr and Kidazqeni Glacier. In the 22 years since the 1970 photograph, the debris-covered, ice-marginal zone has retreated slightly from an end moraine that has developed adjacent to the terminus of the glacier and the individual ogive ridges have become muted. Photograph no. 92–V4–130 by Austin Post, U.S. Geological Survey. Larger versions of* A *and* C *are available online.*

(14 km, 33 km^2) originating on the southeastern side of Mount Spurr and forming the headwaters of Straight Creek; (3) a tephra-covered unnamed glacier draining from Crater Peak (fig. 420) (10 km, 27 km^2), incorrectly labeled as Kidazgeni (with a 'g') Glacier on the USGS 1:63,000-scale Tyonek A–6, Alaska (1958) topographic map, originating on the southern side of Mount Spurr; (4) Kidazqeni Glacier (fig. 420) (9 km, 10 km^2), correctly labeled on the USGS 1:250,000-scale Tyonek, Alaska (1958) topographic map; (5) Barrier Glacier (fig. 421) (see 22 September 1992 vertical aerial photograph by Austin Post, USGS photograph no. 92V4–98), (15 km, 49 km^2), which originates on the western and northern sides of Mount Spurr, so named because it obstructs the flow of water in the Neacola River–Chakachatna River drainage system, forming Chakachamna Lake; (6) stagnant Pothole Glacier (14 km, 56 km^2), which originates on the unnamed accumulation area located between Mount Spurr and Mount Torbert; (7) Harpoon Glacier (13 km, 21 km^2), which heads

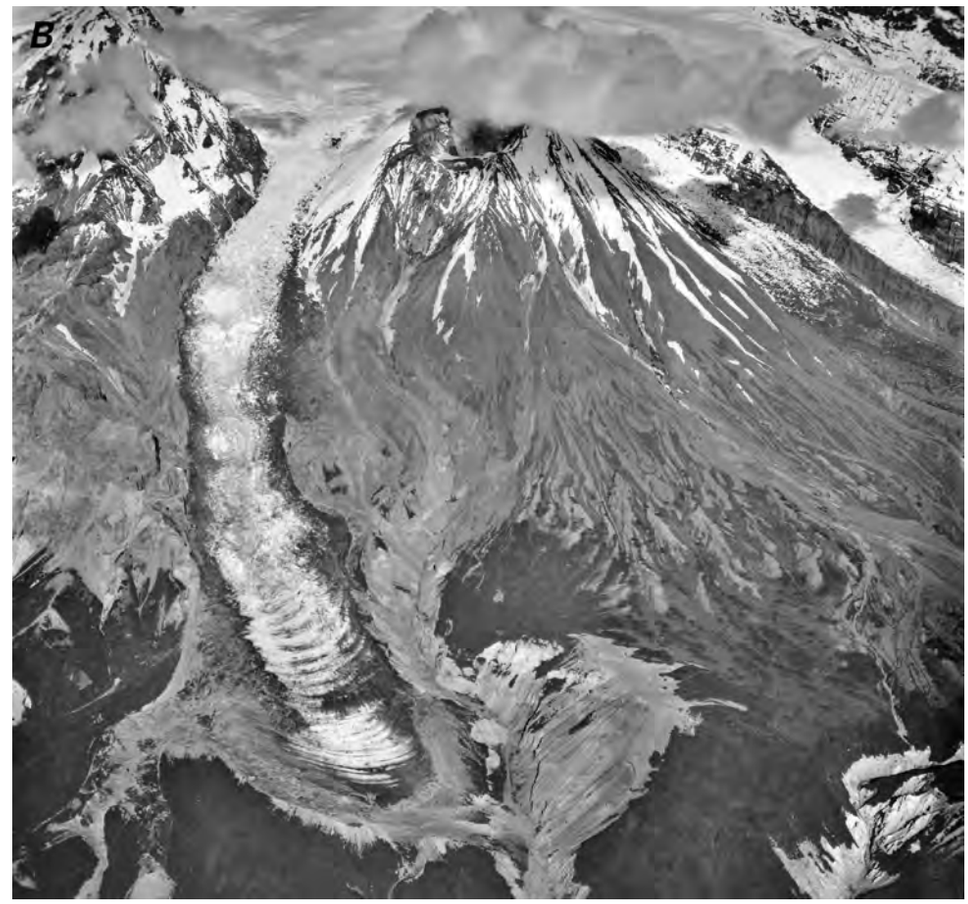

Figure 421.—*Two photographs of Barrier Glacier.* **A**, *4 September 1966 northwest-looking oblique aerial photograph of the summit of Mount Spurr and Barrier Glacier. The southern debris-covered part of the glacier's terminus is the barrier at the head of the Chakachatna River, creating Chakachamna Lake. A trimline on the west side of the glacier, a lobate ice-margin separated by as much as 75 m from its end moraine, and the development of a hummocky, pitted surface on its southern lobe are signs that Barrier Glacier has experienced recent thinning and retreat. In the 8 years between a USGS map (1958; Tyonek A–7) and the photograph, no change could be detected in the glacier. Photograph no. 666–9 by Austin Post, U.S. Geological Survey.* **B**, *8 September 2000 oblique aerial photograph looking northeast across the terminus of Barrier Glacier. Although there has been no change in the position of the debris-covered terminus of the glacier, its surface has been lowered and its bare ice, finger-like lobes continue to retreat. Photograph by William R. Reckert, Volunteer for Science, U.S. Geological Survey. A larger version of* B *is available online.*

on the western side of Mount Torbert and was surging in 1984 (see 4 August 1925 Capps photographs, USGS Photographic Library photographs Capps 1172 and 1173); (8) South Twin Glacier (15 km, 33 km^2); which heads in several cirques located on the western margin of an unnamed accumulation area between Mount Torbert and Mount Gerdine; (9) North Twin Glacier (see 4 August 1925 Capps photograph, USGS Photographic Library photograph Capps 1169) (16 km, 34 km^2), which heads in several cirques located on the southwestern flank of Mount Gerdine; (10) a debris-covered unnamed glacier (19 km, 62 km^2), which drains into the Skwentna River and heads in several isolated cirques west of Mount Gerdine; and (11) Black and Tan Glacier (see 20 July Capps photographs, USGS Photographic Library photographs Capps 1142 and 1143, and 20 July 1982 AHAP false-color infrared vertical aerial photograph no. L102F9238) (17 km, 20 km^2), which drains into the Skwentna River, and heads in several isolated cirques northwest of Mount Gerdine.

In August 1925, Capps photographed several small valley glaciers at a location that he called the head of *Tumbling Creek*, a tributary to the Skwenta River. All showed significant evidence of recent thinning and retreat (see August 1925 Capps photograph, USGS Photographic Library photograph Capps 1149). Because the name *Tumbling Creek* was never formally adopted, the exact location of these glaciers is not known. Photograph numbers indicate that they are probably located between North Twin Glacier and Black and Tan Glacier on the eastern side of the Skwentna River.

Mount Spurr is an active glacier-covered Quaternary stratovolcano located at the southern end of the Alaska Range and the northeastern end of the Aleutian volcanic arc (figs. 1, 420*A*, *C*). Crater Peak (2,309 m) (fig. 420*A*, *B*), a parasitic spatter cone, was the source of recent activity (Riehle, 1985) in 1953 and 1992, when eruptions deposited tephra on glaciers to the east and generated lahars that affected the glaciers on the southern side of the mountain. The eruption that began on 9 July 1953 produced a glacier-covering tephra blanket about 4 mm thick at Anchorage and detectable up to 350 km to the east (Wilcox, 1953). Lahars, including entrained snow and glacier ice, swept down valleys on the southern flank and dammed the Chakachatna River, which raised the level of Chakachamna Lake at least 3 m (Juhle and Coulter, 1955). The 1992 eruption began on 27 June 1992 and lasted more than 3 months. Westerly winds carried tephra to the east and deposited a tephra layer on glaciers as far east as Yakutat. Up to 3 mm of sand-sized tephra fell in Anchorage, while coastal communities more than 1,000 km away reported dustings of fine-grained tephra (Neal and others, 1992). On 16 September 1992, pyroclastic flows entrained snow and other surface debris and formed lahars that again temporarily dammed the Chakachatna River. Beginning in the summer of 2004, Mount Spurr began a new period of activity, including an increase in seismicity and the melting of glacier ice that covered its summit.

In the Tordrillo Mountains, many of the smaller valley glaciers and small cirque glaciers show multiple evidence of recent thinning and retreat (see 20 July 1980 AHAP false-color infrared vertical aerial photograph no. L108F6629). In some cases, retreat predates the 20th century. This continuing trend was documented by Brooks as early as 1902 (see USGS Photographic Library photograph Brooks 847).

Similarly, many upland areas of glacier ice show evidence of rapid thinning. Newly exposed bedrock can be seen in the upper reaches of many glacierized drainage basins in the Tordrillo Mountains, such as on the eastern side of Mount Gerdine (fig. 422).

To the west, in the Revelation Mountains and in isolated accumulation areas on peaks between the Tordrillo and Revelation Mountains, such as Mount Stoney and Mount Estelle, more than 15 glaciers longer than 8 km are located. The lengths and areas of some of these glaciers have been measured by Denton and Field (1975a, p. 597–598) and the others are estimated by

Figure 422.—*8 September 2000 oblique aerial photograph looking northwest across an unnamed ridge west of the South Branch of Trimble Glacier and showing newly exposed bedrock, several detached former tributary glaciers, and several cirques that have recently become deglacierized. Photograph no. C–2 by Austin Post, U.S. Geological Survey.*

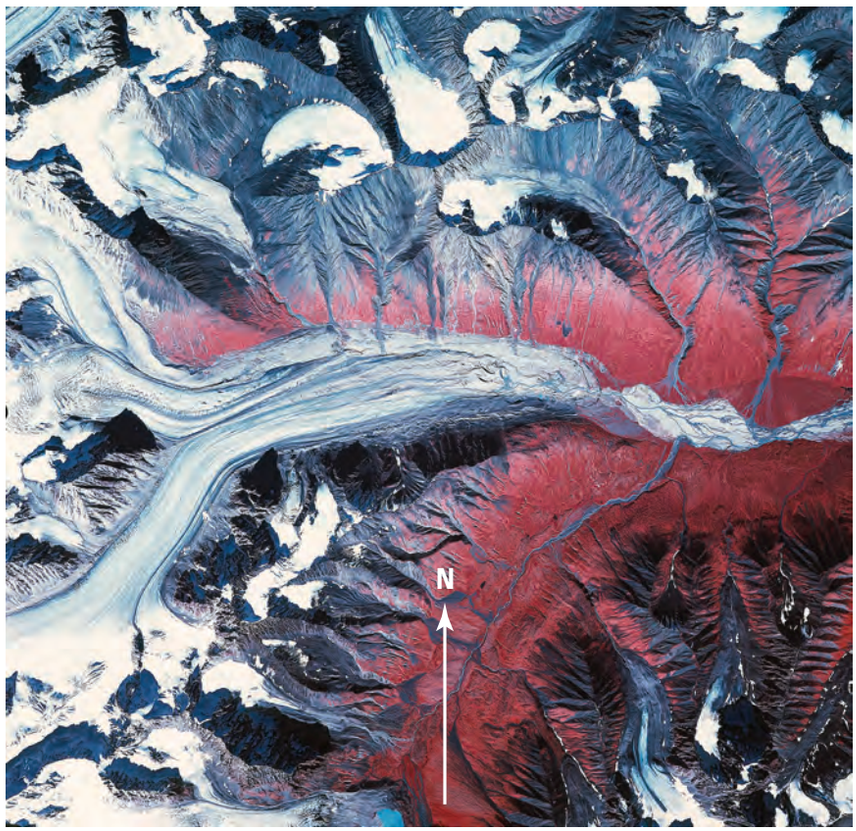

Figure 423.—*26 August 1978 AHAP false-color infrared vertical aerial photograph of the lower part of an unnamed glacier at the head of Hartman River and many small cirque glaciers. In the 20 years since being mapped by the USGS in 1958 (Lime Hills C–2, Alaska), the unnamed glacier has retreated about 1 km and begun to separate into at least four unique tributaries. Of the dozen or so cirque glaciers mapped in 1958, about two-thirds exhibit significant reductions in area, and the other third have completely melted, leaving numerous deglacierized cirques. AHAP photograph no. L103F7860 from the GeoData Center, Geophysical Institute, University of Alaska, Fairbanks, Alaska.*

the author: (1) an unnamed glacier (8 km, 9 km^2) that forms the head of Chilligan River; (2) an unnamed glacier (13 km, 25 km^2) located at the head of the eastern tributary of Stony River; (3) an unnamed south-flowing glacier on the eastern side of 2,540-m-high Mount Snowcap (~14 km, ~18 km^2; estimated by the author); (4) two other unnamed glaciers originating on Mount Snowcap, an east-flowing glacier (~10 km, ~20 km^2, estimated by the author) and a north-flowing glacier (~9 km, ~15 km^2, estimated by the author); (5) an unnamed glacier (~8 km, ~7 km^2, estimated by the author) that drains into Stony River; (6) an unnamed glacier (13 km, 40 km^2) that is located at the head of Hartman River (fig. 423); (7) Tired Pup Glacier, named by Orth in 1956 (Orth, 1967) (9 km, 15 km^2); (8) three unnamed glaciers (10 km, 18 km^2; 9 km, 12 km^2; ~10 km, ~10 km^2, estimated by the author), all eastern tributaries to the Swift River; (9) Stony Glacier (~8 km, ~12 km^2, estimated

by the author), a primary source of the Stony River; (10) an unnamed glacier (15 km, 44 km^2), the source of Fish Creek; (11) an unnamed glacier (14 km, 38 km^2) located at the head of Big River; (12) Revelation Glacier (16 km, 36 km^2) the westernmost named glacier in the Revelation Mountains; (13) an unnamed glacier (~8 km, ~7 km^2); (14) an unnamed glacier (10 km, 22 km^2) located at the head of the Post River; and (15) two unnamed glaciers (11 km, 18 km^2; ~9 km, ~17 km^2, estimated by the author), both sources of meltwater for the Lyman Fork of the Big River.

A number of smaller glaciers lie on the summits and flanks of the Revelation Mountains (see 26 August 1978 AHAP false-color infrared vertical aerial photograph no. L103F7865) and on a number of peaks between the Skwetna, Stoney, and Styx Rivers. These glaciers are generally valley glaciers less than 8 km long and less than 1.5 km wide.

Summary

During the period of the Landsat baseline (1972–81), all of the non-actively surging valley glaciers in the Alaska Range were stagnant, thinning, and (or) retreating. Several glaciers surged early during the baseline period, but no terminus advances were reported. At the end of the 20th century and during the first few years of the 21st century, all of the valley and outlet glaciers in the Alaska Range continued to thin, stagnate, and retreat.

Wood River Mountains

The Wood River Mountains of southwestern Alaska (figs. 1, 424) have maximum elevations of approximately 1,500 m. They are northeast- to southwest-trending mountain ranges that are about 160 km long and about 50 km wide and extend from Bristol Bay to Chikuminuk Lake. They are bounded on the west by Togiak River and Togiak Lake, on the north and northwest by Trail Creek and Milk Creek, on the east by the Tikchik Lakes and the lowlands of the Nuyakuk and Nushagak Rivers, and on the south by Bristol Bay. The total area of glaciers in the Wood River Mountains was estimated at 230 km^2 by Post and Meier (1980, p. 45).

Landsat MSS images that cover the Wood River Mountains area have the following Path/Row coordinates: 80/18 (fig. 425) and 81/18 (fig. 3, table 1). The area is covered by two USGS 1:250,000-scale topographic maps: Bethel (1980) and Goodnews Bay (1979) (appendix A). The maps are based on data collected between 1954 and 1979. The area was photographed from the space shuttle in 1992 (see 26 January 1992 photograph no. STS042–96–071, NASA). A GIS analysis of USGS 1:63,360-scale topographic maps of the Wood River Mountains by William F. Manley determined that 106 glaciers exist at several locations along the crest of the west-central part of the mountains: on the summit and flanks of Mount Waskey, on the ridge crests west of the head of Nuyakuk Lake, on the summit and flanks of Konarut Mountain (1,533 m) west of Lake Chauekuktuli, and along a 25-km-long ridge southwest of Chikuminuk Lake and north and west of Konarut Mountain (figs. 425, 426) (William F. Manley, written commun., 1999, 2000).

Manley (1999, 2000) quantified 32 different parameters of these 106 glaciers. He also determined that the total glacier-covered area was approximately 60 km^2 and that individual glaciers ranged in area from 0.05 to 6.4 km^2 (median area 0.26 km^2). They ranged in average elevation from 581 to 1,176 m (median elevation 937 m), in length from 0.25 to 4.38 km (median length 0.61 km), in width from 0.17 to 2.97 km (median width 0.72 km), and in perimeter from 1.0 to 23.8 km (median perimeter 2.6 km). The ELAs ranged from 545 to 1,155 m (average 929 m) and displayed high local variability.

More than 20 glaciers head along the summit ridge and slopes of 1,532-m-high Mount Waskey, the second highest peak in the Wood River Mountains, and on the nearby peaks and ridges (figs. 427, 428). Another group of more

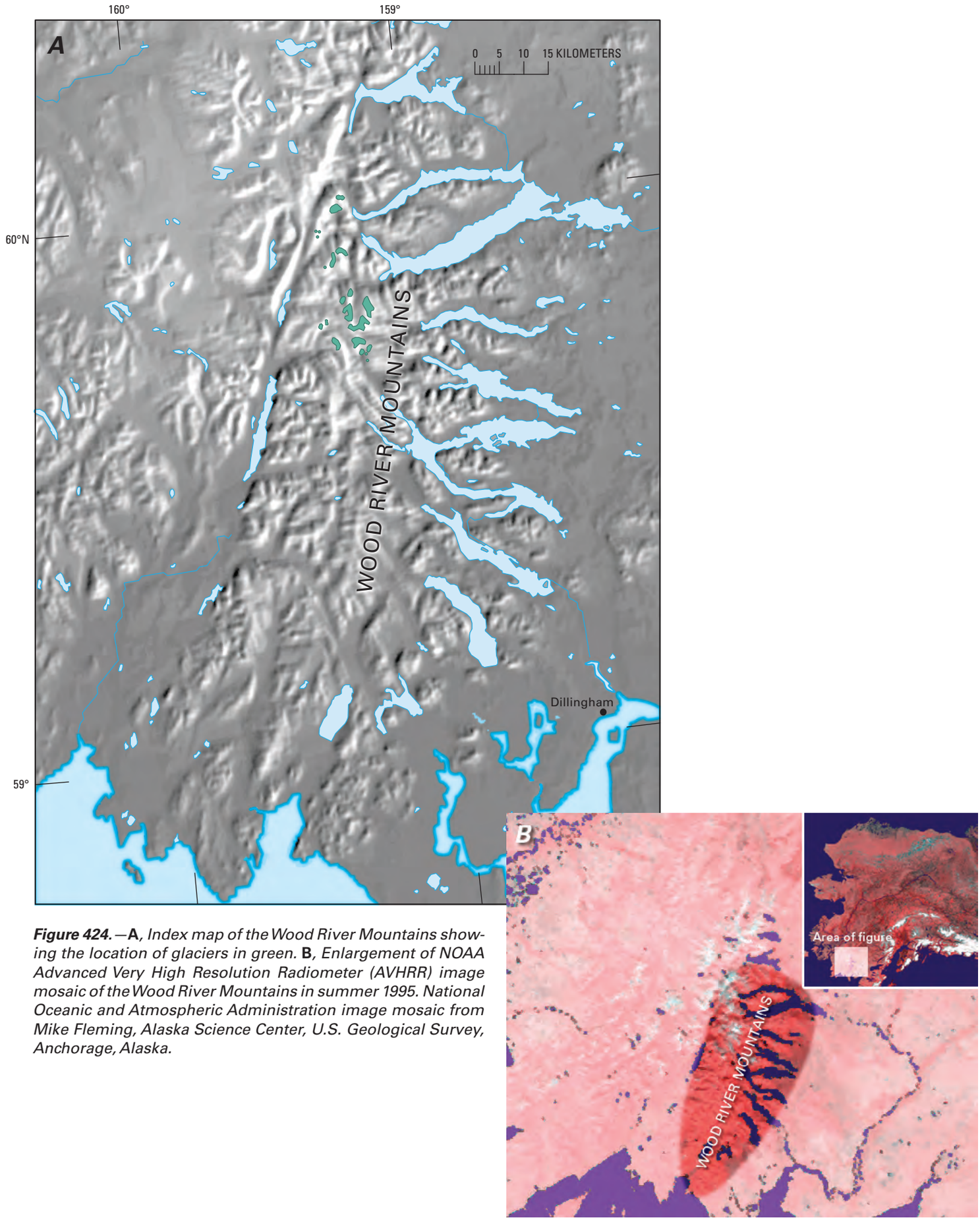

Figure 424. *—***A**, Index map of the Wood River Mountains showing the location of glaciers in green.* **B**, *Enlargement of NOAA Advanced Very High Resolution Radiometer (AVHRR) image mosaic of the Wood River Mountains in summer 1995. National Oceanic and Atmospheric Administration image mosaic from Mike Fleming, Alaska Science Center, U.S. Geological Survey, Anchorage, Alaska.*

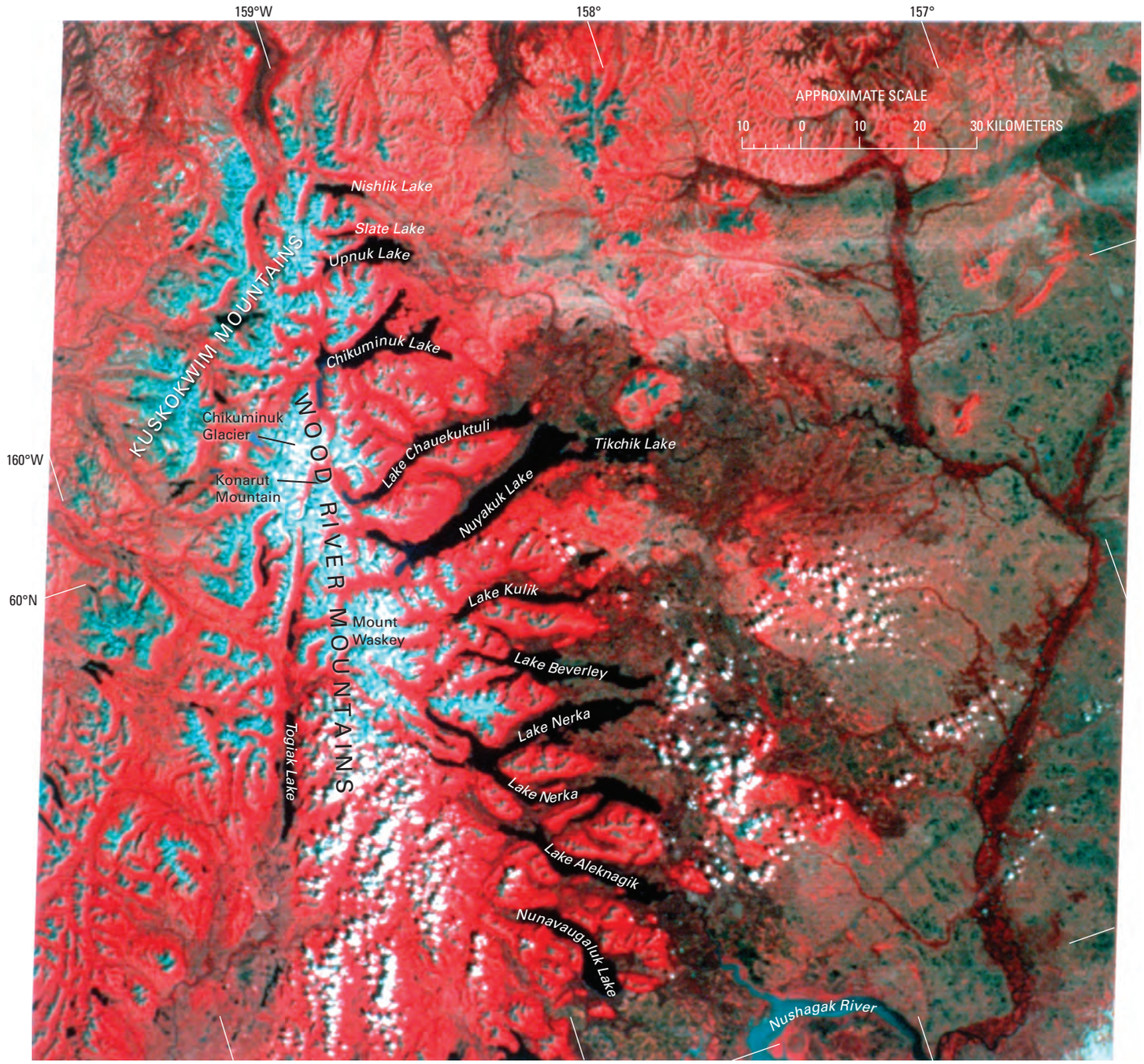

Figure 425. *—Annotated Landsat MSS false-color composite image showing the northern Wood River Mountains and the adjacent Kuskokwim Mountains. East of the mountains are the Tikchik Lakes, a group of more than a dozen finger lakes formed by glacier erosion during the Pleistocene. Also shown are the locations of Togiak Lake, Chikuminuk Glacier, Konarut Mountain, and Mount Waskey. Landsat image (30145–21091, bands 4, 5, 7; 28 July 1978, Path 80, Row 18) is from the USGS, EROS Data Center, Sioux Falls, S. Dak.*

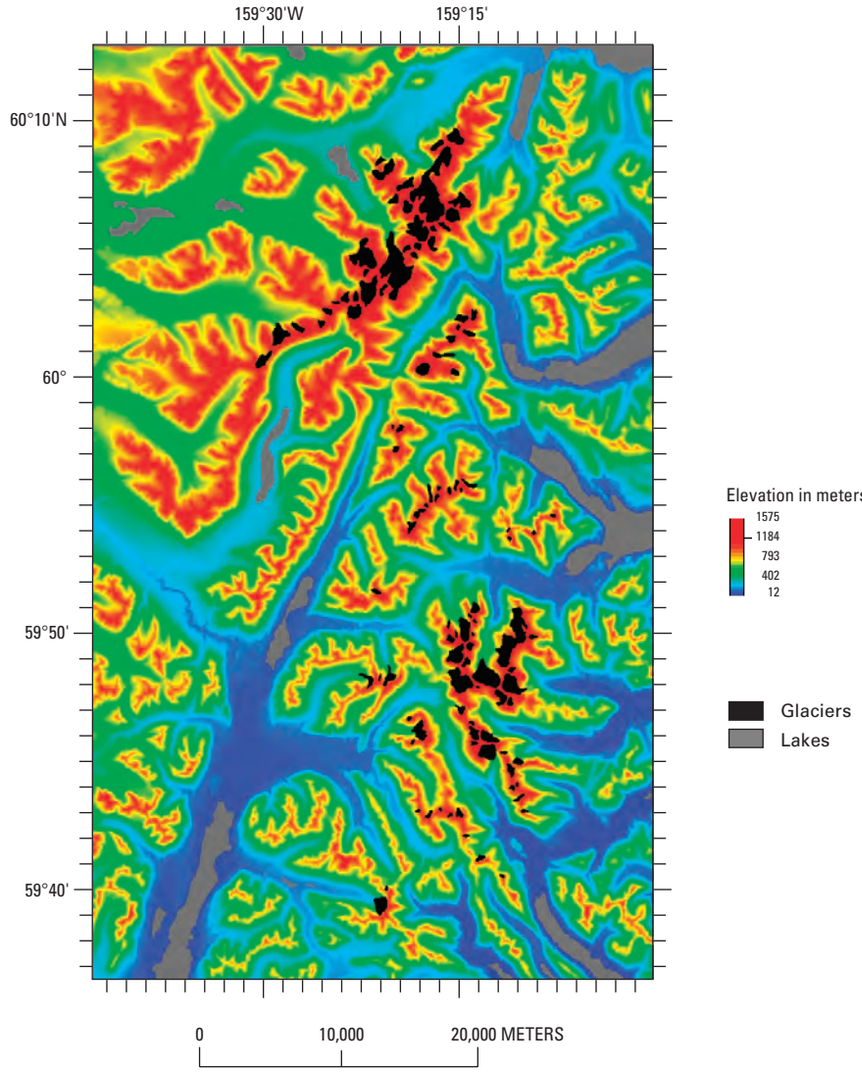

Figure 426.— *Map showing elevations and locations of glaciers in the central Wood River Mountains. Source: unpublished data provided by William F. Manley, University of Colorado, December 2001.*

than a dozen small unnamed glaciers lie along two ridges 8 to 15 km north-northwest of Mount Waskey and drain west into the Izavieknik River and east into Nuyakuk Lake (see 15 August 1984 AHAP false-color infrared vertical aerial photograph no. L121F0066). The area is referred to by some as the Ahklun Mountains, although, on USGS maps, the Ahklun Mountains are an independent parallel mountain range that lies about 60 km northwest of the Wood River Mountains. When they were photographed on 15 August 1984 by the AHAP Program (fig. 427) and in 1999 and 2000 by a University of Northern Arizona field party, all showed evidence of appreciable retreat and thinning. Additional glacial geology research by the University of Northern Arizona and other institutions was directed at Holocene glacier fluctuations (Levy and others, 2004). Another group of more than a dozen glaciers, all less than 2 km long, lies east and northeast of the summit of 1,533 m-high Konarut Mountain, the highest peak in the Wood River Mountains. Most drain eastward into Lake Chauekuktuli.

More than 20 glaciers lie along a 1350- to 1400-m-high, 25-km-long ridge southwest of Chikuminuk Lake and north and west of Konarut Mountain. This group is the greatest concentration of glaciers in the Wood River Mountains area. Their size increases to the north. The largest, the compound Chikuminuk Glacier is located almost at the northeastern end of the ridge. Chikuminuk Glacier, also called Kilbuck Glacier, was mapped at a scale of 1:10,000 during the IGY by the AGS (1960) (see sheet 8, AGS Glacier Mapping Project: Nine Glacier Maps, Northwestern North America). At that time, it was 5.5 km long and 1.0 km wide, had an area of 5.77 km^2, and was

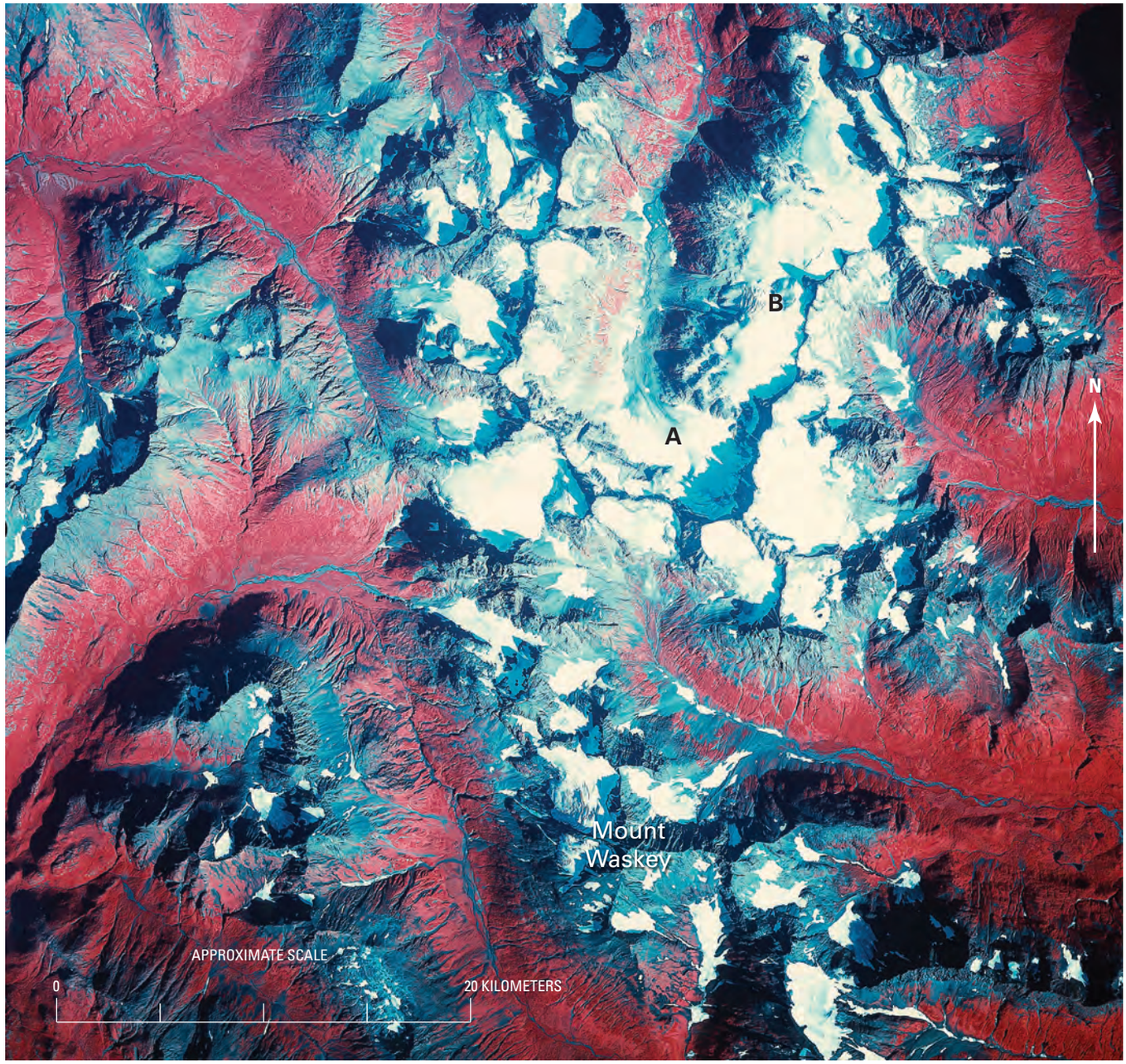

Figure 427.—*15 August 1984 annotated AHAP false-color infrared vertical aerial photograph of Mount Waskey and the adjacent glacier-covered ridges in the central Wood River Mountains. At least seven small glaciers can be seen. In each case, a bare-ice terminus is visible below a snow-covered upper glacier. At least one valley with an unnamed glacier at its head (A) shows evidence of recently hosting a 3- to 4-km-long valley glacier. A former tributary glacier (B) has two well-preserved elevated lateral moraines and an end moraine on the floor of its valley. It has recently retreated more than 1 km. Even in August, many other adjacent cirques are snowfilled, making the identification of glaciers in those cirques difficult. AHAP photograph no. L122F0166 from the GeoData Center, Geophysical Institute, University of Alaska, Fairbanks, Alaska.*

Figure 428.—*July 1999 ground photograph of the glacier-covered summit of the Mount Waskey massif from Waskey Lake. Several recently deglacierized hanging valleys can be seen below the snowline. Photograph by Darrell S. Kaufman, Northern Arizona University.*

Figure 429.—*6 September 1957 east-looking oblique aerial photograph of most of the northern tributary and part of the southern tributary glaciers that form the Chikuminuk Glacier. Most of the larger southern tributary lies off the right edge of the aerial photograph. The terminus shows evidence of recent retreat and thinning. Photograph from the U.S. Navy. Facsimile of photograph published by the American Geographical Society (1960).*

retreating. More than 75 percent of the glacier was located at elevations above approximately 1,000 m. When it was photographed in 1957, the terminus region exhibited much evidence of rapid retreat (fig. 429). Almost the entire surface of the glacier was bare ice, and the accumulation area was very small. Elevated trimline positions indicated that Chikuminuk Glacier was retreating. Other glaciers in the area also show signs of retreat, and areas mapped as glaciers on the USGS 1:63,360-scale topographic maps of this area—Bethel A1 (1979) and Bethel A2 (1979)—are now deglacierized.

Chikuminuk Glacier was one of nine glaciers mapped during the IGY that was resurveyed with a geodetic airborne laser altimeter system to obtain accurate profiles (Sapiano and others, 1998). Interpretation of six profiles collected on 11 May 1996 showed that the terminus of Chikuminuk Glacier had retreated 830 m during the 39 years between surveys, an average annual retreat rate of 21.2 m a^{-1}. The glacier's area had decreased by approximately 9 percent (from 5.77 km^2 in 1957 to 5.33 km^2 in 1996) (Sapiano and others, 1998). Of the nine glaciers mapped during the IGY, the terminus of Chikuminuk Glacier had retreated the most. Between surveys, at an elevation of about 480 m, the glacier thinned as much as about 42 m. Above an elevation of approximately 1,075 m the glacier thickened by an average of about 10 m. Sapiano and others (1998) stated that a comparison of the 1957 and 1996 volumes suggests that the total volume of the glacier increased by 8×10^6 m^3; however, because of 1957 survey errors, there is a large uncertainty in this number.

With the exception of Chikuminuk Glacier, lack of recent information makes it difficult to determine the status of the Wood River Mountains glaciers through the end of the 20th century. However, all of the glaciers show evidence of thinning and retreat. The 1984 AHAP photography indicated that the glaciers near Mount Waskey had actively thinned and retreated during the Landsat baseline period (1972–81).

Summary

The Wood River Mountains is an area in which no glacier observations were reported during the period of the Landsat baseline 1972–81. However, comparing pre-Landsat topographic maps and photographs with AHAP photographs collected during 1984 shows that every glacier depicted in the AHAP photographs had lost length and area during the interval between data sets. Observations by William H. Manley of the University of Colorado suggest that every glacier continued to lose area and volume through the end of the 20th century. The terminus region of Chikuminuk Glacier, the most studied glacier in the region, has been retreating and thinning since it was mapped during the IGY in the middle 1950s.

Kigluaik Mountains

The only glaciers on the Seward Peninsula are located in the 65 km-long east-west trending Kigluaik Mountains (figs. 1, 430). The total glacier area was estimated at about 3 km^2 by Post and Meier (1980, p. 45). Three glaciers exist in drainages on the flanks of 1,437-m-high Mount Osborn and adjacent peaks about 50 km north of Nome. Twentieth century investigations by Brooks in 1900 (Brooks and others, 1901), Henshaw and Parker in 1909 (Henshaw and Parker, 1913), Moffit (1913), Hopkins in 1973 (Hopkins and others, 1983), Kaufman and Calkin (1988), Kaufman and others (1989), and Calkin and others (1998) confirm that (1) from the start of the 20th century through the late 1980s, glaciers existed in the Kigluaik Mountains; (2) during the 20th century, several glaciers have completely disappeared; and (3) the remaining Kigluiak Mountain glaciers, according to the last field observation in 1986, had continued to decrease in area and length. The Kigluaik Mountains can be seen on Landsat MSS Path 88, Row 14 (fig. 3, table 1). Figure 431 is a Landsat 2 MSS false-color composite image acquired on 26 June 1977.

Brooks and others (1901) described two small glaciers that he observed in the vicinity of Mount Osborn in 1900. One was located at the head of the eastern fork of Grand Union Creek and the other near the head of the north fork of the Grand Central River (fig. 432). When they visited the area in 1909, nine years later, Henshaw and Parker (1913) observed a third small glacier, which they described as being located at the head of Pass Creek. David M. Hopkins (personal commun. to Camilla McCauley in correspondence to the

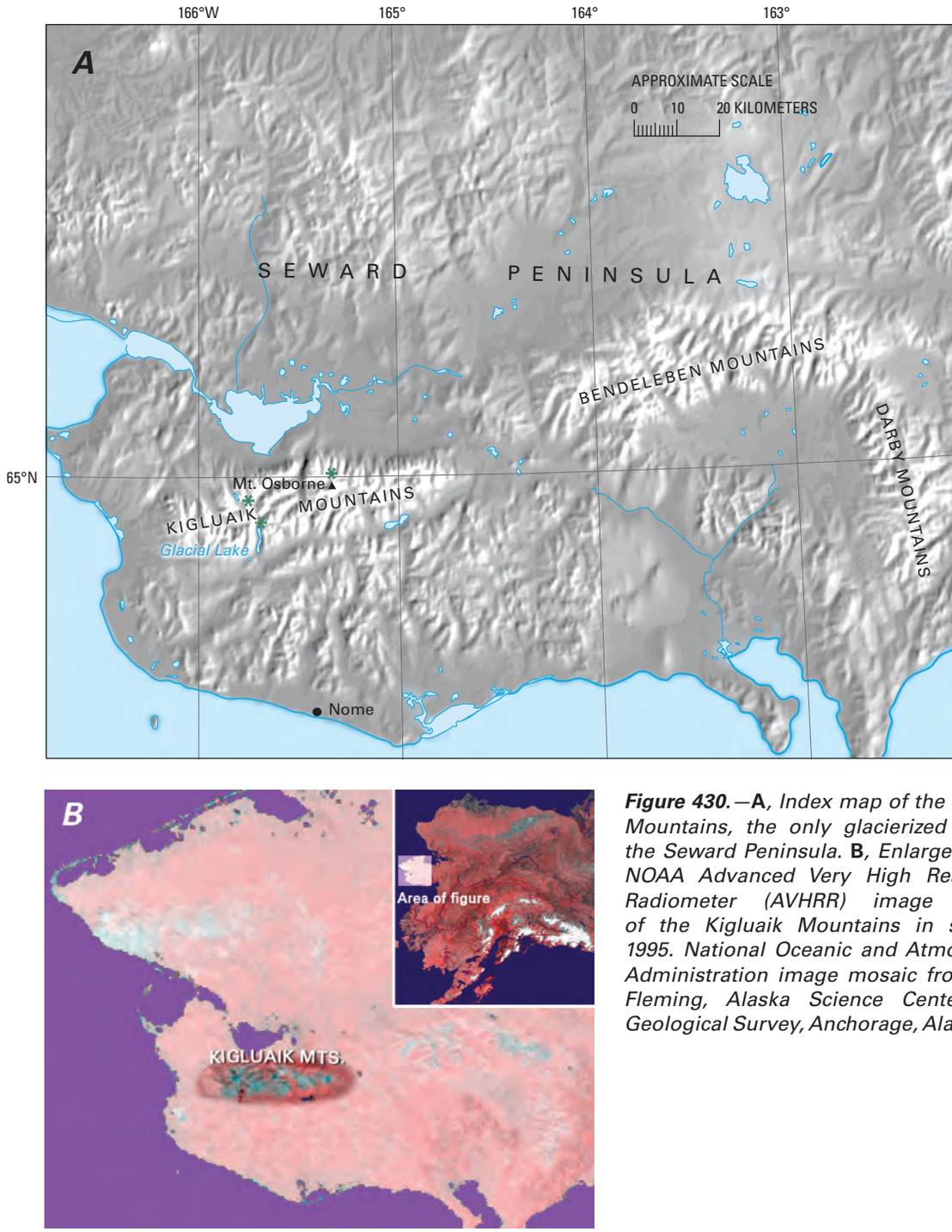

***Figure 430.*—A**, *Index map of the Kigluaik Mountains, the only glacierized part of the Seward Peninsula.* **B**, *Enlargement of NOAA Advanced Very High Resolution Radiometer (AVHRR) image mosaic of the Kigluaik Mountains in summer 1995. National Oceanic and Atmospheric Administration image mosaic from Mike Fleming, Alaska Science Center, U.S. Geological Survey, Anchorage, Alaska.*

AGS, 1956; cited by McCauley, 1975, p. 668) determined that this glacier was actually located in the eastern fork of Smith Creek. His examination of 1949 and 1950 aerial photographs of these locations determined that all three glaciers had completely melted and no longer existed.

Using the same 1949–50 photography, Hopkins discovered three previously "unknown" glaciers elsewhere in the area with a total area of less than 5 km^2. He described the largest of these, *Grand Union Glacier*, "being about a mile long" and having a "prominent vegetation-free moraine a few hundred feet down-valley from the front; presumably the moraine is between a few decades and a century in age" (McCauley, 1975, p. 668). According to Calkin and others (1998), the glacier lies sheltered in a cirque below

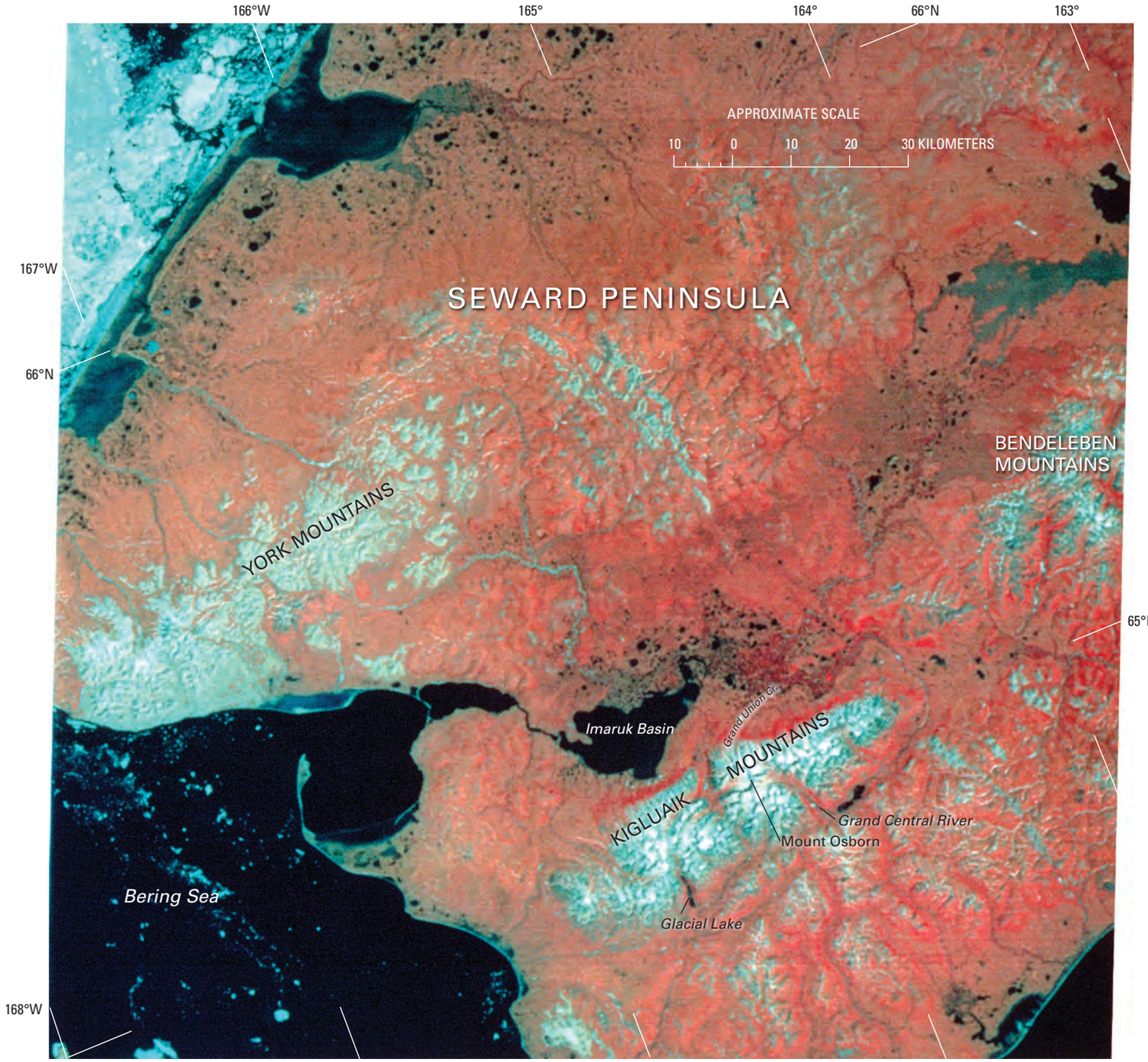

Figure 431.—*Annotated Landsat 2 MSS false-color composite image of much of the Seward Peninsula, including all of the Kigluaik Mountains. The locations of Mount Osborn, Grand Union Creek, Grand Central River, and Glacial Lake are indicated. Landsat 2 image (2886–213155; bands 4, 5, 7; 26 June 1977; Path 88, Row 14) is from the USGS, EROS Data Center, Sioux Falls, S. Dak.*

the northeastern margin of Mount Osborn at the head of the middle fork of Grand Union Creek. Hopkins also identified two other small cirque glaciers, one in the Glacial Lake valley about 12 km southwest of Mount Osborn and one at the head of an unnamed tributary of the Pilgrim River adjacent to Grand Union Creek. When Hopkins visited *Grand Union Glacier* in 1973, he observed that the length of the glacier had decreased to only about 800 m. In the 23 years between the 1950 aerial photography and Hopkins' 1973 field observations, *Grand Union Glacier's* length had decreased approximately 800 m or about 35 m a^{-1}.

Péwé and Reger (1972) and McCauley (1975) also studied the glaciers of the Kigluaik Mountains by using the 1949–50 photography. They reported the length of *Grand Union Glacier*, the westernmost active Alaskan glacier located north of the Aleutian Islands, to be about 1 km. Calkin and others (1998) reported that its length had decreased about 30 percent to about 700 m by 1986. Figure 433 is an AHAP photograph acquired on 1 August

1985 that shows *Grand Union Glacier* and numerous ice-free cirques. In 1986, its area was 0.28 km^2, and its mean altitude was 700 m. Evidence of its recent larger extent is a broad looped terminal moraine that reached 410 m beyond the glacier terminus in a summer 1983 photograph (fig. 434). Local lichen chronology led Calkin and others (1998) to place the date of its Holocene maximum advance at 1645 A.D.

Mass-balance studies were performed in 1985 and 1986 (Przybyl, 1988). Winter balances were 1.5 m (1984–85) and 2.3 m (1985–86); summer balances were -2.3 m (1984–85) and -3.1 m (1985–86). The net mass balance was a loss of about 0.8 m annually. The other two smaller stagnant cirque glaciers, informally called *Thrush Glacier* and *Phalarope Glacier* by Calkin and others (1998), occur in north-facing canyon-like cirques whose mean surface elevations are 630 and 820 m, respectively. *Thrush Glacier* is located at the head of the main northeastern tributary of Glacial Lake in a northwestward-facing cirque. In 1986, its area was 0.10 km^2, and its length was 350 m (Calkin and others, 1998). Its Holocene maximum length was 400 m. Calkin and others (1998) based the 1675 A.D. date of its Holocene maximum advance on local lichen chronology.

Phalarope Glacier, located 7.6 km northwest of *Thrush Glacier* is the smallest of the three. In 1986, its area was 0.06 km^2, and its length was 150 m (Calkin and others, 1998). Its Holocene maximum length was only 160 m. On the basis of local lichen chronology, Calkin and others (1998) dated its Holocene maximum advance at 1825 A.D.

Figure 432.—*Summer 1900 photograph by A.H. Brooks of a small retreating cirque glacier located at the head of the North Fork of the Grand Central River. Photograph Brooks 360 from the USGS Photo Library, Denver, Colo. A larger version of this figure is available online.*

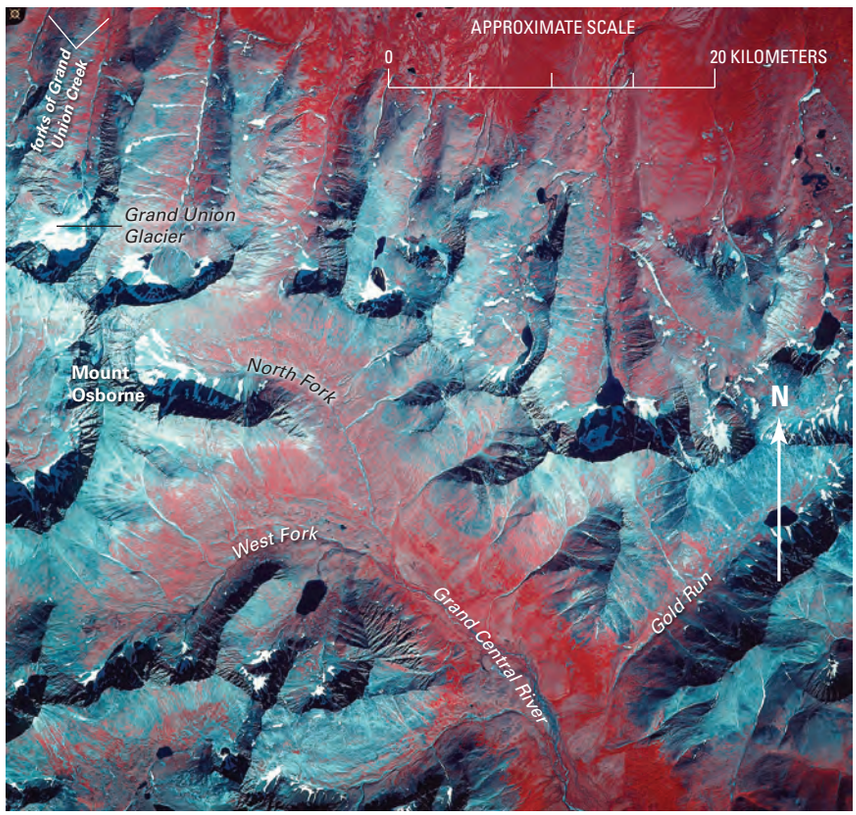

Figure 433.—*1 August 1985 annotated AHAP false-color infrared vertical aerial photograph of the Mount Osborn area showing* Grand Union Glacier *and numerous ice-free cirques. The valley of the North Fork of the Grand Central River where one of Brooks' 1900 glaciers was located is east of Mount Osborn's summit. AHAP photograph no. L168F8277 from the GeoData Center, Geophysical Institute, University of Alaska, Fairbanks, Alaska.*

Figure 434.—*Summer 1983 photograph of the* Grand Union Glacier*, located northeast of Mount Osborn. The retreating glacier is surrounded by a broad, looped terminal moraine that dates from 1645 A.D. Photograph by Darrell Kaufman, University of Northern Arizona.*

Summary

The glaciers of the Kigluaik Mountains have received little recent attention. During the Landsat baseline period (1972–81), three glaciers—*Grand Union Glacier*, *Thrush Glacier*, and *Phalarope Glacier*—existed in the Kigluaik Mountains. Field investigations performed in 1986, 5 years after the end of the Landsat baseline period, confirm that several glaciers had completely disappeared during the first eight decades of the 20th century and document that the remaining three Kigluaik Mountain glaciers were continuing to decrease in area and length. At the rate that these three glaciers were retreating and thinning, it is possible that one or more of them may have disappeared by the beginning of the 21st century.

Brooks Range

Introduction

The Brooks Range (figs. 1, 435), the northernmost mountain group in Alaska, extends for nearly 1,000 km in an east-west direction from the Yukon Territory, Canada-Alaska border, on the east to the Chukchi Sea on the west. It forms the drainage divide between the Arctic Slope to the north and the Kobuk and Yukon Rivers to the south. The Brooks Range contains about a dozen named generally east-west-trending contiguous mountain ranges (from east to west): British, Davidson, Romanzof, Franklin, Sadlerochit, Shublik, Philip Smith, Endicott, Schwatka, Baird, and DeLong Mountains. Glaciers within the eastern and central Brooks Range are found over a distance of about 650 km in the Romanzof, Franklin, Philip Smith, Endicott, and Schwatka Mountains (figs. 1, 435). Because the Brooks Range lies wholly north of the Arctic Circle, glaciers in the region are generally classified as polythermal; most of them are located in steep cirques and have a northern exposure (Denton, 1975b). The largest glaciers and the greatest concentration of ice are located in the eastern ranges. Two of the three highest peaks in the Brooks Range—Mount Isto (2,761 m) and Mount Michelson (2,699 m)—are in the Romanzof Mountains. Mount Chamberlin (2,750 m), the second highest peak, is in the Franklin Mountains. The glaciers of the Brooks Range cover an area of 723 km^2 (C Suzanne Brown, oral commun., 1992; Post and Meier, 1980, p. 45).

Present-day glacierization is significantly less than it was during the late Wisconsinan (Hamilton and Porter, 1975), when individual ice streams and piedmont lobes flowed as much as 50 km beyond the northern and southern

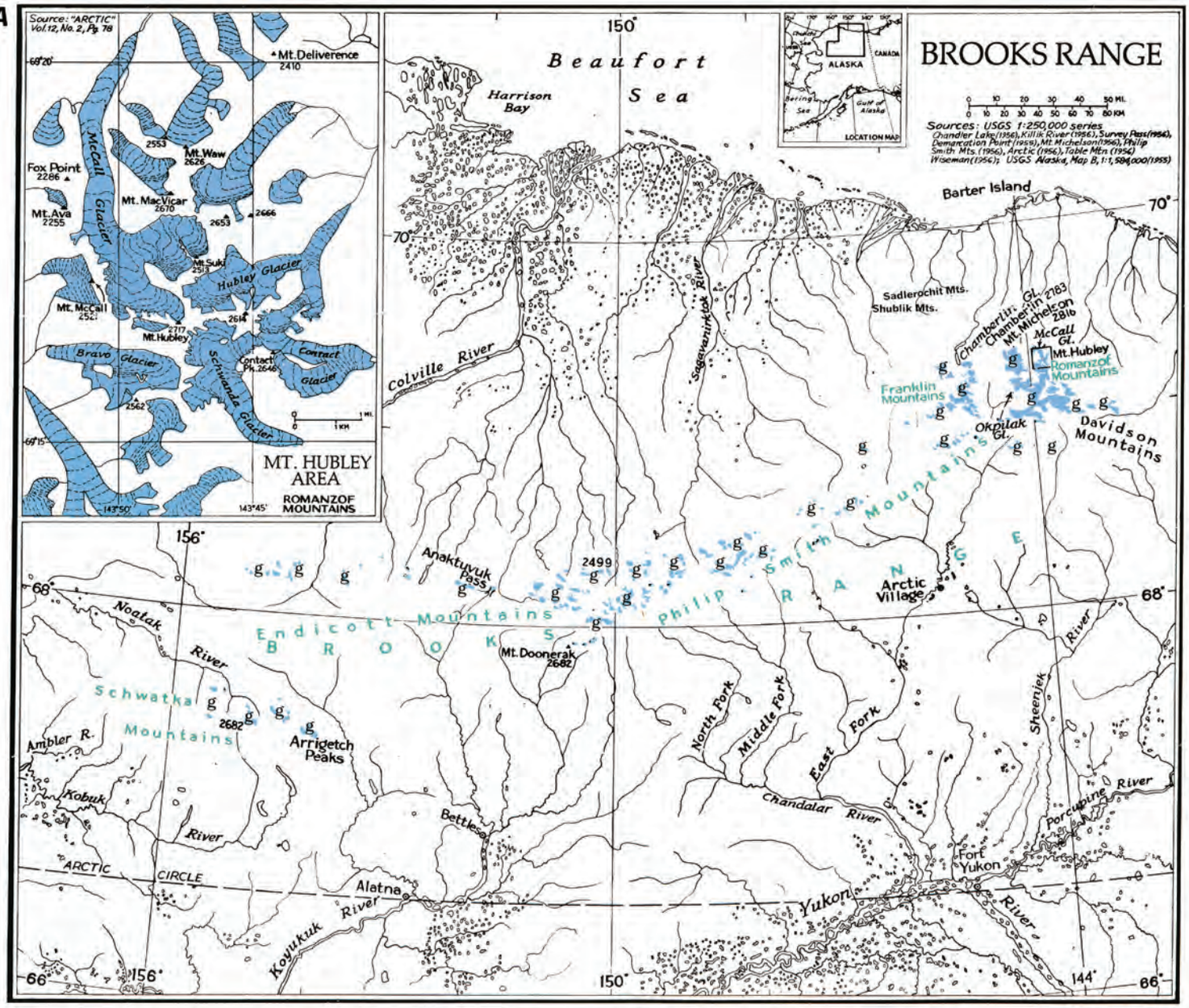
A
BROOKS RANGE
Beaufort Sea
Harrison Bay
Barter Island
Colville River
Sagavanirktok River
Sadlerochit Mts.
Shublik Mts.
Franklin Mountains
Okpilak Gl.
Davidson Mountains
Romanzof Mountains
Mt. Hubley
McCall Gl.
Chamberlin Gl.
Mt. Chamberlin 2783
Mt. Michelson 2810
Arctic Village
Anaktuvuk Pass
2499
Endicott Mountains
Philip Smith Mountains
Noatak River
Mt. Doonerak 2682
Schwatka Mountains
Ambler R.
Kobuk River
Arrigetch Peaks
North Fork
Middle Fork
East Fork
Chandalar River
Sheenjek River
Porcupine River
Fort Yukon
Yukon River
Alatna River
Koyukuk River
ARCTIC CIRCLE
Bettles
ALASKA
CANADA
LOCATION MAP
Sources: USGS 1:250,000 series
Chandler Lake (1956), Killik River (1956), Survey Pass (1956), Demarcation Point (1959), Mt. Michelson (1956), Philip Smith Mts. (1956), Arctic (1956), Table Mtn (1954) Wiseman (1954); USGS Alaska, Map B, 1:1,584,000 (1955)
MT. HUBLEY AREA
ROMANZOF MOUNTAINS
Source: "ARCTIC" Vol. 12, No. 2, Pg. 78
Mt. Deliverence 2410
Fox Point 2286
Mt. Waw 2626
Mt. MacVicar 2670
Mt. Ava 2255
Mt. Suki 2513
Mt. McCall 2521
Mt. Hubley 2717
Hubley Glacier
McCall Glacier
Bravo Glacier
Schwanda Glacier
Contact Glacier
Contact Ph. 2646
B
BROOKS RANGE
Area of figure

◄ ***Figure 435.***—**A**, *Index map of the central and eastern Brooks Range showing major secondary mountain ranges and general location of glaciers (g) (index map modified from Field, 1975a). Names of glacierized ranges shown in green, unglacierized ranges in black.* **B**, *Enlargement of NOAA Advanced Very High Resolution Radiometer (AVHRR) image mosaic of the Brooks Range in summer 1995. National Oceanic and Atmospheric Administration image mosaic from Mike Fleming, Alaska Science Center, U.S. Geological Survey, Anchorage, Alaska.*

margins of the Brooks Range. At least five neoglacial advances occurred in the central Brooks Range, dated at 4,400 yr B.P., 3,500 yr B.P., 2,900 yr B.P., 1,800±500 yr B.P., and 1,120±180 yr B.P. (Ellis and Calkin, 1979, 1984).

Landsat MSS images that cover the Brooks Range have the following Path/Row coordinates: 75/11, 75/12, 76/11, 76/12, 77/11, 77/12, 78/11, 78/12, 79/11, 79/12, 80/11, 80/12, 81/12, 82/12, 83/12, and 84/12 (fig. 3, table 1). Individually, most of the glaciers in the Brooks Range are too small to be delineated on Landsat MSS images; however, many of the glacier tongues in the Romanzof and Franklin Mountains can be discerned. Glacierized areas are mapped on the following 1:250,000-scale USGS topographic quadrangle maps of Alaska: Demarcation Point (1955), Table Mountain (1956), Mount Michelson (1956), Arctic (1956), Philip Smith Mountains (1956), Chandler Lake (1956), Killik River (1956), and Survey Pass (1956) (appendix A).

Very little was known about the glaciers of the Brooks Range until the second half of the 20th century. Writing about northern Alaska glaciers in the first third of the 20th century, Smith and Mertie (1930) described only three. Because USGS reconnaissance surveys made before World War I included photographs of more than a dozen glaciers, Smith and Mertie's work needs to be viewed as applicable only to the larger valley glaciers in the Brooks Range. In June 1907, Leffingwell (1919) mapped in the Romanzof Mountains and took a number of photographs of Okpilak Glacier and adjacent areas (fig. 436). Four years later, in July 1911, Smith photographed several glaciers in the Arrigetch Peaks area in the central Brooks Range. Significant new information began to be collected beginning in the late 1950s, mostly as a direct result of research carried out during the IGY. By the late 20th century, aerial photography and systematic mapping of the Brooks Range revealed that significantly more glaciers existed than previously expected. An inventory of Brooks Range glaciers by the USGS (C Suzanne Brown, oral commun., 1992) identified 1,001 glaciers having a total area of 723 km^2.

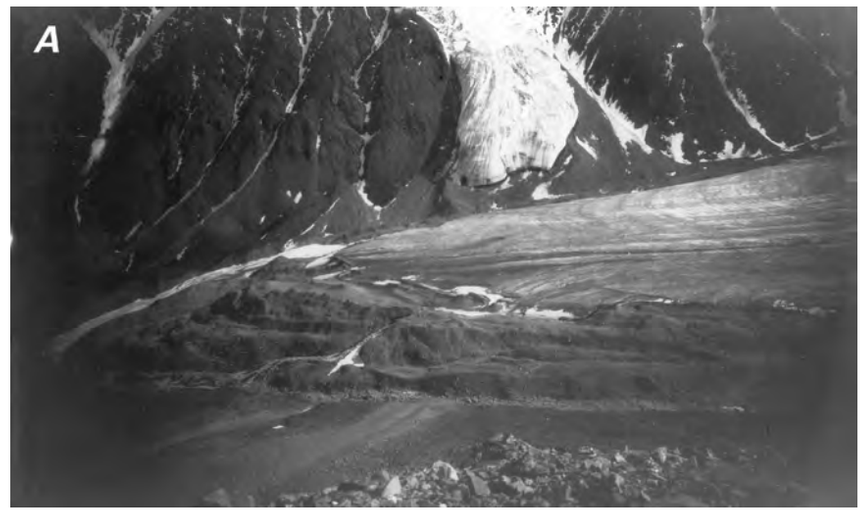

Figure 436.—*Three June 1907 photographs of Okpilak Glacier, Romanzof Mountains.* **A**, *The terminus of Okpilak Glacier and an unnamed hanging glacier. Abandoned lateral moraines on both sides of the hanging glacier and an elevated multiple-lobe terminal-recessional moraine complex at the terminus of Okpilak Glacier suggest that the glaciers had thinned significantly before 1907. The moraine complex may mark Okpilak Glacier's "Little Ice Age" maximum extent. The proximity of the terminus of Okpilak Glacier to the moraine complex suggests that retreat pre-1907 was less than 100 m.* **B** *and* **C**, *see following page.*

Figure 436.—**B**, *View upglacier toward the glacier's source. The low-relief rounded right margin of the glacier and the elevated lateral moraine are all evidence for previous thinning of Okpilak Glacier.* **C**, *View downglacier toward the glacier's terminus. The emergent medial moraine and the three tributary glaciers that enter from the left, all separated from the main ice trunk and mantled by debris, are evidence for previous thinning and retreat of the Okpilak Glacier and its tributaries. Photographs by Ernest de K. Leffingwell. Photographs Leffingwell 84* (A)*, 63* (B)*, and 64f* (C) *are from the USGS Photo Library, Denver, Colo.*

Romanzof Mountains

The 105-km-long Romanzof Mountains (figs. 1, 435, 437), located between the Hulahula and Kongakut Rivers, have a glacier area of about 260 km^2 (Denton, 1975b, p. 653) and contain at least 188 glaciers (Evans, 1977), 4 of which have lengths of 5 km or more. Wendler (1969) determined that no glacier ice was exposed at elevations of less than 1,500 m and that at least 66 percent of the glaciers are located on north-facing slopes (fig. 438); only about 15 percent have south-facing exposures. Studies of two glaciers—8.3-km-long Okpilak Glacier (figs. 436, 439) and 7.6-km-long McCall Glacier (figs. 440, 441)—have provided significant information about 20th century glacier fluctuations and related changes. McCall Glacier was intensively investigated during the IGY, and the International Hydrological Decade (IHD), which ran from 1965 to 1974. Investigations continue to the present.

Okpilak Glacier (figs. 436, 439), which Leffingwell visited in 1907 (Leffingwell, 1919), descends from an unnamed 2,435-m-high mountain about 18 km south of Mount Michelson. In 1958, Sable (1960) examined a number of glaciers in the Romanzof Mountains and revisited several photographic sites occupied by Leffingwell at Okpilak Glacier. A comparison of photographs documents that the Okpilak Glacier retreated more than 300 m in the intervening 51 years. Sable (1960) reported that Okpilak's lateral moraines were 45±6 to 63.5±6 m above the margins of the glacier in 1956–58. In 1907, they ranged from being level to 6 m above the ice (fig. 436). Sable stated (p. 185) that "The average amount of thinning in the lower 1.2 miles (2.3 km) is estimated to be 150 feet (45.3 m), and the mean rate from 1907 to 1958 to be about 3 feet per year (0.9 m)." Hence, the Okpilak Glacier had thinned

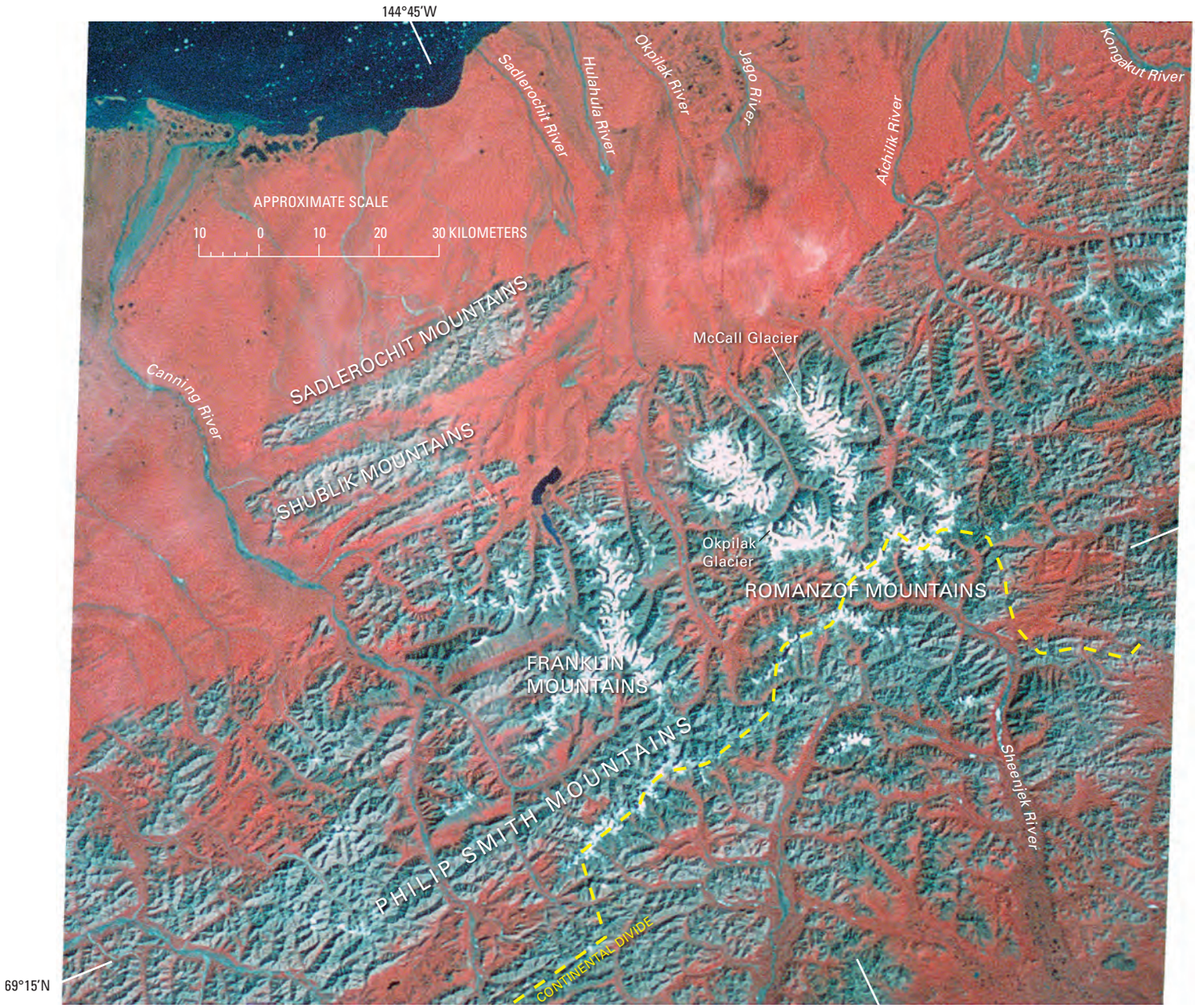

***Figure 437.**—Annotated Landsat 2 MSS false-color composite image of the Brooks Range from just west of Canning River to west of the Kongakut River. Shown are the Romanzof, Franklin, Sadlerochit, and Shublik Mountains, and part of the Phillip Smith Mountains. The location of the largest concentration of glaciers in the Brooks Range occurs north of the Continental Divide in the center of this image. Landsat image (22387–20443, bands 4, 5, 7; 5 August 1981; Path 77, Row 11) is from the USGS, EROS Data Center, Sioux Falls, S. Dak.*

from 33 to 69.5 m (0.65–1.35 m a^{-1}) between 1907 and 1958. Sable also commented that, the ratio of ice lost to thinning versus the ice lost by recession of the Okpilak Glacier terminus is roughly estimated to be at least 25:1. Sable (1960, p. 185) further stated that "All the smaller glaciers in the vicinity of Okpilak Glacier, for which photographic information from 1907 and 1958 can be compared, show evidence of marked recent recession and thinning." Figure 439 is an AHAP false-color infrared vertical aerial photograph of Okpilak Glacier taken on 24 August 1982, 75 years after Leffingwell's ground photographs (fig. 436).

Located about 15 km northeast of Okpilak Glacier, 7.6-km-long McCall Glacier (figs. 440, 441), which has an area of 6.0 km^2, heads on 2,693-m-high Mount Hubley. Its terminus is located at an elevation of about 1,350 m. In August 1956, Walter A. Wood and Richard C. Hubley, accompanied by Robert W. Mason (Mason, 1959), traveled to northern Alaska hoping to find "a valley glacier in the highest area of the Brooks Range... that would lend itself to a micrometeorological and glacier-movement survey program that could be undertaken during the International Geophysical Year" (Mason, 1959, p. 77). They quickly located "a slender valley glacier with a gentle gradient,

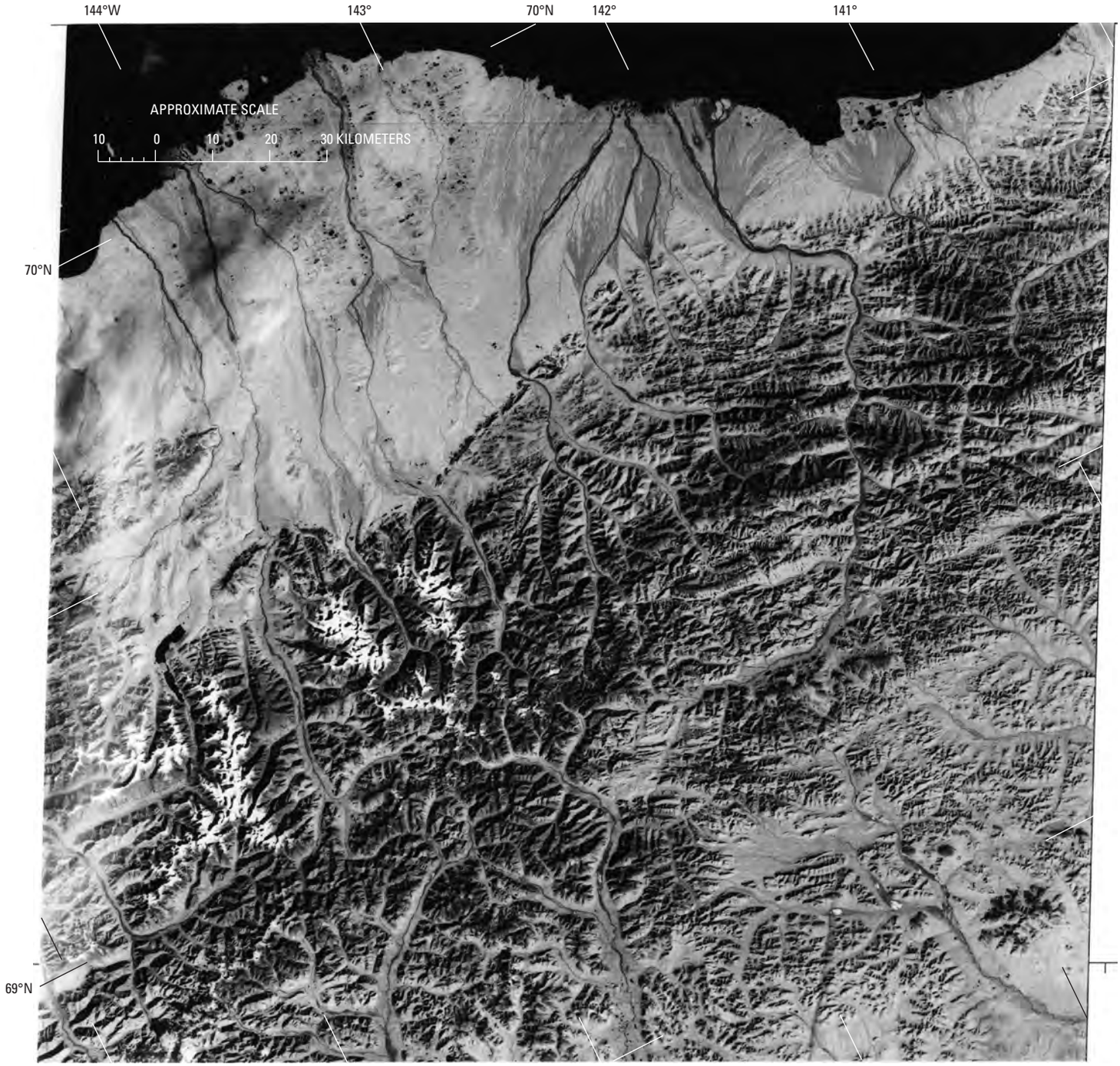

Figure 438.—*Landsat 3 MSS image of the eastern part of the Brooks Range showing glaciers in the Franklin Mountains and Romanzof Mountains (left side of image). The largest glacier in the Brooks Range is less than 10 km long. Most of the glaciers are in steep cirques with northern exposures. The most detailed glacier inventory to date (C Suzanne Brown, oral commun., 1992) counted 1,001 glaciers, with a total area of 723 km^2 in the Brooks Range. Most of these glaciers are too small to be discernible on Landsat MSS images. Many of these glaciers were already retreating before observations by E. de K. Leffingwell in 1907 (Hamilton, 1965). Patches of river ice (aufeis) deposits from the previous winter (1977–1978) remain and can be seen in the lower right corner of the image. Landsat image and caption courtesy of Robert M. Krimmel, U.S. Geological Survey. Landsat image (30177–20435; band 7; 29 August 1978; Path 76, Row 11) is from the USGS, EROS Data Center, Sioux Falls, S. Dak.*

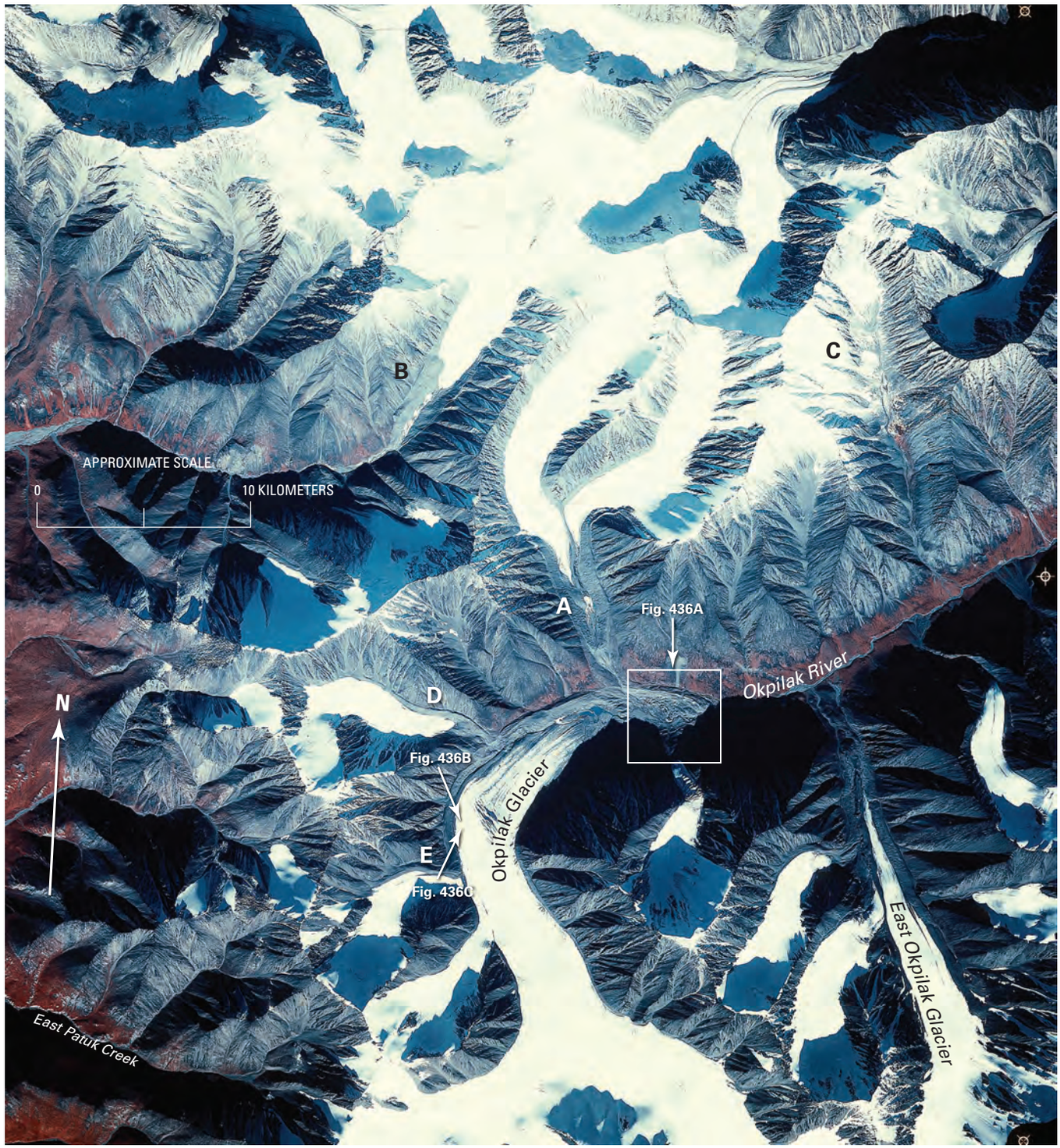

Figure 439.—*24 August 1982 annotated AHAP false-color infrared vertical aerial photograph of the eastern Romanzof Mountains showing Okpilak Glacier, East Okpilak Glacier, and more than a dozen other unnamed glaciers. The location of E. de K. Leffingwell's photograph of the position of the terminus of Okpilak Glacier in 1907 is shown, as well as the view directions of the two other E. de K. Leffingwell photographs (figs. 436*B, C*). The debris-mantled, stagnant termini of many of the glaciers can be seen in this photograph. Five glaciers, labeled A through E and one, informally called East Okpilak Glacier by Raybus and Echelmeyer (1998), show either conspicuous retreat of the terminus or elevated lateral and (or) terminal moraines, clear evidence of glacier thinning and retreat. AHAP photograph no. L28F2321 from GeoData Center, Geophysical Institute, University of Alaska, Fairbanks, Alaska.*

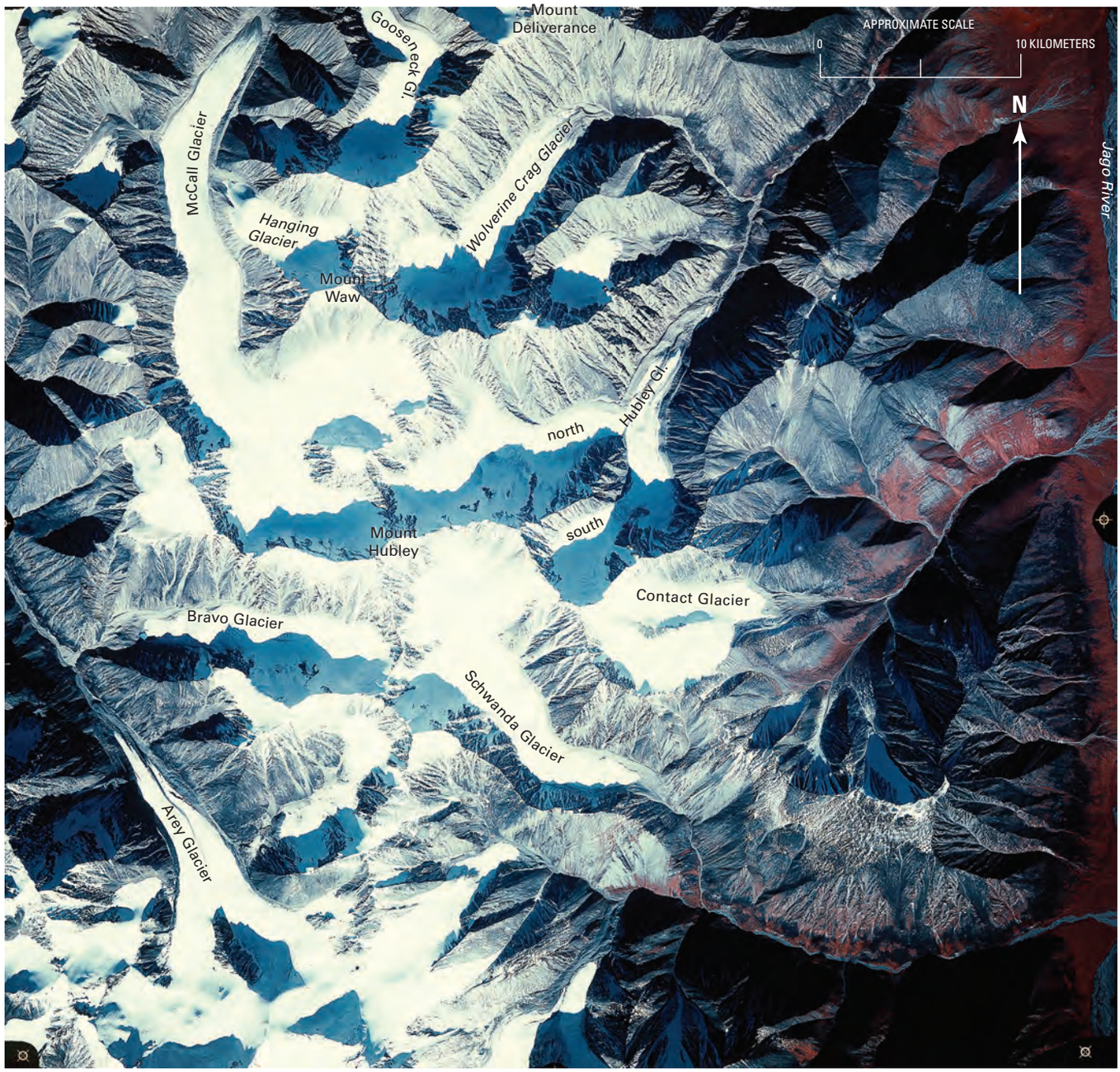

no ice falls, limited crevassing, and no tributary cirque glaciers. The glacier terminus lay almost at the frontal scarp of the mountains. This meant that the glacier could, if necessary, be approached on foot from a low camp on the tundra, that a light plane on skis could probably land on the glacier without difficulty, and that perhaps vehicles could be driven up the valley to transport fragile supplies to a glacier camp site" (Mason, 1959, p. 77–78). Hubley named the glacier for John McCall, an Alaskan geologist who died in 1954. Ironically, Hubley himself died in an accident on McCall Glacier in October 1957. Work started in May 1957 and continued through the end of the summer of 1958. A detailed topographic map (fig. 441) was made by the AGS from geodetic ground control collected in 1957 and aerial photography acquired by the USAF in 1958. Summaries of the results of IGY glaciological and geological investigations of McCall Glacier were presented by Sater (1959) and Keeler (1959).

***Figure 440.**—Annotated 24 August 1982 AHAP false-color infrared vertical aerial photograph of the eastern Romanzof Mountains showing Mount Hubley, Mount Waw, Mount Deliverance, McCall Glacier, Gooseneck Glacier, Bravo Glacier,* Wolverine Crag Glacier*, north Hubley Glacier, south Hubley Glacier, Arey Glacier, and* Hanging Glacier*. All of the named glaciers show evidence of retreat and thinning. AHAP photograph no. L27F2369 from the GeoData Center, Geophysical Institute, University of Alaska, Fairbanks, Alaska.*

Figure 441.—*Topographic map of McCall Glacier produced by the American Geographical Society (1960) based on 1958 vertical aerial photography and 1957 geodetic ground control. More than 75 percent of the glacier exists at an elevation of greater than 1,750 m. A larger version of this figure is available online.*

Between 1969 and 1975, research continued on the following attributes of McCall Glacier: heat balance (Wendler and Weller, 1974); a comparison of monitoring methods (stake measurements versus controlled run-off site measurements versus calculated heat balance) for determining ice melt (Wendler and Ishikawa, 1973); the heat, ice, and water balance of the glacier (Wendler and Ishikawa, 1974a); the effect of slope, exposure, and mountain screening on solar radiation reaching the glacier (Wendler and Ishikawa, 1974b); and climatological change (Dorrer and Wendler, 1976). All work was done as part of the IHD. During four years of observation (1969–72), McCall Glacier's mass balance was consistently negative. Ninety-eight percent of ice loss was owing to melting and 2 percent to evaporation.

During 1993 and 1994, a University of Alaska Fairbanks scientific team returned to the glacier to investigate how it had changed since the IHD. Continuous measurements of temperature, precipitation, short-wave radiation, and snow depth began in June 1993. The ice surface and the outline of the terminus were surveyed using optical and GPS methods, and ice thickness was determined by radio-echo-sounding methods. The survey determined that the maximum ice thickness was 250 m in McCall's overdeepened lower cirque; the average thickness along the glacier's centerline was 140 m (Raybus and Echelmeyer, 1997). A contour map of the bed of McCall Glacier was made from the ice-thickness measurements. The present velocity field, the elevation, the volume change from 1972 to 1993, and the average mass balance during this period were determined from the surveys. Annual velocities measured during 1993 and 1994 were found to be similar to those measured in the 1970s. However, velocities measured in the ablation area during the summer of 1993 were about 30 percent greater than the annual velocities for the same area. This discovery indicated to Raybus and Echelmeyer (1997) that McCall Glacier slides in summer and led them to suggest that it is a polythermal glacier containing a mixture of temperate and polar ice. Ice temperatures in the accumulation area range between -1 and -1.5°C; basal ice is temperate in the accumulation area.

Geodetic airborne laser altimeter surveys (profiles of surface elevation) (Sapiano and others, 1998) show that, since 1958, the elevation of the glacier surface has decreased everywhere, from a few meters in the accumulation zone to more than 70 m at an elevation of about 1,425 m near the terminus. Total volume of ice lost was 6.4×10^7 m^3. The long-term mass balance between 1972 and 1993 was -0.33 m a^{-1} (Raybus and Echelmeyer, 1998). The average mass balance from 1993 to 1996 was -0.60 m a^{-1}. These results document a significant thinning of the glacier during the second half of the 20th century. Because the average mass balance of McCall Glacier between 1958 and 1972 was -0.15 m a^{-1}, the 1993–96 mass balance represents a 400 percent increase in the already negative mass balance and also documents an increase in the rate of volumetric loss since the early 1970s. Individual hydrologic year (HY) annual balances are -42 cm in HY 1969, -8 cm in HY 1970, -14 cm in HY 1971, -19 cm in HY 1972, -48 cm in HY 1993, -74 cm in HY 1994, and -55 cm in HY 1995 (Bernhard Raybus, oral commun., 1996). Repeated surveys of detailed profiles across the lower ablation area from 1969 to 1994 show that a threefold increase in the rate of surface lowering occurred after 1975 (Raybus and Echelmeyer, 1998).

In the 37 years between 1956 and 1993, the area of McCall Glacier decreased from about 6.2 to 6.0 km^2, its length decreased by 353 m, and it thinned an average of 10.5 m. In the 14 years between 1958 and 1972, the terminus retreated 68 m, an average recession rate of 5.7 m a^{-1}. In the 21 years between 1972 and 1993, the terminus retreated 285 m, more than doubling its rate, for an average recession rate of 13.6 m a^{-1}.

Raybus and Echelmeyer (1998) also compared surface-elevation and terminus profiles of 10 other glaciers (fig. 440) located within a 30-km radius of McCall Glacier, collected between 1993 and 1995, with topographic maps

made in 1956 or 1973. Their comparisons showed that nine glaciers had average mass balances of between -20 and -54 cm a^{-1}: 3.1-km-long Gooseneck Glacier (area 1.1 km^2), 3.2-km-long Bravo Glacier (area 1.6 km^2), 3.0-km-long *Wolverine Crag Glacier* (area 1.9 km^2), 3.1-km-long north Hubley Glacier (area 1.8 km^2), 3.0-km-long south Hubley Glacier (area 1.2 km^2), 4.2-km-long Arey Glacier (area 4.6 km^2), 8.3-km-long Okpilak Glacier (called *West Okpilak Glacier* by Raybus and Echelmeyer, 1998) (area 11.0 km^2), 6.0-km-long *East Okpilak Glacier* (area 8.8 km^2), and 7.7-km-long Esetuk Glacier (area 7.1 km^2). A tenth—1.8-km-long *Hanging Glacier*, which has an area of 0.8 km^2—had an average mass balance of -1 cm a^{-1}.

Raybus and Echelmeyer's (1998) data also showed that all 10 glaciers retreated during the period of comparison. They calculated changes in length, changes in ice volume, average changes in elevation, and mean annual mass balances for: Gooseneck Glacier (-16 m, -1.4×10^7 m^3, -12.3 m, -28 cm a^{-1}), Bravo Glacier (-300 m, -1.8×10^7 m^3, -10.2 m, -27 cm a^{-1}), *Wolverine Crag Glacier* (-265 m, -4.6×10^7 m^3, -23.3 m, -27 cm a^{-1}), north Hubley Glacier (-1,030 m, -4.2×10^7 m^3, -22.0 m, -54 cm a^{-1}), south Hubley Glacier (-890 m, -134×10^7 m^3, -10.5 m, -25 cm a^{-1}), Arey Glacier (-570 m, -5.2×10^7 m^3, -11.4 m, -27 cm a^{-1}), *West Okpilak Glacier* (-420 m, -17×10^7 m^3, -15.2 m, -37 cm a^{-1}), *East Okpilak Glacier* (-1,020 m, -7.2×10^7 m^3, -8.1 m, -20 cm a^{-1}), Esetuk Glacier (-814 m, -9.2×10^7 m^3, -12.9 m, -30 cm a^{-1}) [see 24 August 1982 AHAP false-color infrared vertical aerial photograph no. L27F2372], and *Hanging Glacier* (-260 m, -4.0×10^5 m^3, -0.5 m, -1 cm a^{-1}).

Combining Sable's (1960) observations with those of Raybus and Echelmeyer (1998) indicates that Okpilak Glacier underwent a maximum thinning of as much as 84.7 m and retreated more than 750 m during an 85-year observational period during the 20th century. The annual average change is 1.0 m a^{-1} of thinning and 8.8 m a^{-1} of terminus retreat.

A concentration of small cirque and valley glaciers straddles the continental divide on either side of the Sheenjek River (figs. 435, 437). Many glaciers there show multiple evidence of recent retreat and stagnation, and some cirques have recently become ice free (see 24 August 1982 AHAP false-color infrared vertical aerial photograph no. L30F1444).

Franklin Mountains

The Franklin Mountains (figs. 1, 435, 437, 438, 442) support several dozen cirque and small valley glaciers between the Sadlerochit and Hulahula Rivers. The greatest concentrations of glacier ice and the largest glaciers are located along a 25-km-long ridge and upland between the summit of Mount Chamberlin and the head of the Canning River. Two named and two unnamed glaciers descend from 2,739-m-high Mount Chamberlin's summit and flanks. Chamberlin Glacier on the northwest and Peters Glacier on the southwest are the named glaciers (fig. 442). Chamberlin Glacier, which is 2.4 km long and as much as 800 m wide (Denton, 1975b, p. 654), terminates at an elevation above 2,000 m. During the IGY in 1958, meteorological investigations of the glacier were conducted by the USAF Cambridge Research Center (later USAF Cambridge Research Laboratories; now Air Force Phillips Laboratory). Larsson (1960) concluded that the current meteorological regime measured at the glacier was incompatible with the continuing existence of the glacier. A glacier hydrology and hydrochemistry study was carried out on the Chamberlin Glacier by Rainwater and Guy (1961). Several longer unnamed glaciers flow into Carnivore Creek and West Patuk Creek to the south (fig. 442). All of the glaciers examined in the Franklin Mountains show evidence of thinning and retreat.

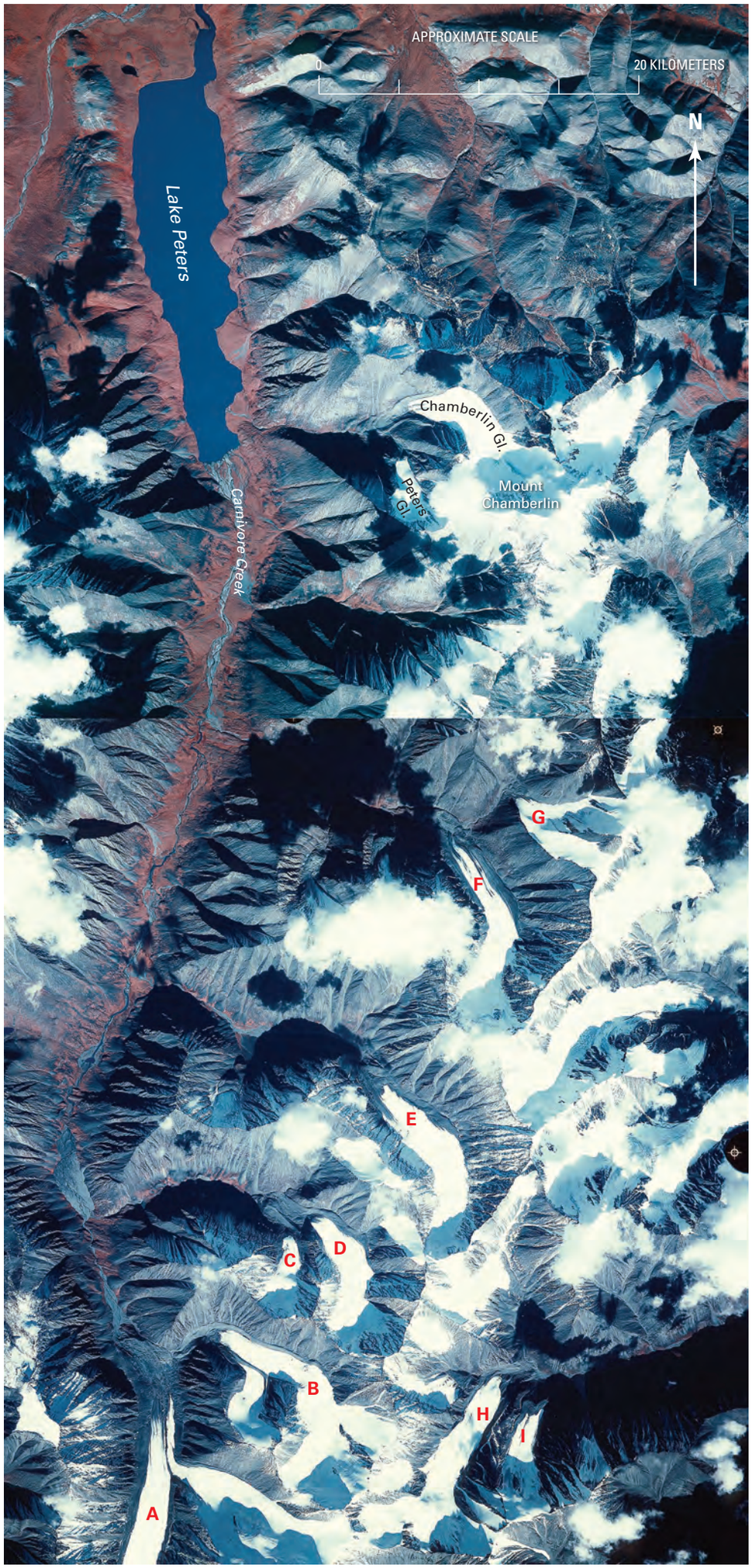

Figure 442.—*24 August 1982 annotated AHAP false-color infrared vertical aerial photographic mosaic of the central Franklin Mountains showing Mount Chamberlin, Lake Peters, Carnivore Creek, Chamberlin Glacier, Peters Glacier, and several unnamed glaciers. Shadows and clouds obscure several of the termini, but Chamberlin Glacier shows a conspicuous, fresh-looking elevated end moraine — lateral moraine complex, several kilometers downvalley from the exposed-ice terminus, evidence of recent glacier thinning, and retreat. On the southern part of the mosaic, two unnamed glaciers, A and B, have separated and retreated into their individual valleys, as have two others labeled C and D. Five other unnamed glaciers, labeled E through I, show multiple evidence of recent retreat and stagnation. Recent end moraine positions are shown for several of the glaciers. AHAP photograph no. L27F2377 (north) and L28F2316 (south) from GeoData Center, Geophysical Institute, University of Alaska, Fairbanks, Alaska.*

Philip Smith and Endicott Mountains

Ellis and Calkin (1979) studied 133 mostly unnamed glaciers in a 4,000-km^2 area of the Philip Smith and Endicott Mountains (fig. 435). The area is centered around Atigun Pass (lat 68°08'N., long 149°29'W.), a rugged area where relief exceeds 1,000 m and peaks rise to 2,300 m. All of the active glaciers occurred at elevations above 1,500 m; 97 percent were located north of the Continental Divide. Glaciers that were fronted by stable moraines varied uniformly in elevation by latitude. Glacier terminus elevations were at about 1,600 m south of the Continental Divide. The further north the glacier, the higher the terminus, maximum elevations being about 2,000 m 25 km to the north. Typically, the glaciers had 220 m of relief, ranged in length from less than 100 m to about 2.5 km, and had areas of 2 km^2 or less. Ellis and Calkin (1979, p. 406) stated that "Under the present climate, the cirque glaciers of the area are wasting away." During July and August of 1977, they observed the complete loss of the previous year's snow accumulation plus the loss of an additional 1 to 2 m of glacier ice at three cirque glaciers near Atigun Pass.

Ellis and Calkin (1979) evaluated glacial deposits adjacent to the ice margins of 102 glaciers. Of these, 55 extended into ice-cored or ice-cemented moraines; 23 extended into ice-cored looping rock glacier ridges located on older rock glacier deposits; 19 extended into ice-cored rock glaciers; and 5 had no associated deposits. They also mapped 113 tongue- and 502 lobate-shaped rock glaciers in the area. Of the 83 tongue-shaped rock glaciers that occur north of the Continental Divide, 76 percent are active, and 46 percent have exposed ice cores. South of the divide, only 30 percent of the tongue-shaped rock glaciers are active, and 9 percent have exposed ice cores. On both sides of the divide, rock glaciers with exposed ice cores have active termini.

Lobate rock glaciers occur in a 500-m-thick altitudinal zone from lat 68°N. to the foothills of the Brooks Range. South of the Continental Divide, only 50 percent of the lobate-shaped rock glaciers are active; north of the Continental Divide, 70 percent of the lobate-shaped rock glaciers are active. Active lobes occur 150 m higher than inactive lobes.

In a later study, Ellis and Calkin (1984) discussed Neoglacial glacier fluctuations in the central Brooks Range, stating that (p. 897) "for the past ~1,100 yr, cirque glaciers have been continuously in more extended positions than they are today... the last two major advances occurred at 800 ±150 (A.D.) and 390 ±90 yr B.P. (A.D. 1410–1600). Glaciers across the central Brooks Range stayed close to their maxima until A.D. 1640–1750. Historical photographs and lichenometry show that retreat was most rapid after A.D. 1870 and decelerated after the mid-1900s. Recession from this most recent Neoglacial maximum has amounted to 150–700 m and continues at present." Results from the eastern Brooks Range suggest that the rate of retreat is again accelerating into the early 21st century.

Elsewhere in this region, Porter's (1966) study of glaciers in the Anaktuvuk Pass area (lat 68°09'N., long 151°43'W.) showed that many lie in deep north-facing cirques and are located at elevations below the present regional snowline. He noted that the snowline was at about 2,070 m, well above the cirque glaciers in the area, and concluded that they are in a state of disequilibrium with present climatic conditions.

In the Arrigetch Peaks area (lat 67°25'N., long 154°13'W.), active glaciers head at elevations of approximately 1,800 m and flow to elevations below 1,500 m. Many stagnant ice bodies lie between 1,200 and 1,500 m. In 1962, Hamilton (1965) reoccupied photographic stations established in 1911 by Philip Smith (1912) and made photographic comparisons of glacier position and glacier mass balance. In the 51 years between studies, Hamilton noted both a recession and a thinning of the glaciers. In one instance, he stated that an ice-cored moraine had thinned by roughly 20 m. In another, he noted "the

ice in the head-wall gully... has thinned appreciably, leaving a pronounced trimline where none was visible in 1911" (Hamilton, 1965, p. 483). In a third observation, he stated that "Present terminal positions are roughly 200 m further up-valley and lie at elevations nearly 100 m higher than in 1911."

Schwatka Mountains

At least four peaks support valley glaciers in the Schwatka Mountains (fig. 435) south of the Noatak River. The largest glaciers descend from the slopes of 2,571-m-high Mount Igikpak and 2,208-m-high Oyukak Mountain. The largest glacier on Mount Igikpak is about 3 km long and unnamed and terminates at an elevation of about 1,150 m. Glaciers also exist on the flanks of Mount Chitiok and Shulakpak Peak.

Summary

During the period of the Landsat baseline (1972–81), all available evidence suggests that the glaciers of the Brooks Range were thinning and retreating. These conclusions are based on published field descriptions, the author's comparison of the size and number of glaciers shown on pre-Landsat baseline USGS topographic maps (ca. 1950s) (appendix A), and 1982 AHAP photography from the end of the Landsat baseline period. Limited information is available about behavior at the end of the 20th and into the early 21st century. However, every glacier described showed significant evidence of thinning and retreat.

Summary and Conclusions

During the period of the Landsat Baseline Decade (1972–1981), glaciers covered about 75,000 km^2 of Alaska (Post and Meier, 1980, p. 45), representing about 5 percent of Alaska's land area. Glacierized regions include 11 mountain ranges (Coast Mountains; Saint Elias Mountains; Chugach Mountains; Kenai Mountains, including Montague Island; Aleutian Range; Wrangell Mountains; Talkeetna Mountains; Alaska Range; Wood River Mountains; Kigluaik Mountains; and Brooks Range), one large island (Kodiak Island), one island archipelago (Alexander Archipelago), and one island chain (Aleutian Islands). Glaciers in Alaska extend over an area from the southeast at lat 55°19'N., long 130°05'W., about 100 km east of Ketchikan to the southwest at Kiska Island at lat 52°05'N., long 177°35'E., in the Aleutian Islands and to the north at lat 69°20'N., long 143°45'W., in the Brooks Range. Because the actual number of glaciers has never been systematically inventoried, it is unknown but probably exceeds 100,000. Alaskan glaciers range in elevation from more than 6,000 m to below sea level. Most of Alaska's glaciers are unnamed; less than 700 have been officially named by the BGN (appendix C) (http://geonames.usgs.gov/).

During the "Little Ice Age," the total glacier-covered area and the number of mountain ranges and islands having glacier cover were significantly larger than they were during the "baseline" period. Since the end of the "Little Ice Age," there has been a decrease in the glacier area and the thickness of most of the Earth's glacierized areas in the middle and low latitudes, along with advances of individual glaciers in some areas including about a dozen in Alaska. However, the timing, magnitude, and complexity of this post-"Little Ice Age" glacier change have been different in each of Alaska's 14 glacierized areas. Although there is almost total thinning of glaciers in lower elevations and a retreat of glacier termini, the details presented in this volume demonstrate that the current status of Alaska's glaciers varies significantly from area to area and with elevation.

Although most Alaskan glaciers at lower elevations are retreating, not all are doing so. At elevations below about 1,500 m, about a dozen glaciers, including Hubbard, Harvard, Meares, Taku, and Lituya Glaciers (all tidewater or former tidewater glaciers), are currently thickening and advancing. Many glaciers at higher elevations are thickening or exhibit no change. Several volcanoes, including Redoubt Volcano, have had 20th century eruptions that melted summit glaciers, but new glaciers have formed in their craters.

The following region-by-region summary details the observed changes in glaciers described in this volume.

Coast Mountains.—During the period of the Landsat Baseline Decade, the glacierized area of the Coast Mountains was approximately 10,500 km^2 (Post and Meier, 1980, p. 45). Taku, Hole-in-the-Wall, and Mead Glaciers were advancing. All other valley and outlet glaciers in the Coast Mountains were thinning and retreating. At the end of the 20th century and early in the 21st century, Taku Glacier was advancing, and Hole-in-the-Wall Glacier was stable. Mead Glacier was advancing in the 1990s and continues in the early 21st century; all other observed valley and outlet glaciers in the Coast Mountains continued to thin and retreat.

Alexander Archipelago.—Glaciers are mapped in mountainous areas on middle 20th century USGS 1:250,000-scale topographic maps on six of the islands in the Alexander Archipelago: Revillagigedo, Prince of Wales, Kupreanof, Baranof, Chichagof, and Admiralty Islands. During the period of the Landsat Baseline Decade, the Alexander Archipelago had a glacierized area of less than 150 km^2. No recent information exists about the status of these glaciers at the beginning of the 21st century. However, their small size, low elevation, and southerly location in an area with late 20th century

temperature increases indicate that they have probably continued to thin and retreat. Some glaciers may have melted completely and no longer exist.

St. Elias Mountains. —During the period of the Landsat Baseline Decade, the glacierized area of the Alaskan St. Elias Mountains was approximately 11,800 km^2 (Post and Meier, 1980, p. 45). Throughout the decade, Johns Hopkins, Grand Pacific, Margerie, Brady, North Crillon, Lituya, Hubbard, and Turner Glaciers were advancing. La Perouse and South Crillon Glacier were stable, although the positions of their termini fluctuated from year to year. All other valley and outlet glaciers in the St. Elias Mountains were thinning and retreating. At the beginning of the 21st century, North Crillon, Lituya, Hubbard, and Turner Glaciers were advancing. Johns Hopkins, La Perouse, and South Crillon Glacier were stable, although the positions of their termini fluctuated from year to year. All other observed valley and outlet glaciers in the St. Elias Mountains continued to thin and retreat.

Chugach Mountains. —During the period of the Landsat Baseline Decade, the glacierized area of the Chugach Mountains was approximately 21,600 km^2 (Post and Meier, 1980, p. 45). Two tidewater glaciers, Meares and Harvard Glaciers, were advancing throughout the decade; Bryn Mawr, Harriman, and Columbia Glaciers advanced during the early part of the "baseline" period. Smith Glacier was stable for most of the period, although the position of its termini fluctuated from year to year. All other valley and outlet glaciers in the Chugach Mountains were thinning and retreating. At the end of the 20th century and during the early 21st century, Meares, Harriman, and Harvard Glaciers were still advancing. All other valley and outlet glaciers in the Chugach Mountains were thinning, retreating, or stagnant.

Kenai Mountains. —During the period of the Landsat Baseline Decade, the glacierized area of the Kenai Mountains was approximately 4,600 km^2 (Post and Meier, 1980, p. 45). With the exception of Aialik and McCarty Glaciers, both of which advanced more than 500 m during the second half of the 20th century, all of the valley and tidewater glaciers in the Kenai Mountains continued to stagnate, thin, and (or) retreat. By the end of the 20th century, all of the valley and outlet glaciers in the Kenai Mountains continued to stagnate, thin, and (or) retreat. When Tiger Glacier was observed in 2000, it was at about the same location as it was in 1908. Because it had been retreating during much of the 20th century, Tiger Glacier must have undergone a late-20th century advance to regain its former position.

Kodiak Island. —During the Landsat Baseline Decade, the glacierized area of Kodiak Island was less than 15 km^2. A comparison of the sizes and numbers of glaciers shown on USGS topographic maps made from 1948 to1952 aerial photographs with AHAP photography from the middle of the "baseline" period (1977–78) show that the glaciers of Kodiak Island were thinning and retreating. No information exists about the status of Kodiak Island's glaciers at the end of the 20th century and the beginning of the 21st century. However, their small size, low elevation, and location on an island that has undergone a temperature increase and is surrounded by temperate ocean water suggest that its glaciers likely have continued to thin and retreat. Some may have melted completely away and no longer exist.

Aleutian Range. —During the period of the Landsat Baseline Decade, the glacierized area of the Aleutian Range was approximately 1,250 km^2 (Post and Meier, 1980, p. 45). All of the nonactive surge-type valley glaciers in the Aleutian Range were stagnant, thinning, and (or) retreating. Several glaciers surged during the "baseline" period, but no termini advances were reported. At the end of the 20th century and into the early 21st century, all of the valley and outlet glaciers in the Aleutian Range continued to thin, stagnate, and retreat. When Tuxedni Glacier was observed in 2000, it showed some evidence of a recent terminus advance. However, trimlines and abandoned moraines document a long-term history of retreat and thinning. The 1912 eruption of Mount Katmai melted and beheaded a number of summit and flank glaciers.

Following the eruption, two small glaciers formed on the talus beneath the crater rim. They continued to exist throughout the "baseline" period and into the early 21st century. Similarly, following the 1989-90 eruption of Mount Redoubt, snow and glacier ice accumulating in the crater have replaced snow and ice melted during the eruption.

Aleutian Islands. —During the period of the Landsat Baseline Decade, the glacierized area of the Aleutian Islands was approximately 960 km^2 (Post and Meier, 1980, p. 45). Glaciers are shown in mountainous areas on mid-20th century USGS 1:250,000-scale topographic maps on at least 10 islands in the eastern and central part of the Aleutian Islands. From east to west, islands where glaciers have been reported are Unimak, Akutan, Unalaska, Umnak, Herbert, Atka, Great Sitkin, Tanaga, Gareloi, and Kiska Islands. All of the mapped glaciers of the Aleutian Islands descend from the summits of active or dormant volcanoes, extending into either calderas or down their flanks. All head at elevations of greater than 1,200 m. No information exists about the status of glaciers in the Aleutian Islands during the "baseline" period or at the end of the 20th century and into the early 21st century. However, their small size, low elevation, and southerly latitudinal location in an area of late-20th century temperature increases indicates that the glaciers likely have continued to thin and retreat. Some may have melted completely and no longer exist.

Wrangell Mountains. —During the period of the Landsat Baseline Decade, the glacierized area of the Wrangell Mountains was approximately 8,300 km^2 (Post and Meier, 1980, p. 45). With the exception of *Athna Glacier* and *South* and *Center Mackeith Glaciers*, which were advancing, apparently in response to heat-flow-related nonclimatic forcing, all of the valley and outlet glaciers in the Wrangell Mountains were retreating, thinning, or stagnant. At the end of the 20th century and into the early 21st century, no additional information was available about *Athna Glacier* and *South* and *Center Mackeith Glaciers*. All other valley and outlet glaciers in the Wrangell Mountains continued to thin, stagnate, and retreat.

Talkeetna Mountains. —During the period of the Landsat Baseline Decade, the glacierized area of the Talkeetna Mountains was approximately 800 km^2 (Post and Meier, 1908, p. 45). Analyzing the comparative sizes and numbers of glaciers shown on topographic maps made from 1948 to 1952 aerial photography and on AHAP photography from the middle of the "baseline" period (1977) and just after the "baseline" period (1983) shows that the glaciers of the Talkeetna Mountains were thinning, retreating, and (or) stagnant. Every glacier observed from the air at the beginning of the 21st century (31 August 2000) showed evidence of thinning and retreat, and many smaller glaciers had completely disappeared.

Alaska Range. —During the period of the Landsat Baseline Decade, the glacierized area of the Alaska Range was approximately 13,900 km^2 (Post and Meier, 1980, p. 45). All of the nonactive, surge-type valley glaciers in the Alaska Range were stagnant, thinning, and (or) retreating. Several glaciers surged early during the "baseline" period, but no terminus advances were reported at the time or documented subsequently. At the end of the 20th century and into the early 21st century, all of the valley and outlet glaciers in the Alaska Range continued to thin, stagnate, and (or) retreat.

Wood River Mountains. —During the period of the Landsat Baseline Decade, the glacierized area of the Wood River Mountains was less than 230 km^2 (Post and Meier, 1980, p. 45; Kilbuk-Wood River Mountains). No reported observations were made of any Wood River Glaciers during the "baseline" period. However, a comparison of pre-"baseline" period topographic maps and photographs with 1984 AHAP photography shows that every glacier visible on the aerial photographs had lost length and area during the interval between the data sets. Every glacier continued to lose area and length through the late 20th century. No early 21st century information exists. Chikuminuk

Glacier was mapped in 1957 and 1958 during the IGY. Since then, its terminus region has thinned and retreated. However, at elevations above 1,000 m, it has thickened by an average of about 10 m.

Kigluaik Mountains. —During the period of the Landsat Baseline Decade, three glaciers—*Grand Union*, *Thrush*, and *Phalarope Glaciers*, which have a collective glacierized area of less than 3 km^2 (Post and Meier, 1980, p. 45; Seward Peninsula)—existed in the Kigluaik Mountains. Since then, they have received little attention. Field investigations performed in 1986, confirmed that other glaciers that existed during the early 20th century have completely disappeared and documented that the remaining three Kigluaik Mountain glaciers were continuing to decrease in area and length. Given the rate at which these three glaciers were retreating and thinning, it is possible that one or more of them may have subsequently disappeared. The absence of recent field observations, including recent aerial photography of the area, renders the continued existence of Kigluaik Mountains glaciers at the end of the 20th century and into the early 21st century a matter of speculation.

Brooks Range. —During the period of the Landsat Baseline Decade, the glacierized area of the Brooks Range was less than 723 km^2 (Post and Meier, 1980, p. 45). Analysis of published field descriptions and a comparison by the author of the sizes and numbers of glaciers shown on pre-Landsat baseline USGS topographic maps and 1982 AHAP photography from the end of the "baseline" period suggest that the glaciers of the Brooks Range are continuing to thin and retreat. Limited information is available about the status of the glaciers at the end of the 20th century and into the early 21st century. However, every glacier described showed evidence of thinning and retreat.

As was noted above, the general thinning and retreat of lower elevation temperate glaciers is one of the most visible manifestations of the post-"Little Ice Age" response of Alaska's glaciers to the changing regional climate. As the regional summaries of the status of Alaska's glaciers presented here document, most Alaskan mountain glaciers at lower elevations are stagnant and (or) retreating and thinning in response to a post-"Little Ice Age" regional warming. In fact, of the more than 1,000 glaciers described in this chapter, more than 98 percent are currently thinning, retreating, or stagnant. As has also been shown, local and regional variability has given every glacier in Alaska its own complex and unique history of change. For example, many glaciers in southeastern Alaska—such as most of the glaciers of the Glacier Bay and the Lynn Canal areas—began to retreat as early as the mid-18th century, some more than 100 years before the advent of systematic meteorological measurements of air temperatures; others in the same area advanced during that entire period. Today most of Alaska's glaciers continue to retreat. Others, such as the tidewater Harvard and Hubbard Glaciers, have been advancing for more than a century.

Nearly all mountain glaciers in Alaska are temperate; that is, meltwater exists in, on, or under the glacier for part, if not all, of the year. Globally, temperate and tropical mountain glaciers are shrinking on all continents and are thus excellent indicators of climate change. Small changes in temperature and precipitation can have an impact on the status of these glaciers. Ongoing glacier melting does, and will continue to substantially reduce the lengths, areas, thicknesses, and volumes of Earth's temperate mountain glaciers. As the glaciers of Alaska melt, their meltwaters flow into the Gulf of Alaska and into the Bering, Chukchi, and Beaufort Seas, contributing to global (eustatic) sea-level rise.

Many investigations have examined the role that temperate glaciers play in present and future sea-level changes; most of the attention has been directed toward the last five decades of the 20th century (National Research Council, 1977, 1983, 1984, 1990; Meier, 1984; 1990 1998; Dyurgerov and Meier, 1997a, 1997b, 1999, 2000; Bahr and Meier, 2000; Dyurgerov and Dwyer, 2000;

Arendt and others, 2002; Meier and Wahr, 2002). Almost all of these reports state that, if all the remaining nonpolar glacier ice were to melt, a sea-level rise of less than 1 m would result. Complete melting of the glacier ice in the Antarctic and Greenland ice sheets would lead to a potential global sea-level rise of about 80 m — 73.4 m from Antarctica, and 6.5 m from Greenland (Williams and Hall, 1993). Several of the studies state that glacier melting and meltwater production have increased significantly during the later part of the 20th century (Arendt and others, 2002; Meier and Dyurgerov, 2002). Of the approximately 4 percent of the glacierized area on Earth that is covered by mountain glaciers, less than one-tenth (<0.4 percent) is Alaskan glaciers. However, as Meier (1984) first showed, the glaciers of the Alaskan coastal region, most of which are melting rapidly under present climatic conditions, may contribute more than one-third of the total annual glacier meltwater entering the global ocean. Because current climate models predict future temperature increases, these glaciers may make even larger contributions to future rising sea level.

Arendt and others (2002), synthesized the result of more than a decade of geodetic airborne laser profiling of 67 glaciers in Alaska and adjacent Canada. The glaciers that they studied represent about 20 percent of the glacierized area of Alaska and adjacent Canada, including glaciers that have all or part of their termini calving into tidewater or into ice-marginal lakes and glaciers that terminate on land. They estimate the total annual volume change of Alaska glaciers, expressed as water equivalent, to be -52±15 $km^3\ a^{-1}$ for the period from the 1950s to the early 1990s and -96±35 $km^3\ a^{-1}$ for the period from the middle 1990s to the late 1990s. These volumes are equivalent to a rise in sea level of 0.14±0.04 mm a^{-1} during the early period and 0.27±0.10 mm a^{-1} during the more recent period.

With respect to thickness change, they report that most glaciers thinned during both periods, an indication of surface lowering. They stated that measurements for both early- and recent-period glaciers indicate that thinning during the recent period was more than twice as much (-1.8 m a^{-1}) as what they calculated for the early period (-0.7 m a^{-1}).

With respect to area, Arendt and others (2002) also reported that most (but not all) of the glaciers that they investigated had retreated. The total area of measured glaciers decreased 0.8 percent (131 km^2) during the early period and 0.4 percent during the recent period. They observed that approximately 10 percent of the sampled glaciers either advanced while simultaneously thinning or (during the early period) retreated while thickening. During the recent period, the 10 largest meltwater contributions came from Columbia (7.1 $km^3\ a^{-1}$), Bering (6.0 $km^3\ a^{-1}$), Malaspina (2.8 $km^3\ a^{-1}$), LeConte (1.0 $km^3\ a^{-1}$), Tazlina (0.56 $km^3\ a^{-1}$), Brady (0.54 $km^3\ a^{-1}$), Baird (0.42 $km^3\ a^{-1}$), Black Rapids (0.19 $km^3\ a^{-1}$), Mendenhall (0.14 $km^3\ a^{-1}$), and Susitna (0.11 $km^3\ a^{-1}$) Glaciers.

The two largest contributors of meltwater during the recent period — Columbia and Bering Glaciers, which together contributed 13.1 $km^3\ a^{-1}$ of water to the global ocean (nearly 15 percent of the annual total) — are not simply responding to changing climate. The significant increase in Columbia Glacier's meltwater production resulted from the onset of its catastrophic calving retreat, which began in the early1980s (Krimmel, this volume), whereas much of the ice lost at Bering Glacier is the result of rapid calving of ice from the surge-advanced terminus. Most of this ice was transported from the accumulation area into the ablation area by surge processes between 1993 and 1995 (see the Chugach Mountains section in this volume). Similarly, much of the increased meltwater contribution from Mendenhall Glacier results from the fact that, since 1990, its eastern terminus has ceased to be grounded on a sediment plain and is now calving into Mendenhall Lake (see the Coast Mountains section in this volume).

The significance of the contribution of Alaskan glaciers to global sea level can be seen by comparing similar data from Greenland. Krabill and others (2000) reported that analysis of 1994-99 aircraft laser altimeter surveys over Greenland indicates a net loss of approximately 51 $km^3\ a^{-1}$ of ice from the entire Greenland ice sheet. They stated that this amount is sufficient to raise sea level by 0.13 mm a^{-1}, approximately 7 percent of the observed rise. The estimated annual volume loss from Alaska during the recent period, $96\pm35\ km^3\ a^{-1}$ (Arendt, and others, 2002), is nearly twice that estimated for the entire Greenland ice sheet during the same period.

This chapter has summarized the areal extent and distribution of Alaska's glaciers during the Landsat Baseline Decade (1972–1981) and, where possible, drawn inferences about the past and speculated about the future. This "baseline" period can be used by both present and future researchers to document changes in the numbers, lengths, and areas of Alaskan glaciers. The diverse data contained herein document that many Alaskan glaciers are rapidly changing, with most glaciers at lower elevations thinning, retreating, and (or) stagnant. The chapter also presents examples of the dynamic behavior of some glaciers, ranging from calving glaciers that have receded a kilometer or more in a year to surge-type glaciers that have advanced more than 10 km during a surge event. These larger scale changes are easily seen at the pixel resolution of Landsat images; in a few instances, Landsat has been the only record of these changes.

Through the use of retrospective and prospective data, this chapter has also shown many examples of the natural variability displayed by glaciers throughout Alaska. For instance, in less than a century, major coastal bays such as Glacier Bay and Icy Bay have formed or expanded in area owing to glacier recession; the catastrophic retreat of Columbia Glacier resulted in the production of icebergs that are a hazard to maritime navigation; the retreat of major glaciers such as Tazlina Glacier resulted in the formation of ice-dammed and ice-marginal lakes that can produce jökulhlaups when the ice dam fails; and, twice since the end of the "baseline" period, the ongoing advance of Hubbard Glacier has blocked Russell Fiord and produced two of the largest jökulhlaups ever witnessed in North America during modern times. Finally, this chapter has reviewed how changing climate has affected the areas (and volumes) of nearly all of Alaska's valley and piedmont glaciers, impacting the storage and release of freshwater and contributing in part to the observed increase in global sea level.

Acknowledgments

Special thanks are offered to Maynard M. Miller, University of Idaho, Moscow, Idaho; Austin Post, U.S. Geological Survey (ret.); and the late William O. "Bill" Field, American Geographical Society. More than 35 years ago, Maynard gave me my first opportunity to become familiar with Alaskan glaciers; Bill gladly shared his data and his experiences in the 20 years that I knew him; and Austin was a good friend who, in addition to providing dozens of photographs included in this volume, accompanied me on many adventures to some of the most spectacular glaciers and fjords in the world—the glaciers and fjords of Alaska. Also, thanks to Darrell S. Kaufman, Department of Geology, Northern Arizona University, Flagstaff, Arizona; Robert M. Krimmel, USGS (ret.); Lawrence C. Mayo, USGS (ret.); and Dennis C. Trabant, USGS (ret.), for providing some of the images and (or) photographs and captions used in this volume. I especially want to recognize series editors Jane G. Ferrigno and Richard S. Williams, Jr., for their thorough technical reviews and comprehensive technical editing of the text and illustrations, Janice G. Goodell for typing multiple revisions and the final preparation of the manuscript, and Kirsten C. Healey for her outstanding work in the preparation of graphics throughout the volume, in both the printed and web versions. I also appreciate Kathie Rankin's fine work in editing the text, graphics, and figure captions.

I also want to acknowledge the assistance provided by Rose Watabe, GeoData Center, Geophysical Institute, University of Alaska, in the correct identification of all of the AHAP false-color infrared vertical aerial photographs used throughout the chapter. I appreciate the efforts of John Pojeta, Jr., USGS (ret.), and Thomas R. Waller, National Museum of Natural History, Smithsonian Institution, to identify the bivalve mollusk *Petricola* sp. shown in figure 217. I am particularly grateful to the following technical reviewers, who freely gave of their time to review all or part of the text and illustrations: Anthony A. Arendt, Keith Echelmeyer, and William D. Harrison, Geophysical Institute, University of Alaska; Austin Post, USGS (ret.); Vashon, Washington; Mark F. Meier, University of Colorado, Institute for Arctic and Alpine Research, Boulder, Colo.; C Suzanne Brown, Tacoma, Wash.; and Parker E. Calkin, University of Colorado, Boulder, Colo.